國立臺灣大學工學院化學工程學系

碩士論文

Department of Chemical Engineering
College of Engineering
National Taiwan University

Master's Thesis

帶電球形軟質粒子在帶電球形孔洞中之擴散泳

Diffusiophoresis of a Charged Soft Sphere in a Charged Spherical Cavity

陳威銍
Wei-Zhi Chen

指導教授：葛煥彰 教授
Advisor: Huan-Jang Keh, Professor

中華民國 114 年 7 月
July 2025

doi:10.6342/NTU202502508

謝辭

首先，要先給所有一路上支持我，給予我幫助、機會、方向與指引的所有人發自內心的感謝。謝謝我的恩師，葛煥彰老師在我碩士班兩年扎實的教導，讓我得以站在巨人的肩上，看到更廣闊的世界。謝謝台南的夥伴們，一路走來都是我最堅強的後盾，讓我再向前邁進的過程中也不至於遺忘自己從何而來。謝謝台北的所有人無論是實驗室、系上與系外的兄弟姐妹們，是你們讓這段時光多了笑聲與力量。最後謝謝我家人，謝謝你們永遠支持我做的任何決定，無論那條路看起來有多麼曲折離奇。

在這不算漫長卻意蘊深遠的求學生涯中，我有著許多後悔的事，有些雲淡風輕也有些刻骨銘心，但我很慶幸我沒有任何遺憾，該做的、不該做的都做了，是場顛簸但精采的冒險。一路走來我的荒唐帶領著我克服許多難以跨越的障礙，而種種經歷的累積，在時間的淬鍊下交織成獨特的紋理，自成一格的構築了現在的我。也希望這樣的鋪陳，在未來，無論是在求學還是職場，無論面對什麼樣的挑戰，也都能保有力量繼續往前。

「人類只要活著，不管在哪裡都可以活下去」。希望在台大的兩年，我所受到的訓練與知識，足以讓我未來不管在怎樣的環境、怎樣的世界，就算到了一個我的學經歷不再具有任何價值的地方，也仍足以讓我牢牢抓住那道僅有的縫隙，那份「活下去的能力」。

最後，我想到上野千鶴子女士的一句話「在大學學習的價值，不是去學已經存在的知識，而是學會發掘至今無人發現的知的能力」，望未來的我，能乘載著在這裡獲得的一切能力，繼續走在探索未知的道路上。不為了什麼偉大的目標，只是為了證明那個曾在星空下對世界充滿好奇的小男孩，仍然活著。

The world is a fine place and worth fighting for. — E. Hemingway

2025. 07. 23

doi:10.6342/NTU202502508

摘要

本研究分析在一個充滿對稱型電解質溶液並具有濃度梯度的同心帶電球形腔體中，由一個不帶電的硬球核心與一個均勻帶電的多孔表面層組成的球形複合軟質粒子的擬穩態擴散泳動現象。藉由對軟質粒子與腔體壁的固定電荷密度進行正規微擾法，求解與流體速度場、電位分佈以及離子濃度分佈相關的線性化電動力方程式。進而獲得了軟質粒子的擴散泳動（包含電泳及化學泳的貢獻）速度的解析結果，此速度為以下幾個無因次群的函數：實心硬核與複合粒子半徑比值（r_0/a）、複合粒子與帶電空腔半徑比值（a/b）、複合粒子半徑與電雙層特性厚度（Debye screening length）的比值（κa）以及複合粒子半徑與多孔層滲透長度（porous layer permeation length）的比值（λa）。

在一般狀況下，帶電的腔體壁對複合粒子的擴散泳動行為具有顯著影響。沿著腔體壁產生的擴散滲透（diffusioosmosis），包含電滲透（electroosmosis）和 化學滲透（chemiosmosis）所造成的流體流動，會大幅改變複合粒子的擴散泳速度，甚至可能使其方向反轉。整體而言，擴散泳速度隨著實心硬核與複合粒子半徑比值、複合粒子與帶電空腔半徑比值、複合粒子半徑與多孔層滲透長度的比值增加而減小，隨著複合粒子半徑與電雙層特性厚度的比值增加而增加。

關鍵詞：擴散泳；擴散滲透；帶電軟質粒子；邊界效應；任意電雙層厚度

doi:10.6342/NTU202502508

Abstract

The quasi-steady diffusiophoresis of a soft particle composed of an uncharged hard sphere core and a uniformly charged porous surface layer in a concentric charged spherical cavity full of a symmetric electrolyte solution with a concentration gradient is analyzed. By using a regular perturbation method with small fixed charge densities of the soft particle and cavity wall, the linearized electrokinetic equations relevant to the fluid velocity field, electric potential profile, and ionic concentration distributions are solved. A closed-form formula for the diffusiophoretic (electrophoretic and chemiphoretic) velocity of the soft particle is obtained as a function of the ratios of core-to-particle radii, particle-to-cavity radii, particle radius to the Debye screening length, and particle radius to porous layer permeation length. In typical cases, the confining charged cavity wall significantly influences the diffusiophoresis of the soft particle.

The fluid flow caused by the diffusioosmosis (electroosmosis and chemiosmosis) along the cavity wall can considerably change the diffusiophoretic velocity of the particle and even reverse its direction. In general, the diffusiohoretic velocity decreases with increasing core-to-particle radius ratio, particle-to-cavity radius ratio, and ratio of particle radius to porous layer permeation length, but increases with increasing ratio of

doi:10.6342/NTU202502508

particle radius to the Debye length.

Keywords: diffusiophoresis; diffusioosmosis; charged soft particle; boundary effect; arbitrary electric double layer

doi:10.6342/NTU202502508

Table of Contents

謝辭 i

摘要 ii

Abstract iii

Table of Contents v

List of Figures vii

Chapter 1 Introduction 1

1.1 Diffusiophoresis 1

1.2 Soft particle 2

Chapter 2 Electrokinetic Equations and Boundary Conditions 5

2.1 Perturbation method 6

2.2 Differential governing equations 6

2.3 Boundary conditions 7

Chapter 3 Solution of the Diffusiophoretic Velocity 9

3.1 Equilibrium electrical potential profile 9

3.2 Solution of the perturbed variables 10

doi:10.6342/NTU202502508

3.3 Forces acting on the particle 12

3.4 Diffusiophoretic velocity of the particle 14

Chapter 4 Results and Discussion 16

4.1 Porous particle velocities 16

4.1.1 First-order electrophoretic velocities 16

4.1.2 Second-order chemiphoretic velocities 22

4.1.3 Diffusiophoretic velocity 28

4.2 Soft particle velocities 30

4.2.1 First-order electrophoretic velocities 30

4.2.2 Second-order chemiphoretic velocities 35

4.2.3 Diffusiophoretic velocity 40

Chapter 5 Conclusions 41

List of Symbols 43

References 47

Appendix A Functions in Equations (21)-(25) and Coefficients in Equation (29) 51

Appendix B Basic Governing Equations in Chapter 2 and Section 3.1 73

doi:10.6342/NTU202502508

List of Figures

Figure 1. Geometric sketch for the diffusiophoresis of a charged soft sphere in a concentric charged spherical cavity. 5

Figure 2. Normalized velocity $U_{01} / \beta U^{*}$ for the electrophoresis of a charged porous sphere ($r_0 = 0$) in a spherical cavity: (a) $a/b = 0.5$; (b) $\lambda a = 10$; (c) $\kappa a = 1$. 18

Figure 3. Normalized velocity $U_{10} / \beta U^{*}$ for a porous sphere ($r_0 = 0$) in a charged spherical cavity with electroosmosis: (**a**) $a/b = 0.5$; (**b**) $\lambda a = 10$; and (**c**) $\kappa a = 1$. 19

Figure 4. Normalized velocity $U_1 / \overline{Q} \beta U^{*}$ for the electrophoresis of a charged porous sphere ($r_0 = 0$) in a charged spherical cavity versus the fixed charge density ratio $\overline{\sigma} / \overline{Q}$: (**a**) $a/b = 0.5$ and $\kappa a = 1$; (**b**) $\lambda a = 10$ and $a/b = 0.5$; and (**c**) $\kappa a = 1$ and $\lambda a = 10$ 21

Figure 5. Normalized velocity U_{02} / U^{*} for the chemiphoresis of a charged porous sphere ($r_0 = 0$) in a spherical cavity: (**a**) $a/b = 0.5$; (**b**) $\lambda a = 10$; and (**c**) $\kappa a = 1$. 23

Figure 6. Normalized velocity U_{11} / U^{*} for a charged porous sphere ($r_0 = 0$) in a charged spherical cavity: (**a**) $a/b = 0.5$; (**b**) $\lambda a = 10$; and (**c**) $\kappa a = 1$. 24

doi:10.6342/NTU202502508

Figure 7. Normalized velocity U_{20}/U^* for a porous sphere ($r_0 = 0$) in a charged spherical cavity with chemiosmosis: (**a**) $a/b = 0.5$; (**b**) $\lambda a = 10$; and (**c**) $\kappa a = 1$. 25

Figure 8. Normalized velocity $U_2/\bar{Q}^2 U^*$ for the chemiphoresis of a charged porous sphere ($r_0 = 0$) in a charged spherical cavity versus the fixed charge density ratio $\bar{\sigma}/\bar{Q}$: (**a**) $a/b = 0.5$ and $\kappa a = 1$; (**b**) $\lambda a = 10$ and $a/b = 0.5$; and (**c**) $\kappa a = 1$ and $\lambda a = 10$. 27

Figure 9. Normalized velocity U/U^* for the diffusiophoresis of a charged porous sphere ($r_0 = 0$) in a charged spherical cavity with $\beta = -0.2$ and $\bar{Q} = 1$ versus the charge density $\bar{\sigma}$: (**a**) $a/b = 0.5$ and $\kappa a = 1$; (**b**) $\lambda a = 10$ and $a/b = 0.5$; and (**c**) $\kappa a = 1$ and $\lambda a = 10$ 29

Figure 10. Normalized velocity $U_{01}/\beta U^*$ for the electrophoresis of a charged soft sphere in a spherical cavity versus r_0/a: (**a**) $a/b = 0.5$ and $\kappa a = 1$; (**b**) $\lambda a = 10$ and $a/b = 0.5$; and (**c**) $\kappa a = 1$ and $\lambda a = 10$. 32

Figure 11. Normalized velocity $U_{10}/\beta U^*$ for a soft sphere in a charged spherical cavity with electroosmosis versus r_0/a: (**a**) $a/b = 0.5$ and $\kappa a = 1$; (**b**) $\lambda a = 10$ and $a/b = 0.5$; and (**c**) $\kappa a = 1$ and $\lambda a = 10$. 33

Figure 12. Normalized velocity $U_1/\bar{Q}\beta U^*$ for the electrophoresis of a charged soft sphere in a charged spherical cavity with $\kappa a = 1$, $\lambda a = 10$, and $a/b = 0.5$

doi:10.6342/NTU202502508

versus the fixed charge density ratio $\bar{\sigma}/\bar{Q}$ 34

Figure 13. Normalized velocity U_{02}/U^* for the chemiphoresis of a charged soft sphere in a spherical cavity versus r_0/a: (**a**) $a/b=0.5$ and $\kappa a=1$; (**b**) $\lambda a=10$ and $a/b=0.5$; and (**c**) $\kappa a=1$ and $\lambda a=10$ 36

Figure 14. Normalized velocity U_{11}/U^* for a charged soft sphere in a charged spherical cavity versus r_0/a : (**a**) $a/b=0.5$ and $\kappa a=1$; (**b**) $\lambda a=10$ and $a/b=0.5$; and (**c**) $\kappa a=1$ and $\lambda a=10$ 37

Figure 15. Normalized velocity U_{20}/U^* for a soft sphere in a charged spherical cavity with chemiosmosis versus r_0/a: (**a**) $a/b=0.5$ and $\kappa a=1$; (**b**) $\lambda a=10$ and $a/b=0.5$; and (**c**) $\kappa a=1$ and $\lambda a=10$ 38

Figure 16. Normalized velocity $U_2/\bar{Q}^2U^*$ for the chemiphoresis of a charged soft sphere in a charged spherical cavity with $\kappa a=1$, $\lambda a=10$, and $a/b=0.5$ versus the fixed charge density ratio $\bar{\sigma}/\bar{Q}$ 39

Figure 17. Normalized velocity U/U^* for the diffusiophoresis of a charged soft sphere in a charged spherical cavity with $\beta=-0.2$, $\kappa a=1$, $\lambda a=10$, $a/b=0.5$ and $\bar{Q}=1$ versus the charge density $\bar{\sigma}$ 40

doi:10.6342/NTU202502508

Chapter 1
Introduction

1.1 Diffusiophoresis

Diffusiophoresis refers to the motion of colloid particles under imposed solute concentration gradients [1–8] and provides the mechanisms for numerous applications in the characterization, separation, transport, and manipulation of particles in microfluidics [9–14] and layered two-dimensional nanocolloid/liquid crystals [15,16], as well as in the autonomous motion of micromotors [17–19]. In a nonionic solution, the particle interacts with solute molecules via the Van der Waals and dipole attractive forces, and diffusi-ophoresis proceeds toward the regions where there is a higher solute concentration [20]. For the diffusiophoresis of a charged particle in an electrolyte solution, the particle–ion interaction is dominated by electrostatics and the range of its electric double layer with a thickness of the order of the Debye screening length [21]. In the past, the diffusiophoretic motion of a hard particle (which is impermeable to ionic fluids) [22,23], a porous particle (which is permeable) [24], and a soft particle (which has a hard core covered by a porous layer) [25–28] with an arbitrary electric double layer thickness were studied analytically (by assuming a weak applied electrolyte concentration gradient) and experimentally.

doi:10.6342/NTU202502508

In various applications of diffusiophoresis, the colloid particles are rarely unbounded, and it is important to understand whether boundaries significantly affect the particle mobility [5,29]. In the limiting case of a very thin double layer, the normalized fluid velocity field around a hard sphere undergoing diffusiophoresis is identical to that of one undergoing electrophoresis, and the already extensively studied boundary effect on electrophoretic motion can be used to explain the effect on diffusiophoretic motion [10]. On the other hand, the boundary effect of diffusiophoresis is different from that of electrophoresis when a double layer polarization is incorporated. By using a boundary collocation technique, the diffusiophoretic motion of a hard sphere with a thin polarized double layer near one or two plates [30] and along the axis of a microtube [31,32] was examined. Also, the diffusiophoresis of a charged sphere in a charged spherical cavity can be used to model diffusiophoretic motions in lab-on-a-chip devices and dead-end pores involving self-regulated drug delivery [33,34].

1.2 Soft particle

The surface of a colloidal particle is generally not hard and smooth as assumed in many theoretical models, instead, it often comprises a complex structure that plays a crucial role in colloidal stability. For instance, surface layers formed by the adsorption of long-chain polymers are commonly employed to enhance colloidal stability against flocculation, producing an extended, gel-like polymeric layer that penetrates into the

doi:10.6342/NTU202502508

suspending medium. Even model colloids such as silica and polystyrene latex exhibit such "hairy" surfaces. Biological cells present even greater complexity, featuring permeable, rough interfaces with appendages ranging from nanometer-scale protein molecules to micrometer-scale cilia. To capture these complexities, colloidal particles are often modeled as soft or composite particles, consisting of a central rigid core surrounded by an outer porous shell; in the limiting case where the core vanishes, the structure effectively becomes a fully permeable particle, analogous to polymer coils or colloidal flocs.

In fact, the diffusiophoresis of a charged hard or porous sphere with a thin polarized or an arbitrary double layer situated at the center of a charged spherical cavity [35,36] and the diffusiophoresis of a charged soft sphere with an arbitrary double layer inside a nonconcentric uncharged spherical cavity [37] have been studied theoretically. However, the effect of a charged boundary on the diffusiophoretic motion of a soft particle has not been investigated. In this thesis, the diffusiophoresis of a charged soft spherical particle inside a concentric charged spherical cavity with an arbitrary electric double layer thickness is analyzed. The fluid velocity field, electric potential profile, and ionic concentration distributions are determined as the power series of the small fixed charge densities of the soft sphere and cavity wall. An explicit formula for the diffusiophoretic mobility of the soft sphere is obtained as a function of the relevant

doi:10.6342/NTU202502508

parameters.

doi:10.6342/NTU202502508

Chapter 2

Electrokinetic Equations and Boundary Conditions

As shown in Figure 1, we consider the diffusiophoresis of a soft spherical particle of radius a, consisting of an uncharged hard sphere core of radius r_0 and a charged porous surface layer of thickness $a - r_0$, situated at the center of a charged spherical cavity of radius b occupied by a symmetric electrolyte solution in a quasi-steady state. A linear electrolyte concentration profile $n^{\infty}(z) = n^{\infty}(0) + \left|\nabla n^{\infty}\right| z$ is imposed along the cavity wall with a constant gradient ∇n^{∞} in the z direction, and the induced particle velocity U in this direction needing to be determined. The origin of the spherical coordinates (r, θ, ϕ) is attached to the particle center (at $z = 0$), and the problem is independent of ϕ (symmetric about the z axis).

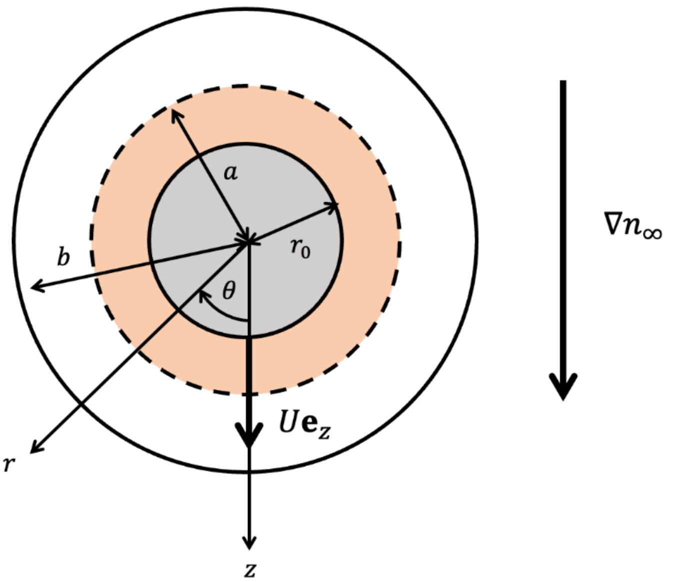

Figure 1. Geometric sketch for the diffusiophoresis of a charged soft sphere in a concentric charged spherical cavity.

doi:10.6342/NTU202502508

2.1 Perturbation method

The normalized electrolyte concentration gradient $\alpha = a\left|\nabla n^{\infty}\right| / n^{\infty}(0)$ is taken to be positive but small, so that the system deviates slightly from equilibrium. Therefore, the cationic and anionic concentration profiles $n_{+}(r,\theta)$ and $n_{-}(r,\theta)$, respectively; the dynamic pressure distribution $p(r,\theta)$; and the electrical potential distribution $\psi(r,\theta)$ can be decomposed into the following:

$$n_{\pm} = n_{\pm}^{(\mathrm{eq})} + \delta n_{\pm}, \tag{1}$$

$$p = p^{(\mathrm{eq})} + \delta p, \tag{2}$$

$$\psi = \psi^{(\mathrm{eq})} + \delta\psi, \tag{3}$$

where $n_{\pm}^{(\mathrm{eq})}(r)$, $p^{(\mathrm{eq})}(r)$, and $\psi^{(\mathrm{eq})}(r)$ are the equilibrium profiles of the ionic concentrations, dynamic pressure, and electrical potential, respectively, and $\delta n_{\pm}(r,\theta)$, $\delta p(r,\theta)$, and $\delta\psi(r,\theta)$ are the pertinent small perturbations.

2.2 Differential governing equations

The small perturbed quantities, $\delta n_{\pm}$, δp, and $\delta\psi$, and the fluid velocity $\mathbf{v}(r,\theta)$ are governed by the linearized ionic continuity equations, modified Stokes–Brinkman equations, and Poisson–Boltzmann equation, respectively, as follows (being discussed in Appendix B):

$$\nabla^2 \delta\mu_{\pm} = \pm\frac{Ze}{kT}[\nabla\delta\mu_{\pm}\cdot\nabla\psi^{(\mathrm{eq})} - \frac{kT}{D_{\pm}}\mathbf{v}\cdot\nabla\psi^{(\mathrm{eq})}], \tag{4}$$

$$[\nabla^2 - \lambda^2 h(r)]\nabla\times\mathbf{v} = -\frac{\varepsilon}{\eta}\nabla\times[\nabla^2\delta\psi\nabla\psi^{(\mathrm{eq})} + \nabla^2\psi^{(\mathrm{eq})}\nabla\delta\psi], \tag{5}$$

$$\nabla^2\delta\psi = \frac{n_0^{\infty}Ze}{\varepsilon kT}\{(\delta\mu_{-} + Ze\delta\psi)\exp[\frac{Ze\psi^{(\mathrm{eq})}}{kT}] - (\delta\mu_{+} - Ze\delta\psi)\exp[-\frac{Ze\psi^{(\mathrm{eq})}}{kT}]\}. \tag{6}$$

doi:10.6342/NTU202502508

In the previous equations, the ionic electrochemical potential energy perturbations are as follows:

$$\delta\mu_{\pm} = \frac{kT}{n_{\pm}^{(\mathrm{eq})}}\delta n_{\pm} \pm Ze\delta\psi\,, \tag{7}$$

Furthermore, λ^{-1} is the flow penetration length or the square root of the permeability in the porous surface layer of the soft sphere; $D_{\pm}$ are the ionic diffusivities in the fluid; Z is the valence of the symmetric electrolyte (which is positive); η and ε are the viscosity and dielectric permittivity, respectively, of the fluid; and $h(r)$ equals unity if $r_0 \le r \le a$ and zero otherwise. The pressure term in Equation (5) disappears owing to the application of a curl to the momentum equation; the fluid velocity $\mathbf{v}$ also satisfies the continuity equation; and the constants $D_{\pm}$, η, and ε inside and outside the porous layer are considered to be the same.

2.3 Boundary conditions

The boundary conditions of the small perturbed quantities along the interface between the hard sphere core and the porous surface layer and at the particle surface are as follows [25]:

$$r = r_0: \ \mathbf{e}_r \cdot \nabla\delta\mu_{+} = 0,\ \ \mathbf{e}_r \cdot \nabla\delta\mu_{\pm} = 0,\ \ \mathbf{v} = \mathbf{0}, \tag{8}$$

$$r = a: \qquad \delta\psi,\ \nabla\delta\psi,\ \delta\mu_{\pm},\ \nabla\delta\mu_{\pm},\ \mathbf{v}\text{, and } \mathbf{e}_r\cdot\boldsymbol{\tau} \text{ are continuous,} \tag{9}$$

where $\boldsymbol{\tau}$ is the hydrodynamic stress tensor of the fluid, $\mathbf{e}_r$ is the unit vector in the r direction, and Equation (8) takes a reference frame traveling with the soft particle.

The boundary conditions at the cavity wall are as follows [35]:

$$r = b: \qquad \delta\psi = -\frac{kT}{Ze}\beta\alpha\frac{r}{a}\cos\theta\,, \tag{10}$$

doi:10.6342/NTU202502508

$$\delta\mu_{\pm} = kT(1 \mp \beta)\alpha \frac{r}{a} \cos\theta \text{, if } a \le r \le b, \tag{11}$$

$$\mathbf{v} = -U\mathbf{e}_z \tag{12}$$

where $\alpha = a\left|\nabla n^{\infty}\right| / n^{\infty}(0)$, $\beta = (D_+ - D_-)/(D_+ + D_-)$, and $\mathbf{e}_z$ is the unit vector in the z direction. Equations (10a) and (10b) for the induced perturbed electrical potential and the ionic electrochemical potential energies result from the electrolyte concentration gradient imposed along the cavity wall and the equality of the anion and cation fluxes in the particle-free fluid. Equation (10c) for the stationary cavity also takes the same reference frame as Equation (8).

doi:10.6342/NTU202502508

Chapter 3

Solution of the Diffusiophoretic Velocity

3.1 Equilibrium electrical potential profile

The equilibrium electrical potential profile of a soft spherical particle, whose porous surface layer has a constant space charge density Q, situated at the center of a spherical cavity, having a constant surface charge density σ, satisfying the continuity of electrical potential and current at the particle surface ($r = a$) and the Gauss condition at the hard core surface ($r = r_0$) and cavity wall ($r = b$) , can be obtained as follows (being discussed in Appendix B):

$$\psi^{(\mathrm{eq})} = \psi_{\mathrm{eq01}}(r)\overline{Q} + \psi_{\mathrm{eq10}}(r)\overline{\sigma} + \mathrm{O}(\overline{Q}^3, \overline{Q}^2\overline{\sigma}, \overline{Q}\overline{\sigma}^2, \overline{\sigma}^3) , \tag{13}$$

where

$$\psi_{\mathrm{eq01}}(r) = \frac{kT\mathrm{e}^{-\kappa r}}{2ZeA\kappa r}\{[\mathrm{e}^{\kappa a}(\kappa a - 1)(\kappa r_0 + 1) - \mathrm{e}^{\kappa(2r_0 - a)}(\kappa a + 1)(\kappa r_0 - 1)][\mathrm{e}^{2\kappa b}(\kappa b - 1) + \mathrm{e}^{2\kappa r}(\kappa b + 1)]\} \quad \text{for} \quad a < r < b , \tag{14}$$

$$\psi_{\mathrm{eq01}}(r) = \frac{kT\mathrm{e}^{\kappa(2b - a + 2r_0 - r)}}{2ZeA\kappa r}\{\frac{1}{A} + \mathrm{e}^{\kappa(a - 2b)}(\kappa b + 1)(\kappa r_0 - 1)[\mathrm{e}^{\kappa a}(\kappa a - 1) - 2\mathrm{e}^{\kappa r}\kappa r] - \mathrm{e}^{\kappa(r - 2r_0)}(\kappa b - 1)(\kappa r_0 + 1)[\mathrm{e}^{\kappa r}(\kappa a + 1) - 2\mathrm{e}^{\kappa a}\kappa r] + \mathrm{e}^{2\kappa(a - b - r_0 + r)}(\kappa a - 1) \times (\kappa b + 1)(\kappa r_0 + 1) + \kappa[b - r_0(\kappa b - 1) - a(\kappa b - 1)(\kappa r_0 - 1)]\} \quad \text{for} \quad r_0 < r < a , \tag{15}$$

$$\psi_{\mathrm{eq10}}(r) = \frac{2kT(\kappa b)^2\,\mathrm{e}^{\kappa(b + r_0)}}{ZeA\kappa r}\{\kappa r_0 \cosh[\kappa(r - r_0)] + \sinh[\kappa(r - r_0)]\} , \tag{16}$$

$$A = \mathrm{e}^{2\kappa b}(\kappa b - 1)(\kappa r_0 + 1) - \mathrm{e}^{2\kappa r_0}(\kappa b + 1)(\kappa r_0 - 1) , \tag{17}$$

doi:10.6342/NTU202502508

Both $\overline{Q} = ZeQ/\varepsilon\kappa^2 kT$ and $\overline{\sigma} = Ze\sigma/\varepsilon\kappa kT$ are dimensionless, whereas $\kappa = (2Z^2 e^2 n_0^\infty / \varepsilon kT)^{1/2}$ is the Debye screening parameter. For the case of a symmetric electrolyte, the second-order terms $O(\overline{Q}^2, \overline{Q}\overline{\sigma}, \overline{\sigma}^2)$ in Equation (13) disappear.

The substitution of Equations (13)-(16) into the Gauss condition at $r = b$ yields a relation between the surface charge density σ and the zeta potential ζ of the cavity wall:

$$\sigma = \{(1-\kappa^2 a r_0)\sinh[\kappa(a-r_0)] - \kappa(a-r_0)\cosh[\kappa(a-r_0)]\}BQ \\ +\varepsilon\kappa^2\{(\kappa^2 b r_0 - 1)\sinh[\kappa(b-r_0)] + \kappa(b-r_0)\cosh[\kappa(b-r_0)]\}B\zeta\,, \tag{18}$$

where

$$B = \{\kappa^2 b \sinh[\kappa(b-r_0)] + \kappa^3 b r_0 \cosh[\kappa(b-r_0)]\}^{-1}. \tag{19}$$

Namely, after the substitution of Equation (18), Equation (13) is also valid for the solution of $\psi^{(\mathrm{eq})}$ in the case of a cavity wall with a constant zeta potential.

3.2 Solution of the perturbed variables

When the parameters $\overline{Q}$ and $\overline{\sigma}$ are small, in order to solve for the perturbed quantities $\delta\mu_\pm$, $\delta\psi$, v_r, v_θ, and δp with the diffusiophoretic velocity U of the soft spherical particle, these variables can be expressed as power expansions of $\overline{Q}$ and $\overline{\sigma}$, such as the following:

$$U = U_{01}\overline{Q} + U_{10}\overline{\sigma} + U_{02}\overline{Q}^2 + U_{11}\overline{Q}\overline{\sigma} + U_{20}\overline{\sigma}^2 + \cdots, \tag{20}$$

where the to-be-determined coefficients U_{01}, U_{10}, U_{02}, U_{11}, U_{20}, etc. do not depend on $\overline{Q}$ and $\overline{\sigma}$ but are dependent on the core-to-particle radius ratio r_0/a, the particle-to-cavity radius ratio a/b, the ratio of the particle radius to the permeation length in the porous layer λa, and the electrokinetic particle radius κa. There are

doi:10.6342/NTU202502508

zeroth-order terms of $\overline{Q}$ and $\overline{\sigma}$ in the expansions of $\delta\psi$ and $\delta\mu_{\pm}$, as shown in Equations (10) and (11).

The substitution of these expansions and Equation (13) into Equations (4)–(12) yields results for $\delta\psi$, $\delta\mu_{\pm}$ (to the orders $\overline{Q}$ and $\overline{\sigma}$), v_r, v_θ, and δp (to the orders $\overline{Q}^2$, $\overline{Q}\overline{\sigma}$, and $\overline{\sigma}^2$) as follows:

$$\delta\psi = \frac{kT}{Ze}\alpha[-\beta F_{\psi 00} + F_{\psi 01}\overline{Q} + F_{\psi 10}\overline{\sigma}]\cos\theta\,, \tag{21}$$

$$\delta\mu_{\pm} = kT(1\mp\beta)\alpha[F_{\mu 00} \mp F_{\mu 01}\overline{Q} \mp F_{\mu 10}\overline{\sigma}]\cos\theta\,, \tag{22}$$

$$\begin{aligned} v_r = {} & [(U_{01}F_{00r} - \frac{kT}{\eta a^2}\beta\alpha F_{01r})\overline{Q} + (U_{10}F_{00r} - \frac{kT}{\eta a^2}\beta\alpha F_{10r})\overline{\sigma} + (U_{02}F_{00r} + \frac{kT}{\eta a^2}\alpha F_{02r})\overline{Q}^2 \\ & + (U_{11}F_{00r} + \frac{kT}{\eta a^2}\alpha F_{11r})\overline{Q}\overline{\sigma} + (U_{20}F_{00r} + \frac{kT}{\eta a^2}\alpha F_{20r})\overline{\sigma}^2\,]\cos\theta\,, \end{aligned} \tag{23}$$

$$v_\theta = -\frac{\tan\theta}{2r}\frac{\partial}{\partial r}(r^2 v_r)\,, \tag{24}$$

$$\begin{aligned} \delta p = {} & \frac{\eta}{a}\{(U_{01}F_{p00} - \frac{kT}{\eta a^2}\beta\alpha F_{p01} - \frac{\varepsilon kT}{\eta Ze}\kappa^2 a\beta\alpha\psi_{\mathrm{eq}01}F_{\psi 00})\overline{Q} \\ & + (U_{10}F_{p00} - \frac{kT}{\eta a^2}\beta\alpha F_{p10} - \frac{\varepsilon kT}{\eta Ze}\kappa^2 a\beta\alpha\psi_{\mathrm{eq}10}F_{\psi 00})\overline{\sigma} \\ & + (U_{02}F_{p00} + \frac{kT}{\eta a^2}\alpha F_{p02} + \frac{\varepsilon kT}{\eta Ze}\kappa^2 a\alpha\psi_{\mathrm{eq}01}F_{\psi 01})\overline{Q}^2 \\ & + [U_{11}F_{p00} + \frac{kT}{\eta a^2}\alpha F_{p11} + \frac{\varepsilon kT}{\eta Ze}\kappa^2 a\alpha(\psi_{\mathrm{eq}01}F_{\psi 10} + \psi_{\mathrm{eq}10}F_{\psi 01})]\overline{Q}\overline{\sigma} \\ & + (U_{20}F_{p00} + \frac{kT}{\eta a^2}\alpha F_{p20} + \frac{\varepsilon kT}{\eta Ze}\kappa^2 a\alpha\psi_{\mathrm{eq}10}F_{\psi 10})\overline{\sigma}^2\}\cos\theta\,, \end{aligned} \tag{25}$$

where the dimensionless functions $F_{\psi ij}(r)$, $F_{\mu ij}(r)$, $F_{ijr}(r)$, and $F_{pij}(r)$ with i and j equal to 0, 1, and 2 are given by Equations (A1)-(A8) and (A20)-(A23) in Appendix A.

doi:10.6342/NTU202502508

3.3 Forces acting on the particle

The electrical force acting on the soft spherical particle can be expressed as [35]

$$\mathbf{F}_{\mathrm{e}} = 2\pi a^2 \varepsilon \int_0^{\pi} [\nabla \delta\psi \nabla \psi^{(\mathrm{eq})}]_{r=a} \cdot \mathbf{e}_r \sin\theta \mathrm{d}\theta \,. \tag{26}$$

The substitution of Equations (13) and (21) into the previous equation results in this force to the second orders,

$$\begin{aligned}\mathbf{F}_{\mathrm{e}} = \frac{4\pi kT\alpha a\varepsilon}{3Ze}\{-\beta[(2F_{\psi 00} + a\frac{\mathrm{d}F_{\psi 00}}{\mathrm{d}r})\frac{\mathrm{d}\psi_{\mathrm{eq01}}}{\mathrm{d}r}\bar{Q} + (2F_{\psi 00} + a\frac{\mathrm{d}F_{\psi 00}}{\mathrm{d}r})\frac{\mathrm{d}\psi_{\mathrm{eq10}}}{\mathrm{d}r}\bar{\sigma}] + (2F_{\psi 01} + a\frac{\mathrm{d}F_{\psi 01}}{\mathrm{d}r})\frac{\mathrm{d}\psi_{\mathrm{eq01}}}{\mathrm{d}r}\bar{Q}^2 \\ +[(2F_{\psi 01} + a\frac{\mathrm{d}F_{\psi 01}}{\mathrm{d}r})\frac{\mathrm{d}\psi_{\mathrm{eq10}}}{\mathrm{d}r} + (2F_{\psi 10} + a\frac{\mathrm{d}F_{\psi 10}}{\mathrm{d}r})\frac{\mathrm{d}\psi_{\mathrm{eq01}}}{\mathrm{d}r}]\bar{Q}\bar{\sigma} + (2F_{\psi 10} + a\frac{\mathrm{d}F_{\psi 10}}{\mathrm{d}r})\frac{\mathrm{d}\psi_{\mathrm{eq10}}}{\mathrm{d}r}\bar{\sigma}^2\}_{r=a}\mathbf{e}_z \,,\end{aligned} \tag{27}$$

The drag force exerted by the fluid on the soft spherical particle can be expressed as

$$\mathbf{F}_{\mathrm{h}} = 2\pi a^2 \int_0^{\pi} \{-\delta p \mathbf{I} + \eta[\nabla \mathbf{v} + (\nabla \mathbf{v})^{\mathrm{T}}]\}_{r=a} \cdot \mathbf{e}_r \sin\theta \mathrm{d}\theta \,, \tag{28}$$

where $\mathbf{I}$ is the unit dyadic. Substituting Equations (23)-(25) into the previous equation, we obtain

$$\begin{aligned}\mathbf{F}_{\mathrm{h}} = -4\pi\{[\eta a U_{01} C_{002} - \frac{kT}{a}\alpha\beta C_{012} - \frac{\varepsilon kT}{3Ze}(\kappa a)^2 \alpha\beta F_{\psi 00}\psi_{\mathrm{eq01}}]\bar{Q} \\ +[\eta a U_{10} C_{002} - \frac{kT}{a}\alpha\beta C_{102} - \frac{\varepsilon kT}{3Ze}(\kappa a)^2 \alpha\beta F_{\psi 00}\psi_{\mathrm{eq10}}]\bar{\sigma} \\ +[\eta a U_{02} C_{002} + \frac{kT}{a}\alpha C_{022} + \frac{\varepsilon kT}{3Ze}(\kappa a)^2 \alpha F_{\psi 01}\psi_{\mathrm{eq01}}]\bar{Q}^2 \\ +[\eta a U_{11} C_{002} + \frac{kT}{a}\alpha C_{112} + \frac{\varepsilon kT}{3Ze}(\kappa a)^2 \alpha (F_{\psi 01}\psi_{\mathrm{eq10}} + F_{\psi 10}\psi_{\mathrm{eq01}})]\bar{Q}\bar{\sigma} \\ +[\eta a U_{20} C_{002} + \frac{kT}{a}\alpha C_{202} + \frac{\varepsilon kT}{3Ze}(\kappa a)^2 \alpha F_{\psi 10}\psi_{\mathrm{eq10}}]\bar{\sigma}^2\}_{r=a}\mathbf{e}_z \,.\end{aligned} \tag{29}$$

doi:10.6342/NTU202502508

where the dimensionless coefficients C_{002}, C_{012}, C_{102}, C_{022}, C_{112} and C_{202}, also appearing in Equations (A1), (A3), (A5), and (A7), are given by Equations (A35) and (A43).

doi:10.6342/NTU202502508

3.4 Diffusiophoretic velocity of the particle

Applying the constraint that the total force on the diffusiophoretic soft sphere is zero to the summation of Equations (27) and (29), we obtain the following:

$$U_{01} = \frac{Ze\beta U^*}{3\varepsilon akTC_{002}}\{3ZeC_{012} + \varepsilon a^2[\kappa^2 aF_{\psi 00}\psi_{\text{eq}01} - (2F_{\psi 00} + a\frac{\mathrm{d}F_{\psi 00}}{\mathrm{d}r})\frac{\mathrm{d}\psi_{\text{eq}01}}{\mathrm{d}r}]\}_{r=a}, \tag{30}$$

$$U_{10} = \frac{Ze\beta U^*}{3\varepsilon akTC_{002}}\{3ZeC_{102} + \varepsilon a^2\kappa^2 aF_{\psi 00}\psi_{\text{eq}10} - (2F_{\psi 00} + a\frac{\mathrm{d}F_{\psi 00}}{\mathrm{d}r})\frac{\mathrm{d}\psi_{\text{eq}10}}{\mathrm{d}r}\}_{r=a}, \tag{31}$$

$$U_{02} = \frac{-ZeU^*}{3\varepsilon akTC_{002}}\{3ZeC_{022} + \varepsilon a^2[\kappa^2 aF_{\psi 01}\psi_{\text{eq}01} - (2F_{\psi 01} + a\frac{\mathrm{d}F_{\psi 01}}{\mathrm{d}r})\frac{\mathrm{d}\psi_{\text{eq}01}}{\mathrm{d}r}]\}_{r=a}, \tag{32}$$

$$\begin{aligned} U_{11} = \frac{-ZeU^*}{3\varepsilon akTC_{002}}\{3ZeC_{112} + \varepsilon a^2[\kappa^2 aF_{\psi 10}\psi_{\text{eq}01} + \kappa^2 aF_{\psi 01}\psi_{\text{eq}10} - (2F_{\psi 10} + a\frac{\mathrm{d}F_{\psi 10}}{\mathrm{d}r})\frac{\mathrm{d}\psi_{\text{eq}01}}{\mathrm{d}r} \\ -(2F_{\psi 01} + a\frac{\mathrm{d}F_{\psi 01}}{\mathrm{d}r})\frac{\mathrm{d}\psi_{\text{eq}10}}{\mathrm{d}r}]\}_{r=a}, \end{aligned} \tag{33}$$

$$U_{20} = \frac{-ZeU^*}{3\varepsilon akTC_{002}}\{3ZeC_{202} + \varepsilon a^2[\kappa^2 aF_{\psi 10}\psi_{\text{eq}10} - (2F_{\psi 10} + a\frac{\mathrm{d}F_{\psi 10}}{\mathrm{d}r})\frac{\mathrm{d}\psi_{\text{eq}10}}{\mathrm{d}r}]\}_{r=a} \tag{34}$$

where

$$U^* = \frac{\varepsilon\alpha}{\eta a}(\frac{kT}{Ze})^2 \tag{35}$$

which is a characteristic particle velocity. After the substitution of Equation (18), Equation (20) is also valid for the diffusiophoretic velocity of the particle in the case of a cavity wall with a constant zeta potential. Equations (30)-(34) for the limit $r_0 = 0$ reduce to the diffusiophoretic velocity of a charged porous spherical particle within a charged spherical cavity obtained earlier, and analytical expressions are available in some limiting cases [36].

In Equation (20) for the diffusiophoretic velocity of the soft spherical particle within the spherical cavity, the first-order terms $\mathrm{O}(\overline{Q}, \overline{\sigma})$ and second-order terms $O(\overline{Q}^2, \overline{Q}\overline{\sigma}, \overline{\sigma}^2)$ denote the contributions from electrophoresis that are caused by the induced electric field in Equation (10) and chemiphoresis, respectively. The fixed

doi:10.6342/NTU202502508

charge at the cavity wall changes the particle motion through the wall-corrected electrical potential distribution and diffusioosmosis-induced (electroosmosis-induced and chemiosmosis-induced) recirculating flows generated by the interaction of the imposed electrolyte concentration gradient with the electrical double layer adjacent to the wall. The terms $U_{01}\overline{Q}+U_{02}\overline{Q}^2$ and $U_{10}\overline{\sigma}+U_{20}\overline{\sigma}^2$ are the diffusiophoretic velocity of a charged soft particle in an uncharged cavity ($\sigma=0$) and the translational velocity of an uncharged soft particle ($Q=0$) in a charged cavity induced by diffusioosmosis, respectively. Equations (30) and (31) agrees with the electrophoretic velocity of a soft spherical particle within a charged cavity available in the literature [38].

doi:10.6342/NTU202502508

Chapter 4

Results and Discussion

4.1 Porous particle velocities

4.1.1 First-order electrophoretic velocities

The analytical formulae for the diffusiophoretic velocity of a charged soft spherical particle within a concentric charged spherical cavity are obtained in Equations (20) and (30)–(35), and the graphical results will be given here. The normalized first-order (electrophoretic) velocities $U_{01}/\beta U^*$ and $U_{10}/\beta U^*$ for the special case of a porous spherical particle ($r_0 = 0$) within a concentric charged cavity as calculated from Equations (30 and (31) are plotted in Figures 2 and 3, respectively, as functions of the hydrodynamic resistance parameter λa, the particle-to-cavity radius ratio a/b, and the electrokinetic particle radius κa. These normalized velocities are always positive; therefore, the sign of the product βQ determines the direction of the electrophoresis and the sign of $\beta\sigma$ determines the direction of the contribution from the electroosmosis at the cavity wall to the particle velocity.

For the fixed values of a/b and λa, both $U_{01}/\beta U^*$ and $U_{10}/\beta U^*$ are the monotonically increasing functions of κa from zero at $\kappa a = 0$. For the specified values of a/b and κa, both $U_{01}/\beta U^*$ and $U_{10}/\beta U^*$ are the monotonically decreasing functions of λa as expected, but $U_{01}/\beta U^*$ may strongly depend on λa, while $U_{10}/\beta U^*$ is only weakly dependent on λa. For fixed λa and κa, both

doi:10.6342/NTU202502508

$U_{01}/\beta U^*$ and $U_{10}/\beta U^*$ are the monotonically decreasing functions of a/b as expected, and $U_{10}/\beta U^*$ equals 1 and 0 if a/b equals 0 and 1, respectively.

doi:10.6342/NTU202502508

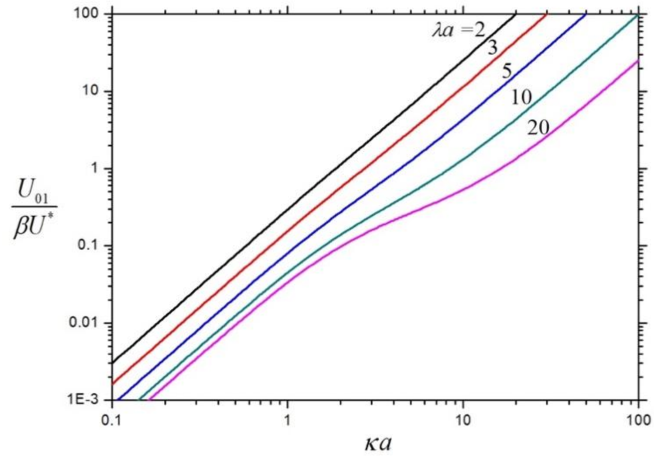

(a)

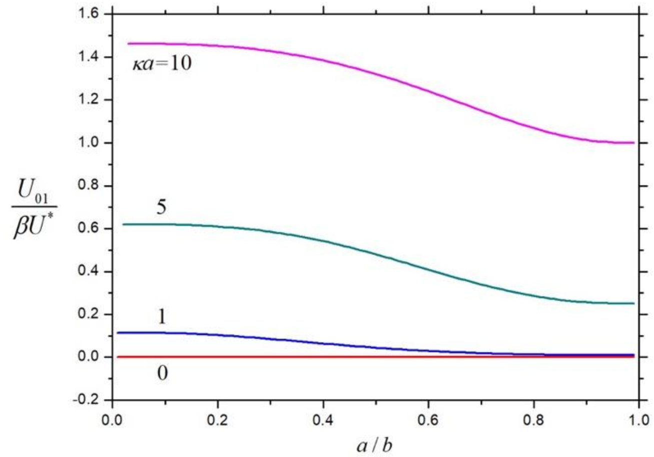

(b)

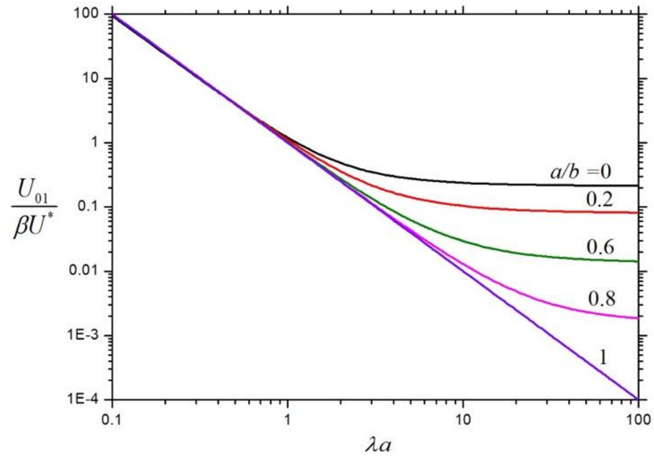

(c)

Figure 2. Normalized velocity $U_{01} / \beta U^*$ for the electrophoresis of a charged porous sphere ($r_0 = 0$) in a spherical cavity: (a) $a / b = 0.5$; (b) $\lambda a = 10$; (c) $\kappa a = 1$.

doi:10.6342/NTU202502508

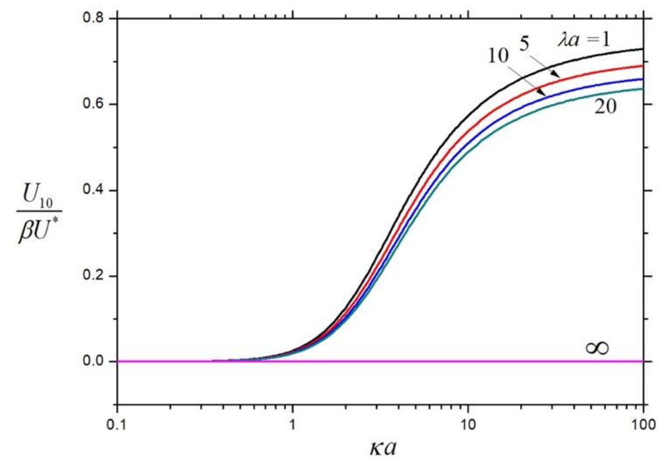

(a)

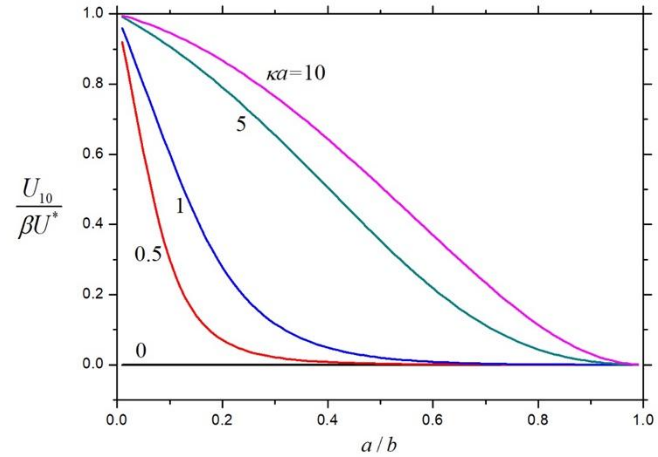

(b)

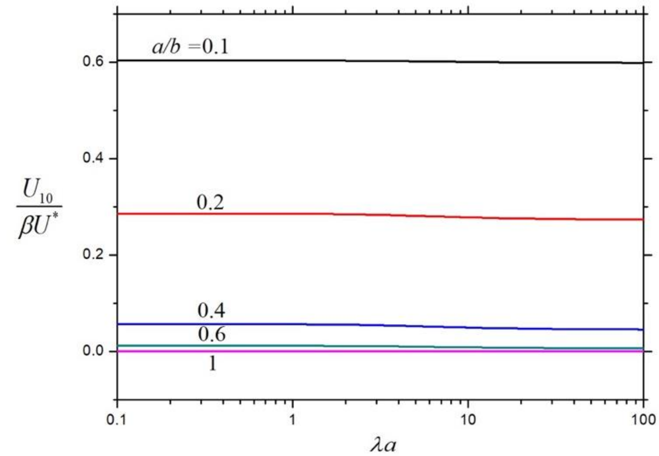

(c)

Figure 3. Normalized velocity $U_{10} / \beta U^*$ for a porous sphere ($r_0 = 0$) in a charged spherical cavity with electroosmosis: (**a**) $a/b = 0.5$; (**b**) $\lambda a = 10$; and (**c**) $\kappa a = 1$.

doi:10.6342/NTU202502508

The normalized net first-order velocity $U_1/\overline{Q}\beta U^*$ (with $U_1 = U_{01}\overline{Q} + U_{10}\overline{\sigma}$) of a charged porous particle inside a charged cavity is plotted versus the fixed charge density ratio $\overline{\sigma}/\overline{Q}$ (equaling $\kappa\sigma/Q$) in Figure 4 (in straight lines with the slope $U_{10}/\beta U^*$) for different values of a/b, λa, and κa. The electroosmotic flow at the cavity wall enhances/reduces this electrophoretic velocity if the fixed charge densities $\overline{Q}$ and $\overline{\sigma}$ are in the same/opposite signs. If the magnitude of $\overline{\sigma}/\overline{Q}$ is large, the wall effect can be significant. When the value of $\overline{\sigma}/\overline{Q}$ is negative and the magnitude is great, the velocity direction of the confined particle may be opposite to the direction of the electrophoresis in an unbounded fluid. The magnitude of $U_1/\overline{Q}\beta U^*$ in general decreases with the increases in λa and a/b, but increases with an increase in κa.

doi:10.6342/NTU202502508

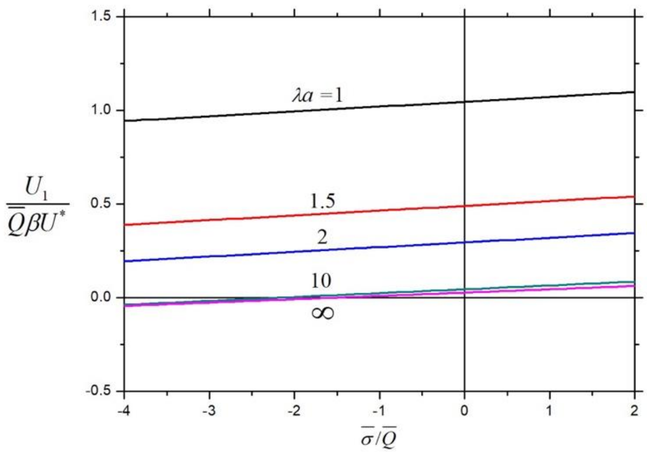

(a)

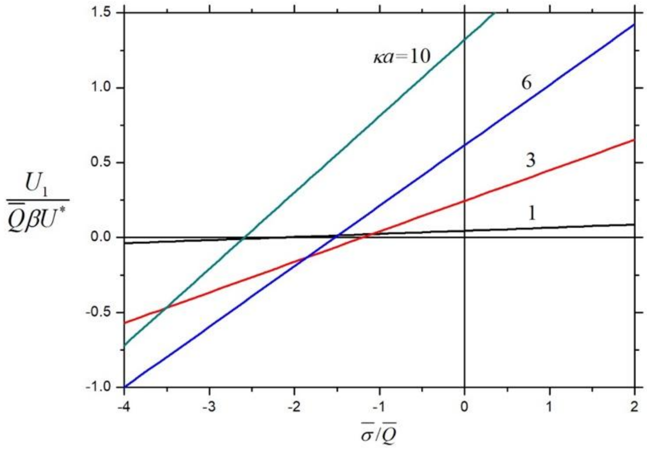

(b)

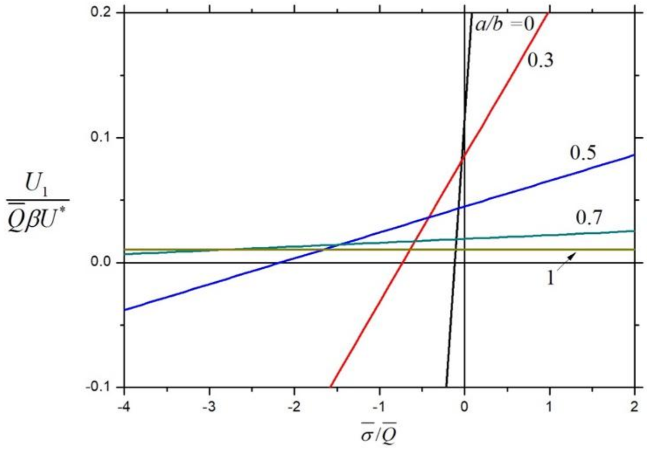

(c)

Figure 4. Normalized velocity $U_1/\overline{Q}\beta U^*$ for the electrophoresis of a charged porous sphere ($r_0 = 0$) in a charged spherical cavity versus the fixed charge density ratio $\overline{\sigma}/\overline{Q}$: (**a**) $a/b = 0.5$ and $\kappa a = 1$; (**b**) $\lambda a = 10$ and $a/b = 0.5$; and (**c**) $\kappa a = 1$ and $\lambda a = 10$.

doi:10.6342/NTU202502508

4.1.2 Second-order chemiphoretic velocities

The normalized second-order velocities U_{02}/U^*, U_{11}/U^*, and U_{20}/U^* of a charged porous sphere inside a charged cavity caused by the chemiphoretic and wall-induced chemiosmotic effects as calculated from Equations (32)-(34) are plotted in Figures 5, 6, and 7, respectively, as functions of the parameters a/b, λa, and κa. All these second-order velocities are monotonically decreasing functions of λa as expected, but none of them is a monotonic function of a/b (local extrema appear at moderate values of a/b), keeping the other parameters unchanged.

For the specified values of a/b and λa, the value of U_{02}/U^* increases monotonically with an increase in κa, whereas U_{11}/U^* and U_{20}/U^* may not be monotonic functions of κa. As expected, $U_{02}/U^* = U_{11}/U^* = U_{20}/U^* = 0$ in the limits $a/b = 1$ and $\kappa a = 0$, while $U_{11}/U^* = 0$ in the limit $a/b = 0$. For the given values of a/b and κa, both U_{11}/U^* and U_{02}/U^* are strongly dependent on λa (inversely proportional to $\lambda^2 a^2$ if λa is smaller than about 10), while U_{20}/U^* only weakly depend on λa.

doi:10.6342/NTU202502508

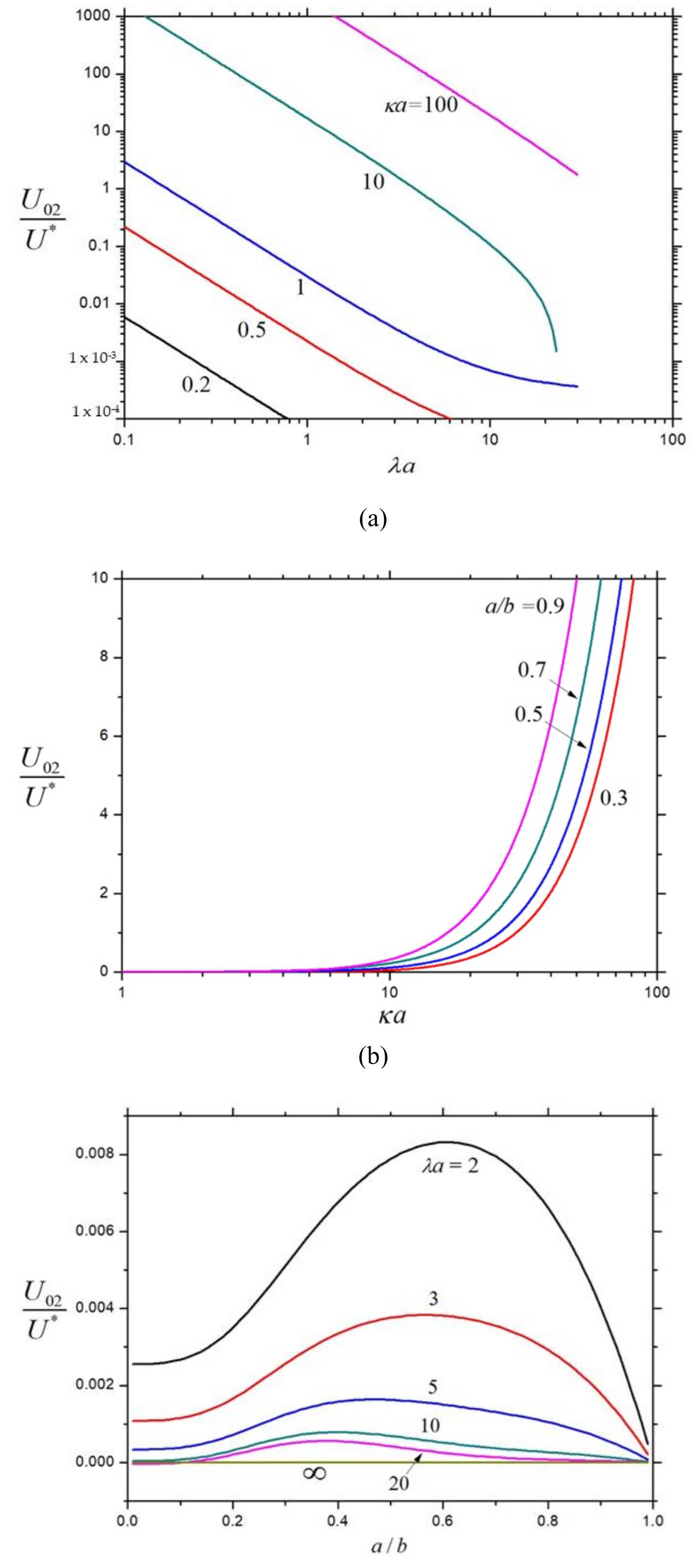

Figure 5. Normalized velocity U_{02}/U^* for the chemiphoresis of a charged porous sphere ($r_0 = 0$) in a spherical cavity: (**a**) $a/b = 0.5$; (**b**) $\lambda a = 10$; and (**c**) $\kappa a = 1$.

doi:10.6342/NTU202502508

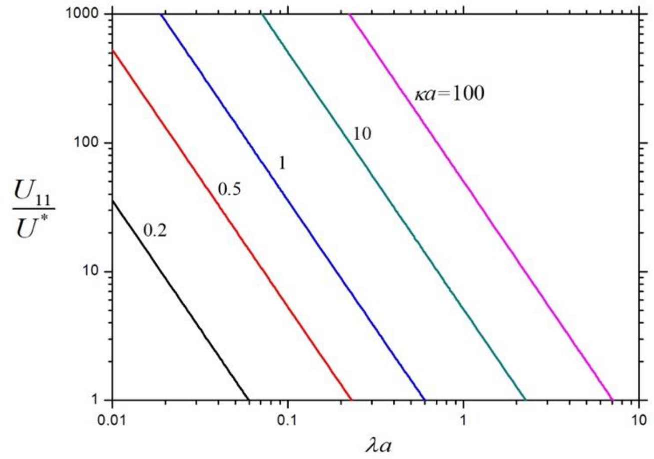

(a)

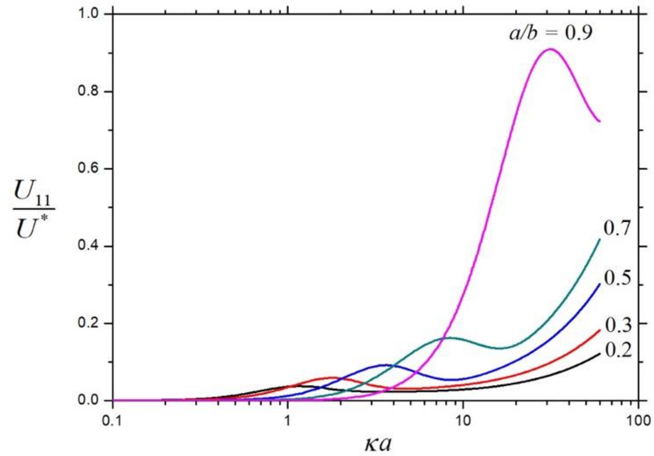

(b)

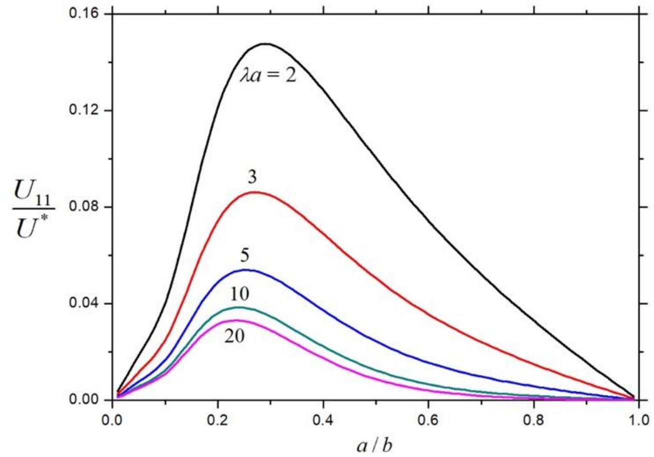

(c)

Figure 6. Normalized velocity U_{11}/U^* for a charged porous sphere ($r_0 = 0$) in a charged spherical cavity: (**a**) $a/b = 0.5$; (**b**) $\lambda a = 10$; and (**c**) $\kappa a = 1$.

doi:10.6342/NTU202502508

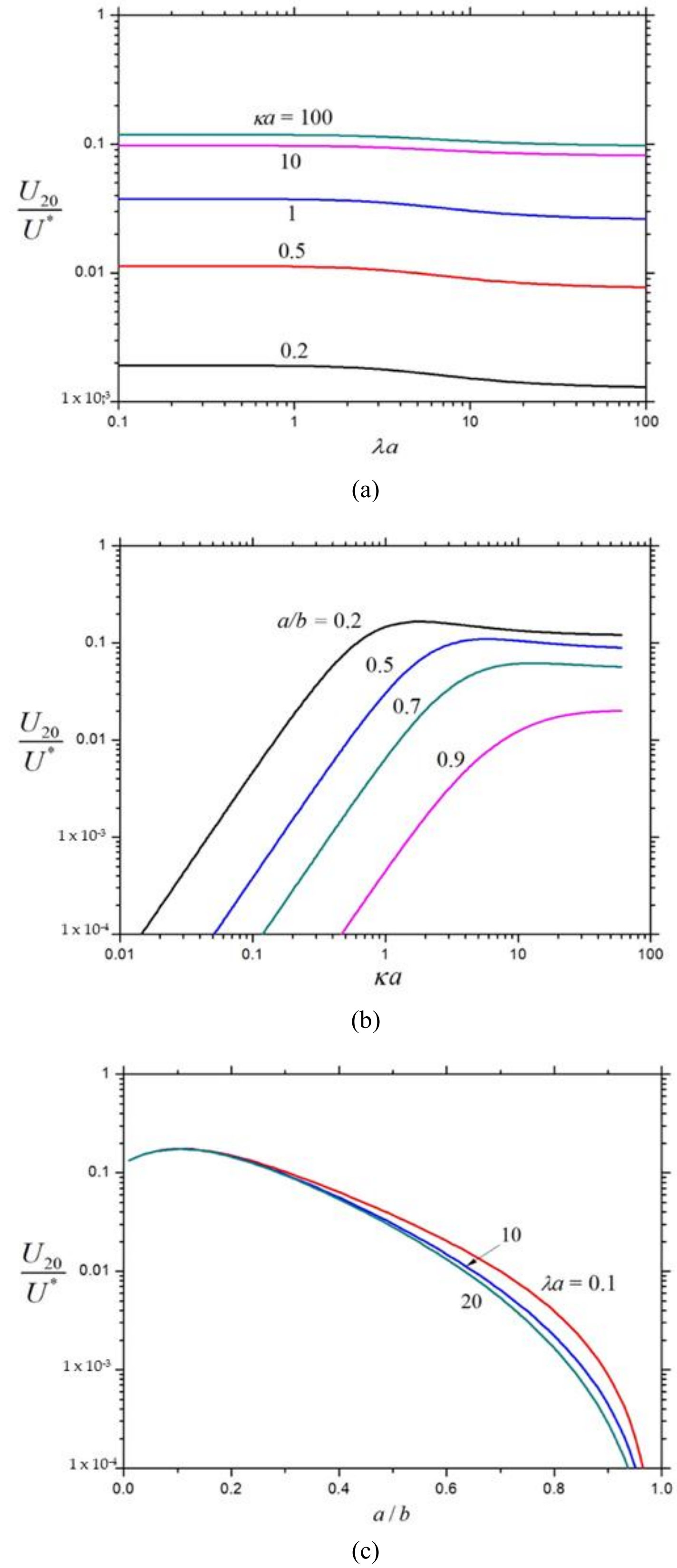

Figure 7. Normalized velocity U_{20} / U^* for a porous sphere ($r_0 = 0$) in a charged spherical cavity with chemiosmosis: (**a**) $a / b = 0.5$; (**b**) $\lambda a = 10$; and (**c**) $\kappa a = 1$.

doi:10.6342/NTU202502508

The normalized net second-order velocity $U_2/\overline{Q}^2U^*$ (with $U_2 = U_{02}\overline{Q}^2 + U_{11}\overline{Q}\overline{\sigma} + U_{20}\overline{\sigma}^2$) of a charged porous particle inside a charged cavity is plotted versus the fixed charge density ratio $\overline{\sigma}/\overline{Q}$ in Figure 8 (in parabolic curves that concave upward) for various values of the parameters a/b, λa, and κa. For the given values of a/b, λa, and κa, this velocity may reverse its direction twice as $\overline{\sigma}/\overline{Q}$ changes, due to the combined effects of chemiphoresis and wall-induced chemiosmosis. If the magnitude of $\overline{\sigma}/\overline{Q}$ is large, the cavity wall effect on the motion of the porous sphere is substantial. The magnitude of $U_2/\overline{Q}^2U^*$ generally diminishes when λa and a/b increase, but increases with an increasing κa. Figure 8 shows the normalized chemiphoretic velocity $U_2/\overline{Q}^2U^*$ for various values of the parameters a/b, λa, and κa, as well as the fixed charge densities $\overline{Q}$ and $\overline{\sigma}$.

doi:10.6342/NTU202502508

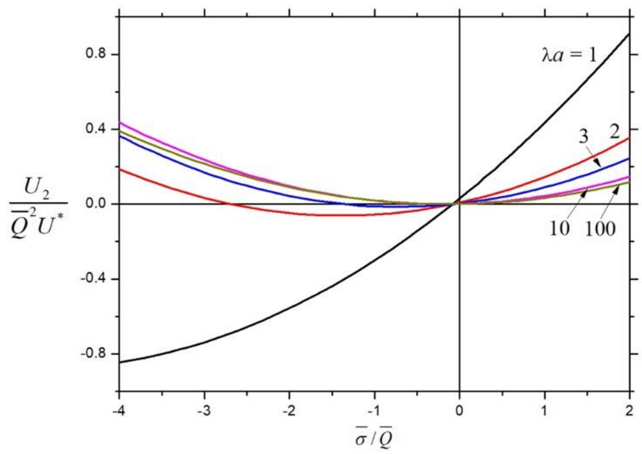

(a)

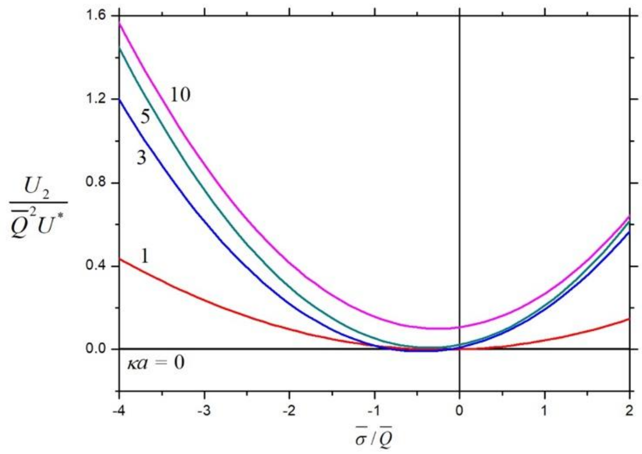

(b)

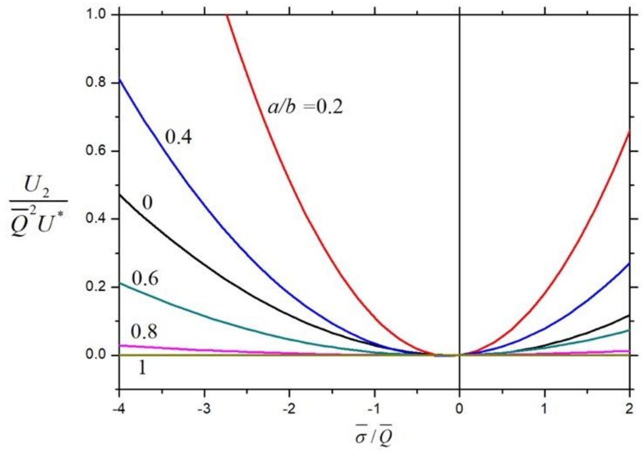

(c)

Figure 8. Normalized velocity $U_2/\overline{Q}^2U^*$ for the chemiphoresis of a charged porous sphere ($r_0 = 0$) in a charged spherical cavity versus the fixed charge density ratio $\overline{\sigma}/\overline{Q}$: **(a)** $a/b = 0.5$ and $\kappa a = 1$; **(b)** $\lambda a = 10$ and $a/b = 0.5$; and **(c)** $\kappa a = 1$ and $\lambda a = 10$.

doi:10.6342/NTU202502508

4.1.3 Diffusiophoretic velocity

For the diffusiophoresis of a porous particle in a symmetric electrolyte whose cation and anion have different diffusivities ($\beta = -0.2$, like the aqueous solution of NaCl), the plots of U/U^* against $\overline{\sigma}$ with $\overline{Q} = 1$ and the different values of a/b, λa, and κa are given in Figure 9 (a combination of Figures 4 and 8), where the contributions from electrophoresis and chemiphoresis, as well as from wall-induced electroosmosis and chemiosmosis, are included. Furthermore, for the fixed values of a/b, λa, and κa, the cavity wall effect is significant as the magnitude of $\overline{\sigma}/\overline{Q}$ is large, and the particle velocity may reverse twice in its direction when $\overline{\sigma}/\overline{Q}$ changes.

doi:10.6342/NTU202502508

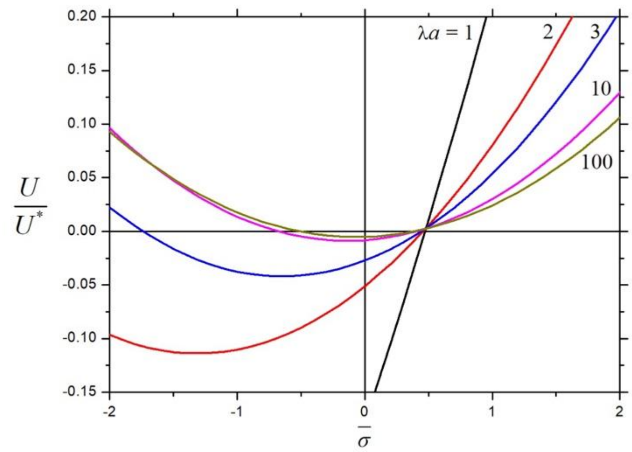

(a)

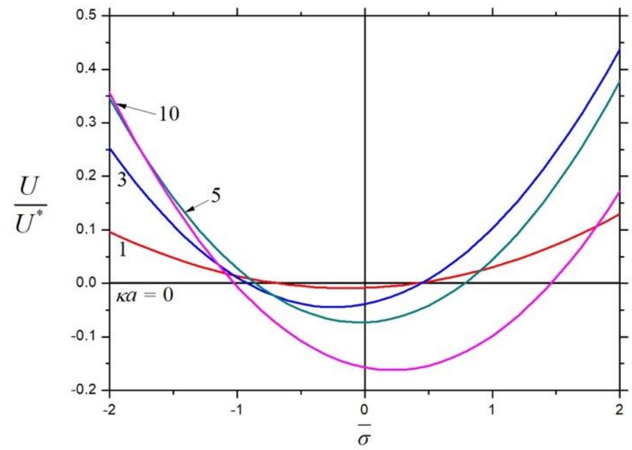

(b)

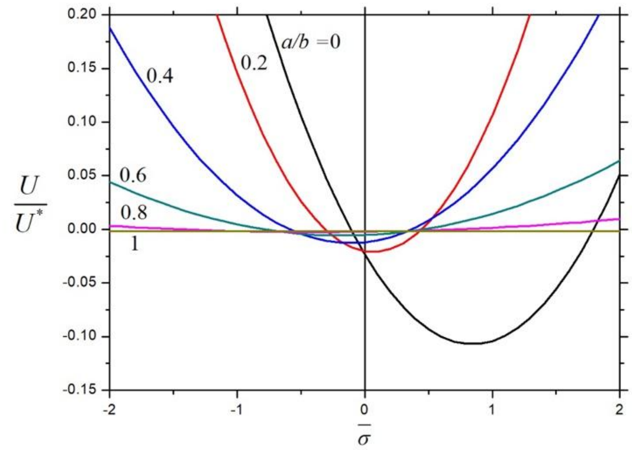

(c)

Figure 9. Normalized velocity U/U^* for the diffusiophoresis of a charged porous sphere ($r_0 = 0$) in a charged spherical cavity with $\beta = -0.2$ and $\overline{Q} = 1$ versus the charge density $\overline{\sigma}$: (**a**) $a/b = 0.5$ and $\kappa a = 1$; (**b**) $\lambda a = 10$ and $a/b = 0.5$; and (**c**) $\kappa a = 1$ and $\lambda a = 10$.

doi:10.6342/NTU202502508

4.2 Soft particle velocities

Having understood the effect of a concentric charged cavity on the diffusiophoretic velocity of a charged porous particle, we can examine the general case of a diffusiophoretic soft particle.

4.2.1 First-order electrophoretic velocities

The normalized first-order velocities $U_{01}/\beta U^*$ and $U_{10}/\beta U^*$ for a soft spherical particle within a concentric charged cavity as calculated from Equations (30) and (31) are plotted versus the core-to-particle radius ratio r_0/a for different values of the hydrodynamic resistance parameter λa, the particle-to-cavity radius ratio a/b, and the electrokinetic particle radius κa in Figures 10 and 11, respectively. Likewise, these normalized velocities are always positive; the sign of the product βQ determines the direction of the electrophoresis; and the sign of $\beta\sigma$ determines the direction of the wall-induced electroosmotic effect on the particle.

Both $U_{01}/\beta U^*$ and $U_{10}/\beta U^*$ are monotonically increasing functions of κa from zero at $\kappa a = 0$, monotonically decreasing functions of λa, and monotonically decreasing functions of a/b to zero at $a/b = 1$, keeping the other parameters unchanged. For the specified values of λa, κa, and a/b, the normalized electrophoretic velocity $U_{01}/\beta U^*$ monotonically decreases with a rise in the radius ratio r_0/a, as expected, from the value for a charged porous sphere at $r_0/a = 0$ to zero for an uncharged rigid (impermeable) sphere at $r_0/a = 1$. On the other hand, the normalized velocity $U_{10}/\beta U^*$ of the soft particle caused by the electroosmotic effect

doi:10.6342/NTU202502508

of the charged cavity wall for the given values of a/b, λa, and κa is generally not a monotonic function of r_0/a and has a maximum at a relatively large value of r_0/a.

doi:10.6342/NTU202502508

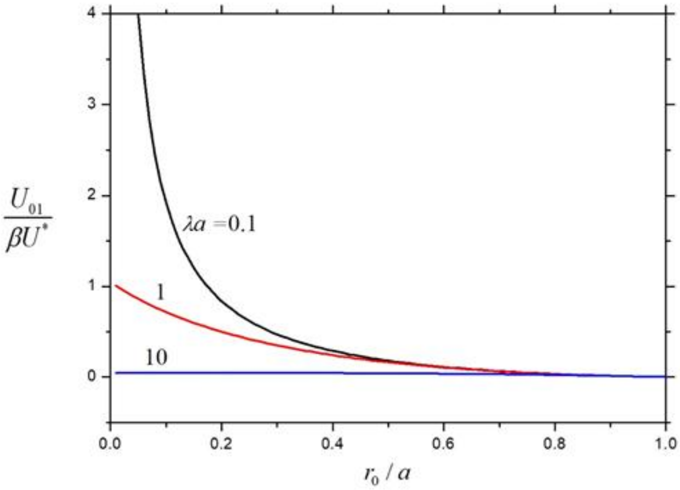

(a)

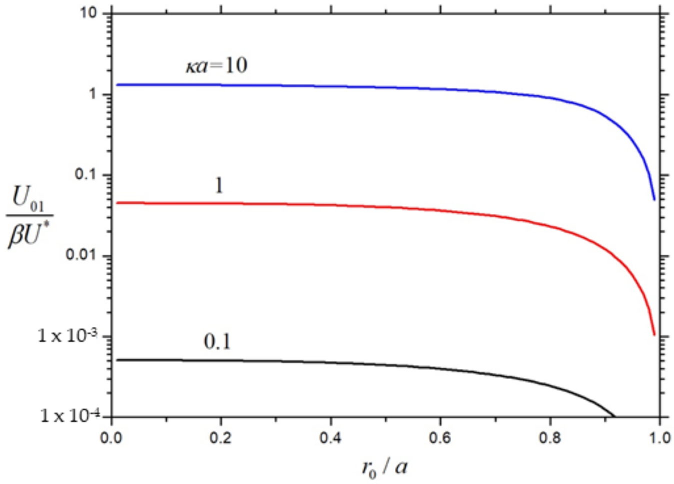

(b)

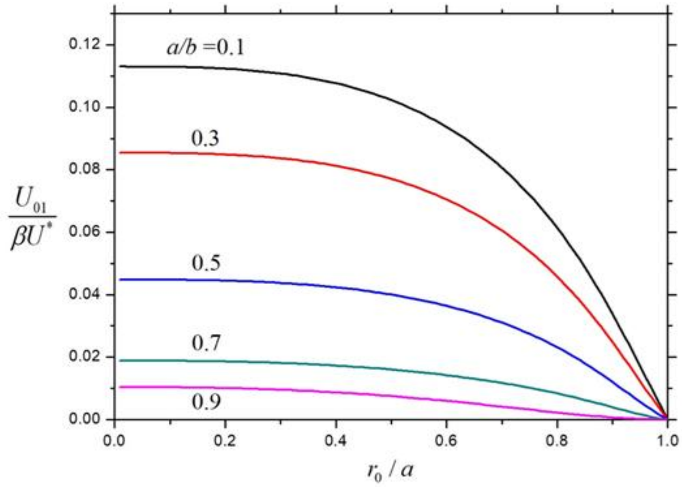

(c)

Figure 10. Normalized velocity $U_{01} / \beta U^*$ for the electrophoresis of a charged soft sphere in a spherical cavity versus r_0 / a: (**a**) $a/b = 0.5$ and $\kappa a = 1$; (**b**) $\lambda a = 10$ and $a/b = 0.5$; and (**c**) $\kappa a = 1$ and $\lambda a = 10$.

doi:10.6342/NTU202502508

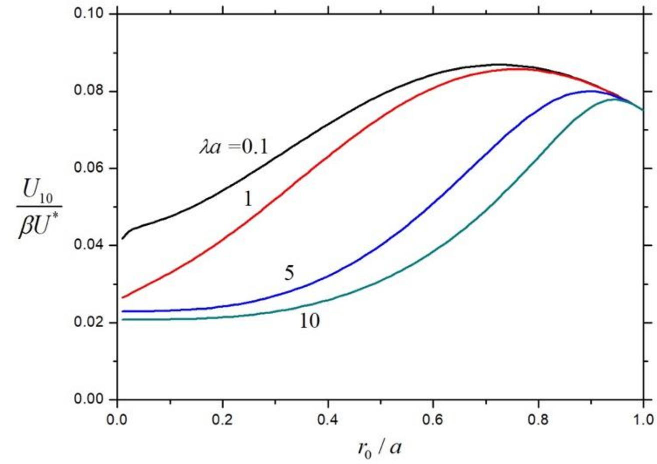

(a)

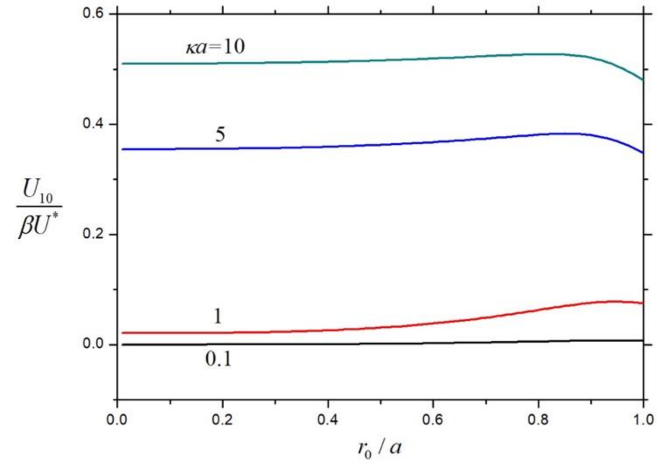

(b)

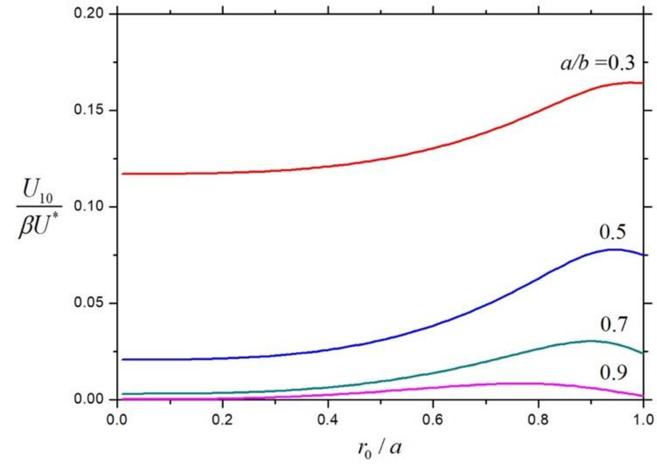

(c)

Figure 11. Normalized velocity $U_{10} / \beta U^*$ for a soft sphere in a charged spherical cavity with electroosmosis versus r_0 / a : (**a**) $a/b = 0.5$ and $\kappa a = 1$; (**b**) $\lambda a = 10$ and $a/b = 0.5$; and (**c**) $\kappa a = 1$ and $\lambda a = 10$.

doi:10.6342/NTU202502508

In Figure 12, the normalized net first-order velocity $U_1/\overline{Q}\beta U^*$ (with $U_1 = U_{01}\overline{Q} + U_{10}\overline{\sigma}$) of a charged soft particle inside a charged cavity is plotted versus the fixed charge density ratio $\overline{\sigma}/\overline{Q}$ for the different values of r_0/a. Again, the electroosmotic effect of the cavity wall enhances/reduces this particle velocity if the fixed charge densities $\overline{Q}$ and $\overline{\sigma}$ are in the same/opposite signs. When the value of $\overline{\sigma}/\overline{Q}$ is negative and the magnitude is great, the velocity direction of the particle may be opposite to the direction of the electrophoresis in an unbounded fluid. The value of $U_1/\overline{Q}\beta U^*$ decreases with an increase in r_0/a, mainly due to the effect of r_0/a on the electrophoretic velocity $U_{01}/\beta U^*$.

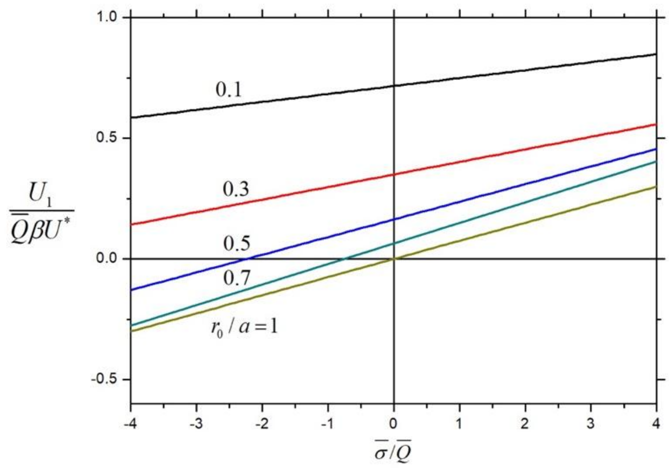

Figure 12. Normalized velocity $U_1/\overline{Q}\beta U^*$ for the electrophoresis of a charged soft sphere in a charged spherical cavity with $\kappa a = 1$, $\lambda a = 10$, and $a/b = 0.5$ versus the fixed charge density ratio $\overline{\sigma}/\overline{Q}$.

doi:10.6342/NTU202502508

4.2.2 Second-order chemiphoretic velocities

The normalized second-order velocities U_{02}/U^*, U_{11}/U^*, and U_{20}/U^* of a charged soft sphere inside a charged cavity caused by the chemiphoretic and wall-induced chemiosmotic effects as calculated from Equations (32)-(34) are plotted versus the core-to-particle radius ratio r_0/a in Figures 13, 14, and 15, respectively, for the different values of a/b, λa, and κa. Likewise, all these velocities are monotonically decreasing functions of λa that generally increase with an increasing κa, but none of them depends monotonically on a/b (local extrema appear at moderate values of a/b), keeping the other parameters unchanged.

For the specified values of a/b, λa, and κa, the normalized velocities U_{02}/U^* and U_{11}/U^* generally decreases with a rise in the radius ratio r_0/a from their values for a charged porous sphere at $r_0/a=0$ to zero for an uncharged rigid sphere at $r_0/a=1$. However, the normalized velocity U_{20}/U^* of the soft particle caused by the chemiosmotic effect of the charged cavity wall for the given values of a/b, λa, and κa is generally not a monotonic function of r_0/a.

doi:10.6342/NTU202502508

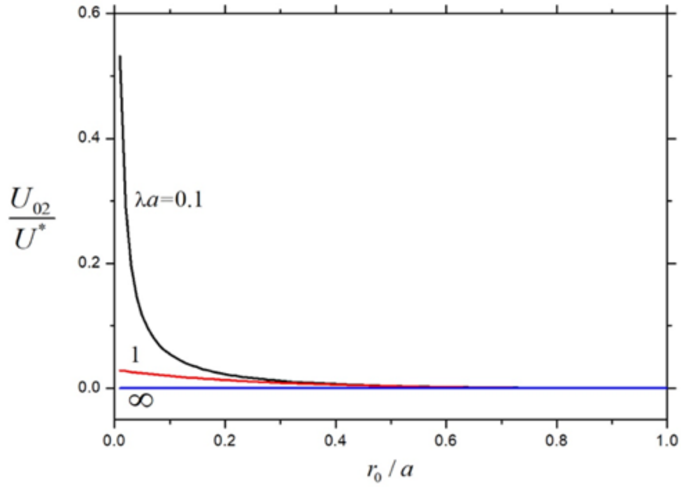

(a)

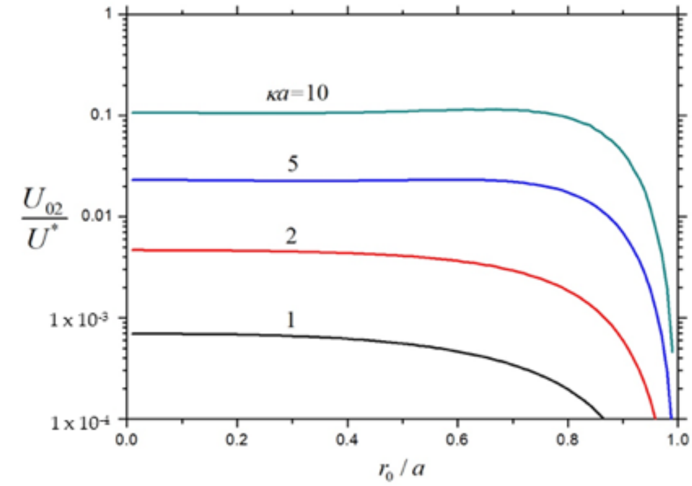

(b)

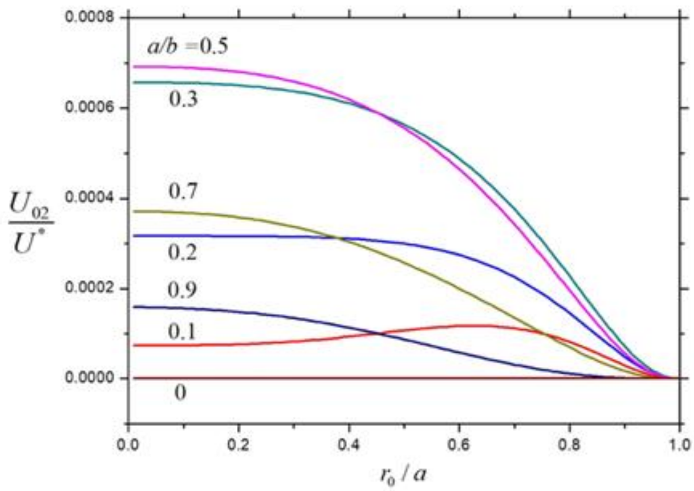

(c)

Figure 13. Normalized velocity U_{02}/U^* for the chemiphoresis of a charged soft sphere in a spherical cavity versus r_0/a: (**a**) $a/b = 0.5$ and $\kappa a = 1$; (**b**) $\lambda a = 10$ and $a/b = 0.5$; and (**c**) $\kappa a = 1$ and $\lambda a = 10$.

doi:10.6342/NTU202502508

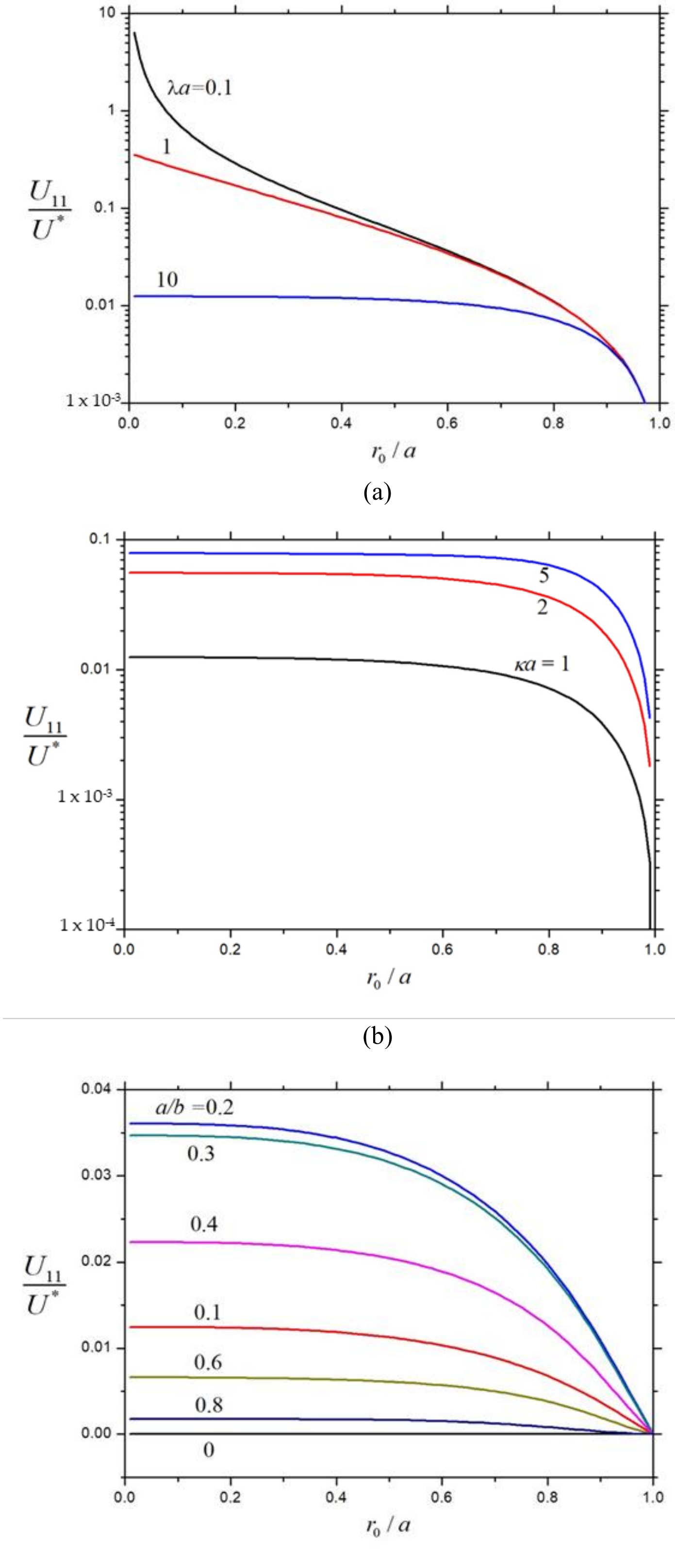

Figure 14. Normalized velocity U_{11}/U^* for a charged soft sphere in a charged spherical cavity versus r_0/a: (**a**) $a/b = 0.5$ and $\kappa a = 1$; (**b**) $\lambda a = 10$ and $a/b = 0.5$; and (**c**) $\kappa a = 1$ and $\lambda a = 10$.

doi:10.6342/NTU202502508

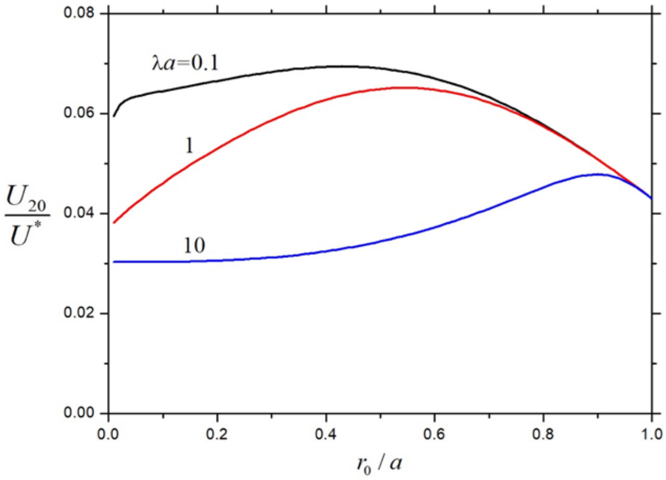

(a)

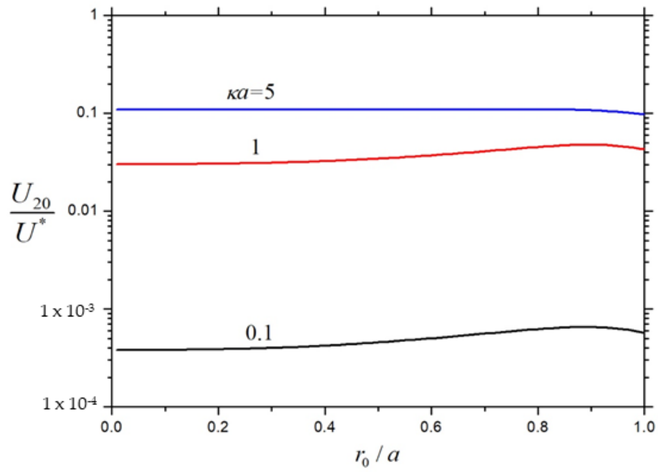

(b)

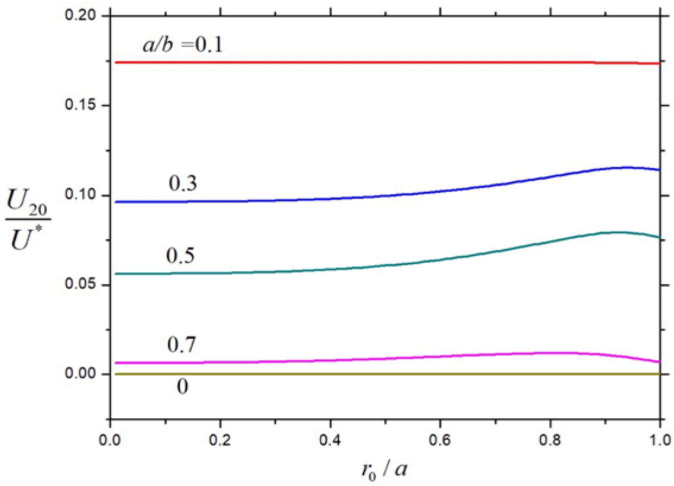

(c)

Figure 15. Normalized velocity U_{20} / U^* for a soft sphere in a charged spherical cavity with chemiosmosis versus r_0 / a : (**a**) $a / b = 0.5$ and $\kappa a = 1$; (**b**) $\lambda a = 10$ and $a / b = 0.5$; and (**c**) $\kappa a = 1$ and $\lambda a = 10$.

doi:10.6342/NTU202502508

In Figure 16, the normalized net second-order velocity $U_2/\overline{Q}^2U^*$ (with $U_2 = U_{02}\overline{Q}^2 + U_{11}\overline{Q}\overline{\sigma} + U_{20}\overline{\sigma}^2$) of a charged soft particle inside a charged cavity is plotted versus the fixed charge density ratio $\overline{\sigma}/\overline{Q}$ for the various values of r_0/a. Furthermore, for the given values of a/b, λa, and κa, this velocity may reverse its direction twice as $\overline{\sigma}/\overline{Q}$ changes, due to the combined effects of chemiphoresis and wall-induced chemiosmosis. In general, the value of $U_2/\overline{Q}^2U^*$ decreases with an increasing r_0/a if $\overline{\sigma}/\overline{Q}$ is positive, but it is not a monotonic function of r_0/a if $\overline{\sigma}/\overline{Q}$ is negative.

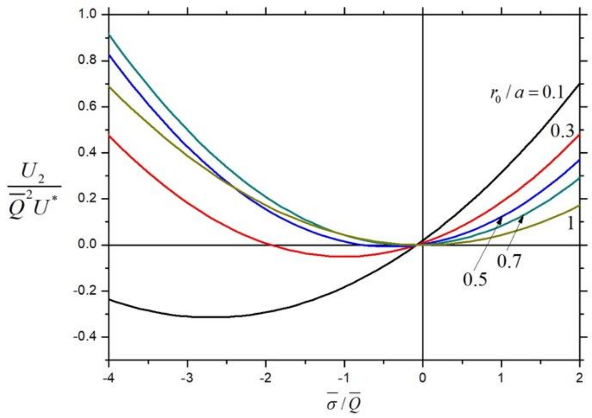

Figure 16. Normalized velocity $U_2/\overline{Q}^2U^*$ for the chemiphoresis of a charged soft sphere in a charged spherical cavity with $\kappa a = 1$, $\lambda a = 10$, and $a/b = 0.5$ versus the fixed charge density ratio $\overline{\sigma}/\overline{Q}$.

doi:10.6342/NTU202502508

4.2.3 Diffusiophoretic velocity

For the diffusiophoresis of a soft particle in a symmetric electrolyte as mentioned previously ($\beta = -0.2$), the plots of U/U^* against $\bar{\sigma}$ with $\bar{Q} = 1$ and the different values of r_0/a is given in Figure 17 (a combination of Figures 12 and 16), where the contributions from electrophoresis and chemiphoresis, as well as from wall-induced electroosmosis and chemiosmosis, are all included. For the fixed values of $\bar{Q}$, r_0/a, a/b, λa, and κa, the cavity wall effect can be significant as the magnitude of $\bar{\sigma}$ is large, and the particle velocity may reverse twice in its direction when $\bar{\sigma}$ changes.

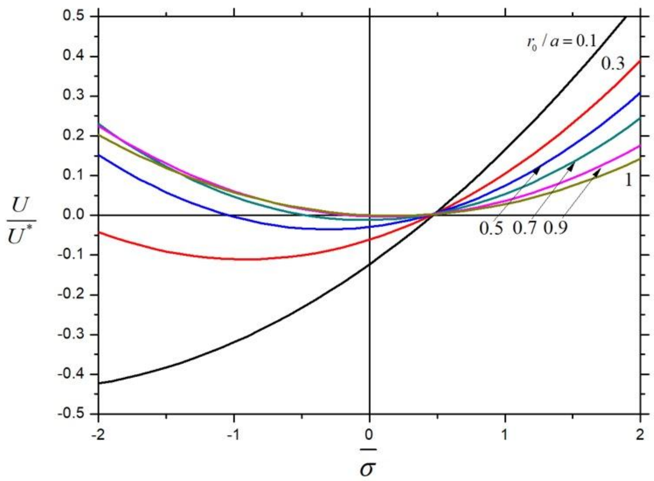

Figure 17. Normalized velocity U/U^* for the diffusiophoresis of a charged soft sphere in a charged spherical cavity with $\beta = -0.2$, $\kappa a = 1$, $\lambda a = 10$, $a/b = 0.5$ and $\bar{Q} = 1$ versus the charge density $\bar{\sigma}$

doi:10.6342/NTU202502508

Chapter 5
Conclusions

In this thesis, the quasi-steady diffusiophoresis of a charged soft spherical particle at the center of a charged spherical cavity under an applied concentration gradient of a symmetric electrolyte is analyzed for the arbitrary values of the core-to-particle radius ratio r_0 / a, the particle-to-cavity radius ratio a/b, the ratio of the particle radius to the permeation length in the porous surface layer λa, and the ratio of the particle radius to the Debye length κa. By using a regular perturbation method with small dimensionless fixed charge densities $\overline{Q}$ and $\overline{\sigma}$ of the porous surface layer and cavity wall, respectively, the linearized electrokinetic differential equations relevant to the fluid velocity field, electric potential profile, and ionic concentration distributions are solved. The balance of the electrostatic and hydrodynamic forces acting on the soft sphere results in an explicit formula, Equation (20) with Equations (30)–(35), for the diffusiophoretic velocity of the particle in terms of r_0 / a, a/b, λa, and κa up to the second orders of $\overline{Q}$ and $\overline{\sigma}$.

The diffusioosmotic flow at the cavity wall can substantially change the particle velocity and even reverse its direction. The normalized electrophoretic and chemiphoretic velocity components $U_{01} / \beta U^*$ and U_{02} / U^* (and also U_{11} / U^*) depend strongly on λa, while the normalized electroosmosis-induced and chemiosmosis-induced velocity components $U_{10} / \beta U^*$ and U_{20} / U^* are weak functions of λa. The diffusiophoretic velocity generally decreases when r_0 / a, a/b, and λa increase, but increases with an increasing κa. The contributions to the

doi:10.6342/NTU202502508

particle velocity from the diffusioosmotic flow taking place along the charged cavity wall and from the wall-corrected diffusiophoretic force are equivalently important, and this diffusioosmotic flow can reverse the direction of the particle velocity.

doi:10.6342/NTU202502508

List of Symbols

a	the radius of the soft particle, [m]
A	non-dimensional coefficient defined in Eq. (17)
b	the radius of the cavity, [m]
B	non-dimensional coefficient defined in Eq. (19)
$C_{002}, C_{012}, C_{102}$ $C_{022}, C_{112}, C_{202}$	dimensionless coefficients defined in Eqs. (A1) to (A8)
D_{+}, D_{-}	the diffusivities of the cation and anion, $[\mathrm{m}^2 \cdot \mathrm{s}^{-1}]$
e	the elementary electric charge, [C]
$\mathbf{e}_r$	the unit vector in the r-direction
$\mathbf{e}_z$	the unit vector in the z-direction
$F_{00r}(r)$	the functions defined in Eqs. (A1) and (A2)
$F_{p00}(r)$	the functions defined in Eqs. (A3) amd (A4)
$F_{01r}(r), F_{10r}(r)$ $F_{02r}(r), F_{11r}(r), F_{20r}(r)$	the functions defined in Eqs. (A5) and (A6)
$F_{p01}(r), F_{p10}(r)$ $F_{p02}(r), F_{p11}(r), F_{p20}(r)$	the functions defined in Eqs. (A7) and (A8)
$F_{\mu 00}(r), F_{\psi 00}(r)$	the functions defined in Eq. (A20)
$F_{\mu 01}(r), F_{\mu 10}(r)$	the functions defined in Eqs. (A21) and (A22)
$F_{\psi 01}(r), F_{\psi 10}(r)$	the functions defined in Eq. (A23)

doi:10.6342/NTU202502508

$\mathbf{F}_{\mathrm{e}}$	the electric force acting on the charged soft particle, $[\mathrm{N}]$
$\mathbf{F}_{\mathrm{h}}$	the hydrodynamic drag force acting on the charged soft particle, $[\mathrm{N}]$
$h(r)$	unit step function
$\mathbf{I}$	unit dyadic tensor
k	Boltzmann's constant, $[\mathrm{J \cdot K^{-1}}]$
n_m	the concentration profiles of type-m ions, $[\mathrm{m^{-3}}]$
$n_m^{(\mathrm{eq})}$	the equilibrium concentrations of type-m ions, $[\mathrm{m^{-3}}]$
n_m^{∞}	the bulk concentrations of type-m ions, $[\mathrm{m^{-3}}]$
p	the pressure distribution, $[\mathrm{N \cdot m^{-2}}]$
$p^{(\mathrm{eq})}$	the equilibrium pressure distribution, $[\mathrm{N \cdot m^{-2}}]$
Q	the fixed charge density within porous layer, $[\mathrm{C \cdot m^{-3}}]$
$\overline{Q}$	non-dimensional fixed charge density within porous layer
(r, θ, ϕ)	spherical coordinates
r_0	the radius of the hard core, $[\mathrm{m}]$
T	the absolute temperature, $[\mathrm{K}]$
$\mathbf{v}$	the fluid velocity distribution, $[\mathrm{m \cdot s^{-1}}]$
v_r, v_θ	r and θ components, respectively, of $\mathbf{v}$, $[\mathrm{m \cdot s^{-1}}]$
U	the diffusiophoretic velocity of the soft particle, $[\mathrm{m \cdot s^{-1}}]$

doi:10.6342/NTU202502508

U_{01}, U_{10}, U_{02}, U_{11}, U_{20}	the velocities defined in Eqs. (30) to (34), $[\mathrm{m \cdot s^{-1}}]$
U^*	the characteristic particle velocity, $[\mathrm{m \cdot s^{-1}}]$
Z	the valence of the symmetric electrolyte

Greek letters

α	normalized electrolyte concentration gradient
β	defined by $(D_+ - D_-)/(D_+ + D_-)$
δn_m	the small deviation from the equilibrium concentration of type-m ions, $[\mathrm{m^{-3}}]$
$\delta\mu_m$	perturbed electrochemical potential energy, the linear combination of δn_m and $\delta\psi$, [J]
$\delta\psi$	the small deviation from the equilibrium electric potential distribution, [V]
δp	the small deviation from the equilibrium pressure, $[\mathrm{N \cdot m^{-2}}]$
ε	the permittivity of the fluid, $[\mathrm{C^2 \cdot J^{-1} \cdot m^{-1}}]$
η	the viscosity of the fluid, $[\mathrm{kg \cdot m^{-1} \cdot s^{-1}}]$
κ	reciprocal of the Debye screening length, $[\mathrm{m^{-1}}]$
λ	reciprocal of the characteristic length of flow penetration inside the porous layer, $[\mathrm{m^{-1}}]$

doi:10.6342/NTU202502508

σ	the fixed charge density on the spherical cavity, $[\mathrm{C{\cdot}m^{-2}}]$
$\bar{\sigma}$	non-dimensional fixed charge density of on the cavity
ψ	the electric potential distribution, [V]
$\psi^{(eq)}$	the equilibrium electric potential distribution, [V]
ψ_{eq01}, ψ_{eq10},	the functions defined in Eqs. (14) to (16), [V]
ζ	zeta potential on the spherical cavity, [V]

Superscripts

(eq)	equilibrium state
∞	in the bulk solution
*	characteristic value

Subscripts

+	the cation
−	the anion
m	the type- m ions

doi:10.6342/NTU202502508

References

1. Dukhin, S.S.; Derjaguin, B.V. In *Surface and Colloid Science*; Matijevic, E., Ed.; Wiley: New York, NY, USA, 1974; Volume 7.
2. Prieve, D.C.; Anderson, J.L.; Ebel, J.P.; Lowell, M.E. Motion of a particle generated by chemical gradients. Part 2. Electrolytes. *J. Fluid Mech*. **1984**, *148*, 247–269.
3. Pawar, Y.; Solomentsev, Y.E.; Anderson, J.L. Polarization effects on diffusiophoresis in electrolyte gradients. *J. Colloid Interface Sci.* **1993**, *155*, 488–498.
4. Khair, A.S. Diffusiophoresis of colloidal particles in neutral solute gradients at finite Péclet number. *J. Fluid Mech.* **2013**, *731*, 64–94.
5. Keh, H.J. Diffusiophoresis of charged particles and diffusioosmosis of electrolyte solutions. *Curr. Opin. Colloid Interface Sci.* **2016**, *24*, 13–22.
6. Prieve, D.C.; Malone, S.M.; Khair, A.S.; Stout, R.F.; Kanj, M.Y. Diffusiophoresis of charged colloidal particles in the limit of very high salinity. *Proc. Natl. Acad. Sci. USA* **2019**, *116*, 18257–18262.
7. Shin, S. Diffusiophoretic separation of colloids in microfluidic flows. *Phys. Fluids* **2020**, *32*, 101302.
8. Lee, S.; Lee, J.; Ault, J.T. The role of variable zeta potential on diffusiophoretic and diffusioosmotic transport. *Colloids Surf. A* **2023**, *659*, 130775.
9. Smith, R.E.; Prieve, D.C. Accelerated deposition of latex particles onto a rapidly dissolving steel surface. *Chem. Eng. Sci.* **1982**, *37*, 1213–1223.
10. Anderson, J.L. Colloid transport by interfacial forces. *Annu. Rev. Fluid Mech.* **1989**, *21*, 61–99.

doi:10.6342/NTU202502508

11. Abecassis, B.; Cottin-Bizonne, C.; Ybert, C.; Ajdari, A.; Bocquet, L. Osmotic manipulation of particles for microfluidic applications. *New J. Phys.* **2009**, *11*, 075022.

12. Wanunu, M.; Morrison, W.; Rabin, Y.; Grosberg, A.Y.; Meller, A. Electrostatic focusing of unlabeled DNA into nanoscale pores using a salt gradient. *Nat. Nanotechnol.* **2010**, *5*, 160–165.

13. Hatlo, M.M.; Panja, D.; van Roij, R. Translocation of DNA molecules through nanopores with salt gradients: The role of osmotic flow. *Phys. Rev. Lett.* **2011**, *107*, 68101.

14. Velegol, D.; Garg, A.; Guha, R.; Kar, A.; Kumar, M. Origins of concentration gradients for diffusiophoresis. *Soft Matter* **2016**, *12*, 4686–4703.

15. Shen, T.Z.; Hong, S.H.; Song, J.K. Electro-optical switching of graphene-oxide liquid crystals with an extremely large Kerr coefficient. *Nat. Mater.* **2014**, *13*, 394–399.

16. Shen, T.Z.; Perera, K.N.A.; Masud, A.R.; Priyadharshana, P.A.N.S.; Park, J.-Y.; Wang, Q.-H.; Hong, S.H.; Song, J.K. A dual-frequency photonic crystal nanocolloid with hue- and brightness-tunable structural colors. *Cell Rep. Phys. Sci.* **2023**, *4*, 101343.

17. Sen, A.; Ibele, M.; Hong, Y.; Velegol, D. Chemo and phototactic nano/microbots. *Faraday Discuss.* **2009**, *143*, 15–27.

18. Brown, A.; Poon, W. Ionic effects in self-propelled Pt-coated Janus swimmers. *Soft Matter.* **2014**, *10*, 4016–4027.

19. Oshanin, G.; Popescu, M.N.; Dietrich, S. Active colloids in the context of chemical kinetics. *J. Phys. A Math. Theor.* **2017**, *50*, 134001.

doi:10.6342/NTU202502508

20. Staffeld, P.O.; Quinn, J.A. Diffusion-induced banding of colloid particles via diffusiophoresis 2. Non-electrolytes. *J. Colloid Interface Sci.* **1989**, *130*, 88–100.
21. Bohinc, K.; Bossa, G.V.; May, S. Incorporation of ion and solvent structure into mean-field modeling of the electric double layer. *Adv. Colloid Interface Sci.* **2017**, *249*, 220–233.
22. Prieve, D.C.; Roman, R. Diffusiophoresis of a rigid sphere through a viscous electrolyte solution. *J. Chem. Soc. Faraday Trans. 2* **1987**, *83*, 1287–1306.
23. Keh, H.J.; Wei, Y.K. Diffusiophoretic mobility of spherical particles at low potential and arbitrary double-layer thickness. *Langmuir* **2000**, *16*, 5289–5294.
24. Wei, Y.K.; Keh, H.J. Diffusiophoretic mobility of charged porous spheres in electrolyte gradients. *J. Colloid Interface Sci.* **2004**, *269*, 240–250.
25. Huang, P.Y.; Keh, H.J. Diffusiophoresis of a spherical soft particle in electrolyte gradients. *J. Phys. Chem. B* **2012**, *116*, 7575–7589.
26. Ohshima, H. Diffusiophoretic velocity of a spherical soft particle. *Colloid Polym. Sci.* **2022**, *300*, 153–157.
27. Ohshima, H. Diffusiophoresis of a soft particle as a model for biological cells. *Colloids Interfaces* **2022**, *6*, 24.
28. Akdeniz, B.; Wood, J.A.; Lammertink, R.G.H. Diffusiophoretic behavior of polyelectrolyte-coated particles. *Langmuir* **2024**, *40*, 5934−5944.
29. Joo, S.W.; Lee, S.Y.; Liu, J.; Qian, S. Diffusiophoresis of an elongated cylindrical nanoparticle along the axis of a nanopore. *ChemPhysChem* **2010**, *11*, 3281–3290.
30. Chang, Y.C.; Keh, H.J. Diffusiophoresis and electrophoresis of a charged sphere perpendicular to one or two plane walls. *J. Colloid Interface Sci.* **2008**, *322*, 634–653.

doi:10.6342/NTU202502508

31. Lee, S.Y.; Yalcin, S.E.; Joo, S.W.; Sharma, A.; Baysal, O.; Qian, S. The effect of axial concentration gradient on electrophoretic motion of a charged spherical particle in a nanopore. *Microgravity Sci. Technol.* **2010**, *22*, 329–338.

32. Chiu, H.C.; Keh, H.J. Diffusiophoresis of a charged particle in a microtube. *Electrophoresis* **2017**, *38*, 2468–2478.

33. Kar, A.; Chiang, T.-S.; Rivera, I.O.; Sen, A.; Velegol, D. Enhanced transport into and out of dead-end pores. *ACS Nano* **2015**, *9*, 746–753.

34. Shin, S.; Um, E.; Sabass, B.; Ault, J.T.; Rahimi, M.; Warren, P.B.; Stone, H.A. Size-dependent control of colloid transport via solute gradients in dead-end channels. *Proc. Natl. Acad. Sci. USA* **2016**, *113*, 257–261.

35. Chiu, Y.C.; Keh, H.J. Diffusiophoresis of a charged particle in a charged cavity with arbitrary electric-double-layer thickness. *Microfluid. Nanofluid.* **2018**, *22*, 84.

36. Chiu, Y.C.; Keh, H.J. Diffusiophoresis of a charged porous particle in a charged cavity. *J. Phys. Chem. B* **2018**, *122*, 9803–9814.

37. Chang, X.; Hsu, W.-L.; Hsu, J.-P.; Tseng, S. Diffusiophoresis of a soft spherical particle in a spherical cavity. *J. Phys. Chem. B* **2009**, *113*, 8646–8656.

38. Chen, W.J.; Keh, H.J. Electrophoresis of a charged soft particle in a charged cavity with arbitrary double-layer thickness. *J. Phys. Chem. B* **2013**, *117*, 9757–9767.

doi:10.6342/NTU202502508

Appendix A
Functions in Equations (21)-(25) and Coefficients in Equation (29)

In Equations (23)-(25),

$$F_{00r}(r)=C_{001}+C_{002}\frac{a}{r}+C_{003}(\frac{a}{r})^3+C_{004}(\frac{r}{a})^2 \quad \text{if } a<r<b, \tag{A1}$$

$$F_{00r}(r)=C_{005}+(\frac{a}{r})^3[C_{006}+C_{007}\alpha_1(\lambda r)+C_{008}\beta_1(\lambda r)] \quad \text{if } r_0<r<a \tag{A2}$$

$$F_{p00}(r)=C_{002}(\frac{a}{r})^2+10C_{004}\frac{r}{a} \quad \text{if } a<r<b, \tag{A3}$$

$$F_{p00}(r)=(\lambda a)^2[\frac{1}{2}C_{006}(\frac{a}{r})^2-C_{005}\frac{r}{a}] \quad \text{if } r_0<r<a, \tag{A4}$$

$$\begin{aligned}F_{ijr}(r)=&C_{ij1}+\frac{1}{3}J_{ij}^{(2)}(r)+[C_{ij2}-\frac{1}{3}J_{ij}^{(3)}(r)]\frac{a}{r}\\ &+[C_{ij3}+\frac{1}{15}J_{ij}^{(5)}(r)](\frac{a}{r})^3+[C_{ij4}-\frac{1}{15}J_{ij}^{(0)}(r)](\frac{r}{a})^2 \quad \text{if } a<r<b,\end{aligned} \tag{A5}$$

$$\begin{aligned}F_{ijr}(r)=&C_{ij5}+[C_{ij6}+C_{ij7}\alpha_1(\lambda r)+C_{ij8}\beta_1(\lambda r)](\frac{a}{r})^3+\frac{2}{3(\lambda a)^2}[J_{ij}^{(0)}(r)-(\frac{a}{r})^3J_{ij}^{(3)}(r)]\\ &+2(\lambda a)^{-5}[\alpha_1(\lambda r)J_{ij}^{(\beta)}(r)-\beta_1(\lambda r)J_{ij}^{(\alpha)}(r)](\frac{a}{r})^3 \quad \text{if } r_0<r<a,\end{aligned} \tag{A6}$$

$$F_{pij}(r)=[C_{ij2}-\frac{1}{3}J_{ij}^{(3)}(r)](\frac{a}{r})^2+2[5C_{ij4}-\frac{1}{3}J_{ij}^{(0)}(r)]\frac{r}{a} \quad \text{if } a<r<b, \tag{A7}$$

$$F_{pij}(r)=-\frac{2}{3}J_{ij}^{(0)}(r)\frac{r}{a}-\frac{1}{3}J_{ij}^{(3)}(r)(\frac{a}{r})^2+(\lambda a)^2[-C_{ij5}\frac{r}{a}+\frac{1}{2}C_{ij6}(\frac{a}{r})^2] \quad \text{if } r_0<r<a, \tag{A8}$$

where $(i,j)=(0,1)$, $(1,0)$ (for the first-order fluid velocity field), $(0,2)$, $(1,1)$, and $(2,0)$ (for the second-order fluid velocity field), the dimensionless coefficients $C_{001}\sim C_{008}$ and $C_{ij1}\sim C_{ij8}$ are given by Eqations (A34)–(A52),

doi:10.6342/NTU202502508

$$\alpha_1(x) = x\cosh(x) - \sinh(x), \tag{A9}$$

$$\beta_1(x) = x\sinh(x) - \cosh(x), \tag{A10}$$

$$J_{ij}^{(n)}(r) = \int_a^r \left(\frac{r}{a}\right)^n G_{ij}(r)\mathrm{d}r, \tag{A11}$$

$$J_{ij}^{(\alpha)}(r) = \int_a^r \alpha_1(\lambda r) G_{ij}(r)\mathrm{d}r, \tag{A12}$$

$$J_{ij}^{(\beta)}(r) = \int_a^r \beta_1(\lambda r) G_{ij}(r)\mathrm{d}r, \tag{A13}$$

$$G_{01}(r) = \frac{\varepsilon\kappa^2 a^4}{Zer} F_{\mu 00}(r)\frac{\mathrm{d}\psi_{\mathrm{eq}01}}{\mathrm{d}r}, \tag{A14}$$

$$G_{10}(r) = \frac{\varepsilon\kappa^2 a^4}{Zer} F_{\mu 00}(r)\frac{\mathrm{d}\psi_{\mathrm{eq}10}}{\mathrm{d}r}, \tag{A15}$$

$$G_{02}(r) = -\frac{\varepsilon\kappa^2 a^4}{Zer} W_{01}(r)\frac{\mathrm{d}\psi_{\mathrm{eq}01}}{\mathrm{d}r}, \tag{A16}$$

$$G_{11}(r) = -\frac{\varepsilon\kappa^2 a^4}{Zer}\left[W_{01}(r)\frac{\mathrm{d}\psi_{\mathrm{eq}10}}{\mathrm{d}r} + W_{10}(r)\frac{\mathrm{d}\psi_{\mathrm{eq}01}}{\mathrm{d}r}\right], \tag{A17}$$

$$G_{20}(r) = -\frac{\varepsilon\kappa^2 a^4}{Zer} W_{10}(r)\frac{\mathrm{d}\psi_{\mathrm{eq}10}}{\mathrm{d}r}, \tag{A18}$$

$$W_{ij}(r) = \left[\frac{Ze}{kT}\psi_{\mathrm{eq}ij}(r) F_{\mu 00}(r) + F_{\mu ij}(r)\right], \tag{A19}$$

The functions $\alpha_1(x)$ and $\beta_1(x)$ defined by Equations (A9) and (A10) have no relation to the parameters α and β in the main text.

In Equations (21) and (22),

$$F_{\mu 00}(r) = F_{\psi 00}(r) = \frac{2r^3 + r_0^3}{2ar^2\chi}, \tag{A20}$$

$$\begin{aligned} F_{\mu ij}(r) = {} & -rK_{ij}^{(0)}(a,r) + \frac{1}{2b^3\chi r^2}[-r_0^6 K_{ij}^{(3)}(r,b) + 2b^3 r_0^3 K_{ij}^{(3)}(r_0,r) - 2r^3 r_0^3 K_{ij}^{(3)}(r_0,b) \\ & +2b^3(r^3 + r_0^3)K_{ij}^{(0)}(a,b) + (b^3 - r^3)r_0^3 K_{ij}^{(0)}(r_0,a)] \quad \text{if } a \le r \le b, \end{aligned} \tag{A21}$$

$$F_{\mu ij}(r) = -rK_{ij}^{(0)}(r_0,r) - \frac{1}{2b^3\chi r^2}[r_0^6 K_{ij}^{(3)}(r,b) - 2b^3 r^3 K_{ij}^{(0)}(r_0,b) + 2r^3 r_0^3 K_{ij}^{(3)}(r_0,b) \tag{A22}$$

doi:10.6342/NTU202502508

$$-b^3 r_0^3 K_{ij}^{(0)}(r_0,b) - 2b^3 r_0^3 K_{ij}^{(3)}(r_0,r)] \quad \text{if } r_0 < r < a,$$

$$F_{\psi ij}(r) = \frac{1}{A(r)\kappa^2 r^2}\{A(r)[\alpha_1(\kappa r)L_{ij}^{\gamma}(r) - \gamma_1(\kappa r)L_{ij}^{\alpha}(r)] + L_{ij}^{\alpha}(r_0)B(r) + L_{ij}^{\alpha}(b)C(r) - L_{ij}^{\gamma}(r_0)D(r) - L_{ij}^{\gamma}(b)E(r)\}, \tag{A23}$$

where $(i,j) = (0,1)$ and $(1,0)$.

$$\chi = 1 + \frac{r_0^3}{2b^3}, \tag{A24}$$

$$\gamma_1(x) = \mathrm{e}^{-x}(1+x), \tag{A25}$$

$$K_{ij}^{(n)}(r_1,r_2) = \frac{Ze}{3akT\chi}\int_{r_1}^{r_2}\left(\frac{r}{r_0}\right)^n\left[1-\left(\frac{r_0}{r}\right)^3\right]\frac{\mathrm{d}\psi_{\mathrm{eq}ij}}{\mathrm{d}r}\mathrm{d}r, \tag{A26}$$

$$L_{ij}^{(\alpha)}(r) = \int_a^r \kappa\alpha_1(\kappa r)W_{ij}(r)\mathrm{d}r, \tag{A27}$$

$$L_{ij}^{(\gamma)}(r) = \int_a^r \kappa\gamma_1(\kappa r)W_{ij}(r)\mathrm{d}r, \tag{A28}$$

$$A(r) = \mathrm{e}^{2\kappa r_0}(\kappa b+1)[2+\kappa r_0(\kappa r_0-2)] + \mathrm{e}^{2\kappa b}(\kappa b-1)[2+\kappa r_0(\kappa r_0+2)], \tag{A29}$$

$$B(r) = \mathrm{e}^{-\kappa r}[\mathrm{e}^{2\kappa b}(\kappa b-1)(\kappa r+1) - \mathrm{e}^{2\kappa r}(\kappa b+1)(\kappa r-1)][2+\kappa r_0(\kappa r_0+2)], \tag{A30}$$

$$C(r) = \mathrm{e}^{-\kappa r}(\kappa b+1)\{\mathrm{e}^{2\kappa r_0}(\kappa r+1)[2+\kappa r_0(\kappa r_0-2)] + \mathrm{e}^{2r\kappa}(\kappa r-1)[2+\kappa r_0(\kappa r_0+2)]\}, \tag{A31}$$

$$D(r) = \mathrm{e}^{\kappa(r_0-r)}[\mathrm{e}^{2\kappa r}(\kappa b+1)(\kappa r-1) - \mathrm{e}^{2\kappa b}(\kappa b-1)(\kappa r+1)][(\kappa^2 r_0^2+2)\sinh(\kappa r_0) - 2\kappa r_0\cosh(\kappa r_0)], \tag{A32}$$

$$E(r) = [1+\kappa b+\mathrm{e}^{2\kappa b}(\kappa b-1)][2+\kappa r_0(\kappa r_0+2)][\kappa r\cosh(\kappa r) - \sinh(\kappa r)] + 2\mathrm{e}^{\kappa(b-r+r_0)}(\kappa r+1)[\kappa b\cosh(\kappa b) - \sinh(\kappa b)][(\kappa^2 r_0^2+2)\sinh(\kappa r_0) - 2\kappa r_0\cosh(\kappa r_0)], \tag{A33}$$

where $(i,j) = (0,1)$ and $(1,0)$.

In Equations (29) and (A1)-(A8),

$$\begin{aligned} C_{001} = &-M^{-1}\lambda^4(b\{6\lambda[180a^3 + (54a^5 - 5a^3b^2 - 4b^5)\lambda^2]r_0 + 3\sinh[\lambda(a-r_0)]\{180a^3 \\ &+\lambda^4[30a^7 - 10a^5b^2 + r_0^2(-9a^5 + 5a^3b^2 + 4b^5 + 5(3a^4 - a^2b^2)r_0)] \\ &+\lambda^2[144a^5 - 4b^5 + 45a^4r_0 - 15a^2b^2r_0 - 20a^3(b^2 + 9r_0^2)]\} \\ &+\lambda\cosh[\lambda(a-r_0)]\{-540a^3(a+r_0) - (9a^5 - 5a^3b^2 - 4b^5)\lambda^4(2a^3 + r_0^3) \\ &-3\lambda^2[84a^6 - 20a^4b^2 - 4ab^5 + r_0(9a^5 - 5a^3b^2 - 4b^5 + 15a^2r_0(-3a^2 + b^2 + 4ar_0))]\}\}) \end{aligned} \tag{A34}$$

,

doi:10.6342/NTU202502508

$$
\begin{aligned}
C_{002} = {} & (aM)^{-1}\lambda^{4}(6b[60a^{6}\lambda^{3}r_{0}+\sinh[\lambda(a-r_{0})]\{135a^{3}r_{0}+\lambda^{4}[12a^{8}-2a^{3}b^{5} \\
& +r_{0}^{2}(-3a^{6}+3ab^{5}+(6a^{5}-b^{5})r_{0})]+3\lambda^{2}[10a^{6}+r_{0}(6a^{5}-b^{5}+15a^{3}r_{0}(-3a+r_{0}))]\} \\
& -\lambda\cosh[\lambda(a-r_{0})]\{135a^{3}(a-r_{0})r_{0}+a(a^{5}-b^{5})\lambda^{4}(2a^{3}+r_{0}^{3}) \\
& +3\lambda^{2}[10a^{7}+r_{0}(a^{6}-ab^{5}+r_{0}(-6a^{5}+b^{5}+15a^{4}r_{0}))]\}])
\end{aligned}
\quad , \qquad \text{(A35)}
$$

$$
\begin{aligned}
C_{003} = {} & (aM)^{-1}\lambda^{4}(2b^{3}[6a(-10a^{3}+b^{3})\lambda^{3}r_{0}+3\sinh[\lambda(a-r_{0})]\{-45ar_{0} \\
& +\lambda^{4}[-4a^{6}+2a^{3}b^{3}+r_{0}^{2}(a^{4}-ab^{3}+(-2a^{3}+b^{3})r_{0})] \\
& +\lambda^{2}[-10a^{4}+4ab^{3}+3r_{0}(-2a^{3}+b^{3}+5a(3a-r_{0})r_{0})]\} \\
& +\lambda\cosh[\lambda(a-r_{0})]\{135a(a-r_{0})r_{0}+a(a^{3}-b^{3})\lambda^{4}(2a^{3}+r_{0}^{3}) \\
& +3\lambda^{2}[10a^{5}-4a^{2}b^{3}+r_{0}(a^{4}-ab^{3}+3r_{0}(-2a^{3}+b^{3}+5a^{2}r_{0}))]\}])
\end{aligned}
\quad , \qquad \text{(A36)}
$$

$$
\begin{aligned}
C_{004} = {} & -M^{-1}\lambda^{4}(3a^{2}b\lambda^{2}[-6a^{3}\lambda r_{0}+\lambda\cosh[\lambda(a-r_{0})]\{3[4a^{4}+a(a^{2}-b^{2})r_{0} \\
& +(-3a^{2}+b^{2})r_{0}^{2}]+a(a^{2}-b^{2})\lambda^{2}(2a^{3}+r_{0}^{3})\} \\
& +\sinh[\lambda(a-r_{0})]\{2a^{3}[-6+(-3a^{2}+b^{2})\lambda^{2}] \\
& +r_{0}[-9a^{2}+3b^{2}+\lambda^{2}r_{0}(3a(a^{2}-b^{2})+(-3a^{2}+b^{2})r_{0})]\}])
\end{aligned}
\quad , \qquad \text{(A37)}
$$

$$
\begin{aligned}
C_{005} = {} & M^{-1}\lambda^{4}(6b\{2a\lambda[45a^{3}+(6a^{5}-5a^{3}b^{2}-b^{5})\lambda^{2}]\cosh[\lambda(a-r_{0})] \\
& +2[-21a^{5}\lambda^{2}+b^{5}\lambda^{2}+5a^{3}(-9+b^{2}\lambda^{2})]\sinh[\lambda(a-r_{0})] \\
& +[3a^{5}\lambda^{3}+2b^{5}\lambda^{3}-5a^{3}\lambda(18+b^{2}\lambda^{2})]r_{0}\})
\end{aligned}
\quad , \qquad \text{(A38)}
$$

$$
\begin{aligned}
C_{006} = {} & (a^{3}M)^{-1}\lambda^{2}(12br_{0}\{a^{3}(3a^{5}-5a^{3}b^{2}+2b^{5})\lambda^{5}+\lambda\cosh[\lambda(a-r_{0})][-135a^{3}(a-r_{0}) \\
& +a(-6a^{5}+5a^{3}b^{2}+b^{5})\lambda^{4}r_{0}^{2}-3\lambda^{2}(a-r_{0})(6a^{5}-5a^{3}b^{2}-b^{5}-15a^{4}r_{0})] \\
& +\sinh[\lambda(a-r_{0})][135a^{3}+\lambda^{4}r_{0}(3a(-6a^{5}+5a^{3}b^{2}+b^{5})+(21a^{5}-5a^{3}b^{2}-b^{5})r_{0}) \\
& +3\lambda^{2}(21a^{5}-5a^{3}b^{2}-b^{5}+15a^{3}r_{0}(-3a+r_{0}))]\})
\end{aligned}
\quad , \qquad \text{(A39)}
$$

$$
\begin{aligned}
C_{007} = {} & (a^{3}M)^{-1}\lambda^{2}(6b[-2a^{3}(3a^{5}-5a^{3}b^{2}+2b^{5})\lambda^{4}\cosh(\lambda r_{0}) \\
& +r_{0}\{6[-21a^{5}\lambda^{2}+b^{5}\lambda^{2}+5a^{3}(-9+b^{2}\lambda^{2})]\cosh(\lambda a) \\
& +6a\lambda[45a^{3}+(6a^{5}-5a^{3}b^{2}-b^{5})\lambda^{2}]\sinh(\lambda a) \\
& -[3a^{5}\lambda^{2}+2b^{5}\lambda^{2}-5a^{3}(18+b^{2}\lambda^{2})][-3\lambda\sinh(\lambda r_{0})r_{0}+\cosh(\lambda r_{0})(3+\lambda^{2}r_{0}^{2})]\}])
\end{aligned}
\quad , \qquad \text{(A40)}
$$

$$
\begin{aligned}
C_{008} = {} & (a^{3}M)^{-1}\lambda^{2}(6b[2a^{3}(3a^{5}-5a^{3}b^{2}+2b^{5})\lambda^{4}\sinh(\lambda r_{0}) \\
& +r_{0}\{6a\lambda[-6a^{5}\lambda^{2}+b^{5}\lambda^{2}+5a^{3}(-9+b^{2}\lambda^{2})]\cosh(\lambda a) \\
& +6[45a^{3}+(21a^{5}-5a^{3}b^{2}-b^{5})\lambda^{2}]\sinh(\lambda a) \\
& +[3a^{5}\lambda^{2}+2b^{5}\lambda^{2}-5a^{3}(18+b^{2}\lambda^{2})][-3\lambda\cosh(\lambda r_{0})r_{0}+\sinh(\lambda r_{0})(3+\lambda^{2}r_{0}^{2})]\}])
\end{aligned}
\quad , \qquad \text{(A41)}
$$

doi:10.6342/NTU202502508

$$
\begin{aligned}
C_{ij1} = {} & (a^2 O)^{-1} 4 e^{\lambda(a+r_0)} \lambda^2 \{-3[60 a^3 J_{ij}^{(\alpha)}(r_0) + 60 a^4 J_{ij}^{(\beta)}(r_0)\lambda \\
& +(28a^5 + 5a^2 b^3 - 3b^5) J_{ij}^{(\alpha)}(r_0)\lambda^2 \\
& +a(8a^5 - 5a^2 b^3 - 3b^5) J_{ij}^{(\beta)}(r_0)\lambda^3] \cosh(\lambda a) r_0 \\
& +3[60 a^3 J_{ij}^{(\beta)}(r_0) + 60 a^4 J_{ij}^{(\alpha)}(r_0)\lambda \\
& +(28a^5 + 5a^2 b^3 - 3b^5) J_{ij}^{(\beta)}(r_0)\lambda^2 \\
& +a(8a^5 - 5a^2 b^3 - 3b^5) J_{ij}^{(\alpha)}(r_0)\lambda^3] \sinh(a\lambda) r_0 \\
& +\sinh(\lambda r_0)[-180 a^3 J_{ij}^{(\beta)}(r_0) r_0 - 180 a^3 J_{ij}^{(\alpha)}(r_0)\lambda r_0^2 \\
& +3(2a^5 - 5a^2 b^3 + 3b^5) J_{ij}^{(\alpha)}(r_0)\lambda^3 r_0^2 \\
& +(a-b)^2 (2a^3 + 4a^2 b + 6ab^2 + 3b^3) J_{ij}^{(\beta)}(r_0)\lambda^4 (2a^3 + r_0^3) \\
& +3 J_{ij}^{(\beta)}(r_0)\lambda^2 \{-10 a^3 b^3 + (2a^5 - 5a^2 b^3 + 3b^5) r_0 - 20 a^3 r_0^3\}] \\
& +\cosh(\lambda r_0)[180 a^3 J_{ij}^{(\alpha)}(r_0) r_0 + 180 a^3 J_{ij}^{(\beta)}(r_0)\lambda r_0^2 \\
& -3(2a^5 - 5a^2 b^3 + 3b^5) J_{ij}^{(\beta)}(r_0)\lambda^3 r_0^2 \\
& -(a-b)^2 (2a^3 + 4a^2 b + 6ab^2 + 3b^3) J_{ij}^{(\alpha)}(r_0)\lambda^4 (2a^3 + r_0^3) \\
& +3 J_{ij}^{(\alpha)}(r_0)\lambda^2 \{10 a^3 b^3 + (-2a^5 + 5a^2 b^3 - 3b^5) r_0 + 20 a^3 r_0^3\}]\} \\
& +(3a^2 \lambda^2 M)^{-1} \lambda^4 \{6 a^3 \lambda^3 [-30\{b^3 J_{ij}^{(0)}(r_0) + 2a^3(-2J_{ij}^{(3)}(b) + J_{ij}^{(3)}(r_0))\} \\
& +\{a^2 b^3 (-10 J_{ij}^{(0)}(r_0) + 2 J_{ij}^{(5)}(b) - 5 J_{ij}^{(3)}(r_0)) \\
& +3b^5 (2 J_{ij}^{(0)}(r_0) - 2 J_{ij}^{(3)}(b) + J_{ij}^{(3)}(r_0)) \\
& +2a^5 (2 J_{ij}^{(0)}(r_0) + 18 J_{ij}^{(3)}(b) - J_{ij}^{(5)}(b) + J_{ij}^{(3)}(r_0))\}\lambda^2] r_0 \\
& +6 \sinh[\lambda(a - r_0)][180 a^3 J_{ij}^{(0)}(r_0) r_0 \\
& +3\lambda^2 \{20 a^6 (J_{ij}^{(3)}(b) - J_{ij}^{(3)}(r_0)) + (28a^5 + 5a^2 b^3 - 3b^5) J_{ij}^{(0)}(r_0) r_0 \\
& -60 a^4 J_{ij}^{(0)}(r_0) r_0^2 + 20 a^3 J_{ij}^{(0)}(r_0) r_0^3\} \\
& +\lambda^4 \{4a^8 (12 J_{ij}^{(3)}(b) - J_{ij}^{(5)}(b) - 7 J_{ij}^{(3)}(r_0)) + a^5 b^3 (J_{ij}^{(5)}(b) - 5 J_{ij}^{(3)}(r_0)) \\
& +3a^3 b^5 (-J_{ij}^{(3)}(b) + J_{ij}^{(3)}(r_0)) + 3a^7 (5 J_{ij}^{(3)}(b) - J_{ij}^{(5)}(b)) r_0 \\
& +3a[5a^2 b^3 J_{ij}^{(0)}(r_0) + 3b^5 J_{ij}^{(0)}(r_0) - 4a^5 (2 J_{ij}^{(0)}(r_0) + 5 J_{ij}^{(3)}(b))] r_0^2 \\
& +(28a^5 + 5a^2 b^3 - 3b^5) J_{ij}^{(0)}(r_0) r_0^3\} \\
& +a^3 \lambda^6 \{2a^7 (5 J_{ij}^{(3)}(b) - J_{ij}^{(5)}(b)) \\
& +[3b^5 J_{ij}^{(3)}(b) - a^2 b^3 J_{ij}^{(5)}(b) + a^5(-3 J_{ij}^{(3)}(b) + J_{ij}^{(5)}(b))] r_0^2 \\
& +a^4 (5 J_{ij}^{(3)}(b) - J_{ij}^{(5)}(b)) r_0^3\}] \\
& -2\lambda \cosh[\lambda(a - r_0)][540 a^3 J_{ij}^{(0)}(r_0)(a - r_0) r_0 \\
& +9\lambda^2 \{20 a^7 (J_{ij}^{(3)}(b) - J_{ij}^{(3)}(r_0)) \\
& +[-5a^3 b^3 J_{ij}^{(0)}(r_0) - 3ab^5 J_{ij}^{(0)}(r_0) + 4a^6 (2 J_{ij}^{(0)}(r_0) + 5 J_{ij}^{(3)}(b))] r_0 \\
& +(-28a^5 - 5a^2 b^3 + 3b^5) J_{ij}^{(0)}(r_0) r_0^2 + 20 a^4 J_{ij}^{(0)}(r_0) r_0^3\} \\
& +3a\lambda^4 \{4a^8 (7 J_{ij}^{(3)}(b) - J_{ij}^{(5)}(b) - 2 J_{ij}^{(3)}(r_0)) + 3a^3 b^5 (-J_{ij}^{(3)}(b) + J_{ij}^{(3)}(r_0)) \\
& +a^5 b^3 (J_{ij}^{(5)}(b) + 5 J_{ij}^{(3)}(r_0)) + [-3a^2 b^5 J_{ij}^{(3)}(b) \\
& +a^7 (3 J_{ij}^{(3)}(b) - J_{ij}^{(5)}(b)) + a^4 b^3 J_{ij}^{(5)}(b)] r_0
\end{aligned}
$$

doi:10.6342/NTU202502508

$$
\begin{aligned}
&+3a^6(-5J_{ij}^{(3)}(b)+J_{ij}^{(5)}(b))r_0^2+[-5a^2b^3J_{ij}^{(0)}(r_0)\\
&-3b^5J_{ij}^{(0)}(r_0)+4a^5(2J_{ij}^{(0)}(r_0)+5J_{ij}^{(3)}(b))]r_0^3\}\\
&+a^3\lambda^6\{-6a^3b^5J_{ij}^{(3)}(b)+a^8(6J_{ij}^{(3)}(b)-2J_{ij}^{(5)}(b))+2a^5b^3J_{ij}^{(5)}(b)\\
&+[-3b^5J_{ij}^{(3)}(b)+a^5(3J_{ij}^{(3)}(b)-J_{ij}^{(5)}(b))+a^2b^3J_{ij}^{(5)}(b)]r_0^3\}]\}\\
&+\{bJ_{ij}^{(2)}(b)[6\lambda\{-180a^3+(-54a^5+5a^3b^2+4b^5)\lambda^2\}r_0\\
&+\lambda\cosh[\lambda(a-r_0)]\{540a^3(a+r_0)\\
&+(9a^5-5a^3b^2-4b^5)\lambda^4(2a^3+r_0^3)\\
&+3\lambda^2[84a^6-20a^4b^2-4ab^5\\
&+(9a^5-5a^3b^2-4b^5)r_0\\
&+15a^2(-3a^2+b^2)r_0^2+60a^3r_0^3\}\\
&-3\sinh[\lambda(a-r_0)]\{180a^3+\lambda^4[30a^7-10a^5b^2\\
&+(-9a^5+5a^3b^2+4b^5)r_0^2+5(3a^4-a^2b^2)r_0^3]\\
&+\lambda^2[144a^5-4b^5+45a^4r_0-15a^2b^2r_0-20a^3(b^2+9r_0^2)]\}]\}\\
&\times\{-36\lambda[20a^6\lambda^2-27a^5b\lambda^2+2b^6\lambda^2+5a^3b(-18+b^2\lambda^2)]r_0\\
&+3\lambda\cosh[\lambda(a-r_0)][-540a^3\{ab+(-a+b)r_0+r_0^2\}\\
&+(a-b)^4(4a^2+7ab+4b^2)\lambda^4(2a^3+r_0^3)\\
&+3\lambda^2\{4a(10a^6-21a^5b+10a^3b^3+b^6)\\
&+(a-b)^4(4a^2+7ab+4b^2)r_0\\
&-3(a-b)^3(8a^2+9ab+3b^2)r_0^2+60a^3(a-b)r_0^3\}]\\
&-9[180a^3(-b+r_0)+\lambda^2\{4(10a^6-36a^5b+10a^3b^3+b^6)\\
&+3(a-b)^3(8a^2+9ab+3b^2)r_0-180a^3(a-b)r_0^2+60a^3r_0^3\}\\
&+(a-b)^3\lambda^4\{2a^3(8a^2+9ab+3b^2)-(a-b)(4a^2+7ab+4b^2)r_0^2\\
&+(8a^2+9ab+3b^2)r_0^3\}]\\
&-N^{-1}\lambda^4 3a^2b^3J_{ij}^{(0)}(r_0)\lambda^2\sinh[\lambda(a-r_0)]\{a^3\lambda^2(a\lambda\cosh[\lambda(a-r_0)]\\
&+\sinh[\lambda(a-r_0)]+\lambda r_0)+M^{-1}\lambda^4[2a\lambda\{15a\\
&+(2a^3-3ab^2+b^3)\lambda^2\}\cosh[\lambda(a-r_0)]\\
&+2(-7a^3\lambda^2+b^3\lambda^2+3a(-5+b^2\lambda^2))\sinh[\lambda(a-r_0)]\\
&-30a\lambda r_0+(a-b)^2(a+2b)\lambda^3r_0][6a\lambda\{60b^3+(-2a^5+20a^2b^3-3b^5)\lambda^2\}r_0\\
&-3\sinh[\lambda(a-r_0)]\{-60ab^3+\lambda^2[8a^6-50a^3b^3+12ab^5+3(2a^5-5a^2b^3+3b^5)r_0\\
&+60ab^3r_0^2]+(a-b)^2(2a^3+4a^2b+6ab^2+3b^3)\lambda^4(2a^3-ar_0^2+r_0^3)\} \quad ,\\
&+\lambda\cosh[\lambda(a-r_0)]\{-180ab^3(a+r_0)\\
&+a(a-b)^2(2a^3+4a^2b+6ab^2+3b^3)\lambda^4(2a^3+r_0^3)\\
&+3\lambda^2[8a^7-30a^4b^3+12a^2b^5+(2a^6-5a^3b^3+3ab^5)r_0\\
&-3(2a^5-5a^2b^3+3b^5)r_0^2-20ab^3r_0^3]\}]\}\}^{-1}
\end{aligned}
\tag{A42}
$$

doi:10.6342/NTU202502508

$$
\begin{aligned}
C_{ij2} = {} & (3a^2 M)^{-1}\lambda^2\{-36b[-45a^3 J_{ij}^{(\alpha)}(r_0) - 45a^4 J_{ij}^{(\beta)}(r_0)\lambda \\
& +(-21a^5+5a^3b^2+b^5)J_{ij}^{(\alpha)}(r_0)\lambda^2 \\
& +a(-6a^5+5a^3b^2+b^5)J_{ij}^{(\beta)}(r_0)\lambda^3]\cosh(\lambda a) r_0 \\
& +6[90a^6 b J_{ij}^{(3)}(r_0)\lambda^3 - a^3\{40a^6 J_{ij}^{(3)}(b) + 5a^3b^3(4J_{ij}^{(0)}(b) \\
& -2J_{ij}^{(0)}(r_0)+J_{ij}^{(3)}(b)-J_{ij}^{(3)}(r_0)) + 2b^6(-J_{ij}^{(0)}(b)+2J_{ij}^{(0)}(r_0) \\
& +J_{ij}^{(3)}(r_0)) + 3a^5 b(2J_{ij}^{(0)}(r_0) - 20J_{ij}^{(2)}(b) - J_{ij}^{(5)}(b) + J_{ij}^{(3)}(r_0))\}\lambda^5 \\
& +6b\{-45a^3J_{ij}^{(\beta)}(r_0) - 45a^4 J_{ij}^{(\alpha)}(r_0)\lambda \\
& +(-21a^5+5a^3b^2+b^5)J_{ij}^{(\beta)}(r_0)\lambda^2 \\
& +a(-6a^5+5a^3b^2+b^5)J_{ij}^{(\alpha)}(r_0)\lambda^3\}\sinh(\lambda a)]r_0 \\
& +\lambda\cosh[\lambda(a-r_0)][1620a^3bJ_{ij}^{(0)}(r_0)(a-r_0)r_0 \\
& +a^3(a-b)\{2b^5(J_{ij}^{(0)}(b)-3J_{ij}^{(2)}(b)) + 4a^5J_{ij}^{(3)}(b) \\
& +a^2b^3(2J_{ij}^{(0)}(b)-6J_{ij}^{(2)}(b)+9J_{ij}^{(3)}(b)) \\
& +ab^4(2J_{ij}^{(0)}(b)-6J_{ij}^{(2)}(b)+9J_{ij}^{(3)}(b)) \\
& +a^4b(-6J_{ij}^{(2)}(b)+4J_{ij}^{(3)}(b)-3J_{ij}^{(5)}(b)) \\
& +a^3b^2(-6J_{ij}^{(2)}(b)+4J_{ij}^{(3)}(b)-3J_{ij}^{(5)}(b))\}\lambda^6(2a^3+r_0^3) \\
& +3a\lambda^4\{4a^3[10a^6J_{ij}^{(3)}(b)+b^6(-2J_{ij}^{(0)}(b)+J_{ij}^{(3)}(r_0)) \\
& +5a^3b^3(J_{ij}^{(0)}(b)+J_{ij}^{(3)}(b)+J_{ij}^{(3)}(r_0)) \\
& -3a^5b(5J_{ij}^{(2)}(b)+J_{ij}^{(5)}(b)+2J_{ij}^{(3)}(r_0))] \\
& +a^2[-2b^6(J_{ij}^{(0)}(b)-3J_{ij}^{(2)}(b)) \\
& +4a^6J_{ij}^{(3)}(b)-9ab^5J_{ij}^{(3)}(b)-3a^5b(2J_{ij}^{(2)}(b)+J_{ij}^{(5)}(b)) \\
& +a^3b^3(2J_{ij}^{(0)}(b)+5J_{ij}^{(3)}(b)+3J_{ij}^{(5)}(b))]r_0 \\
& -3a[2b^6(-J_{ij}^{(0)}(b)+J_{ij}^{(2)}(b))+8a^6J_{ij}^{(3)}(b) \\
& -3ab^5J_{ij}^{(3)}(b)-3a^5b(4J_{ij}^{(2)}(b)+J_{ij}^{(5)}(b)) \\
& +a^3b^3(4J_{ij}^{(0)}(b)+5J_{ij}^{(3)}(b)+J_{ij}^{(5)}(b))]r_0^2 \\
& +[10a^3b^3(3J_{ij}^{(0)}(b)-2J_{ij}^{(0)}(r_0))-4b^6J_{ij}^{(0)}(r_0) \\
& +6a^5b(4J_{ij}^{(0)}(r_0)-15J_{ij}^{(2)}(b))+60a^6J_{ij}^{(3)}(b)]r_0^3\} \\
& -18\lambda^2\{30a^7bJ_{ij}^{(3)}(r_0)-(a-r_0)r_0[5a^3b^3(3J_{ij}^{(0)}(b)-2J_{ij}^{(0)}(r_0)) \\
& -2b^6J_{ij}^{(0)}(r_0)+3a^5b(4J_{ij}^{(0)}(r_0)-15J_{ij}^{(2)}(b)) \\
& +30a^6J_{ij}^{(3)}(b)-30a^4bJ_{ij}^{(0)}(r_0)r_0]\}] \\
& +6b\cosh(\lambda r_0)[2a^3(3a^5-5a^3b^2+2b^5)J_{ij}^{(\alpha)}(r_0)\lambda^4
\end{aligned}
$$

doi:10.6342/NTU202502508

$$
\begin{aligned}
&+r_0\{3a^5\lambda^2+2b^5\lambda^2-5a^3(18+b^2\lambda^2)\}\{3J_{ij}^{(\alpha)}(r_0)\\
&+\lambda r_0(3J_{ij}^{(\beta)}(r_0)+J_{ij}^{(\alpha)}(r_0)\lambda r_0)\}]\\
&-6b\sinh(\lambda r_0)[2a^3(3a^5-5a^3b^2+2b^5)J_{ij}^{(\beta)}(r_0)\lambda^4\\
&+r_0\{3a^5\lambda^2+2b^5\lambda^2-5a^3(18+b^2\lambda^2)\}\{3J_{ij}^{(\beta)}(r_0)\\
&+\lambda r_0(3J_{ij}^{(\alpha)}(r_0)+J_{ij}^{(\beta)}(r_0)\lambda r_0)\}]\\
&-3\sinh[\lambda(a-r_0)][540a^3bJ_{ij}^{(0)}(r_0)r_0+a^2\lambda^6\{2a^3[2b^6(-J_{ij}^{(0)}(b)\\
&+J_{ij}^{(2)}(b))+8a^6J_{ij}^{(3)}(b)-3ab^5J_{ij}^{(3)}(b)-3a^5b(4J_{ij}^{(2)}(b)+J_{ij}^{(5)}(b))\\
&+a^3b^3(4J_{ij}^{(0)}(b)+5J_{ij}^{(3)}(b)+J_{ij}^{(5)}(b))]\\
&+a[2b^6(J_{ij}^{(0)}(b)-3J_{ij}^{(2)}(b))-4a^6J_{ij}^{(3)}(b)\\
&+9ab^5J_{ij}^{(3)}(b)+3a^5b(2J_{ij}^{(2)}(b)+J_{ij}^{(5)}(b))\\
&-a^3b^3(2J_{ij}^{(0)}(b)+5J_{ij}^{(3)}(b)+3J_{ij}^{(5)}(b))]r_0^2\\
&+[2b^6(-J_{ij}^{(0)}(b)+J_{ij}^{(2)}(b))+8a^6J_{ij}^{(3)}(b)\\
&-3ab^5J_{ij}^{(3)}(b)-3a^5b(4J_{ij}^{(2)}(b)+J_{ij}^{(5)}(b))\\
&+a^3b^3(4J_{ij}^{(0)}(b)+5J_{ij}^{(3)}(b)+J_{ij}^{(5)}(b))]r_0^3\}\\
&-6\lambda^2\{30a^6bJ_{ij}^{(3)}(r_0)+r_0[2b^6J_{ij}^{(0)}(r_0)+5a^3b^3(-3J_{ij}^{(0)}(b)+2J_{ij}^{(0)}(r_0))\\
&+a^5b(-42J_{ij}^{(0)}(r_0)+45J_{ij}^{(2)}(b))\\
&-30a^6J_{ij}^{(3)}(b)+30a^3bJ_{ij}^{(0)}(r_0)(3a-r_0)r_0]\}\\
&+\lambda^4\{4a^3[10a^6J_{ij}^{(3)}(b)+b^6(-2J_{ij}^{(0)}(b)+J_{ij}^{(3)}(r_0))\\
&+5a^3b^3(J_{ij}^{(0)}(b)+J_{ij}^{(3)}(b)+J_{ij}^{(3)}(r_0))-3a^5b(5J_{ij}^{(2)}(b)\\
&+J_{ij}^{(5)}(b)+7J_{ij}^{(3)}(r_0))]+r_0[3a^2\{2b^6(-J_{ij}^{(0)}(b)+J_{ij}^{(2)}(b))\\
&+8a^6J_{ij}^{(3)}(b)-3ab^5J_{ij}^{(3)}(b)-3a^5b(4J_{ij}^{(2)}(b)+J_{ij}^{(5)}(b))\\
&+a^3b^3(4J_{ij}^{(0)}(b)+5J_{ij}^{(3)}(b)+J_{ij}^{(5)}(b))\}\\
&+2r_0\{6ab^6J_{ij}^{(0)}(r_0)+15a^4b^3(-3J_{ij}^{(0)}(b)+2J_{ij}^{(0)}(r_0))\\
&+9a^6b(-4J_{ij}^{(0)}(r_0)+15J_{ij}^{(2)}(b))\\
&-90a^7J_{ij}^{(3)}(b)+[5a^3b^3(3J_{ij}^{(0)}(b)-2J_{ij}^{(0)}(r_0))-2b^6J_{ij}^{(0)}(r_0)\\
&+a^5b(42J_{ij}^{(0)}(r_0)-45J_{ij}^{(2)}(b))+30a^6J_{ij}^{(3)}(b)]r_0\}]\}]\}
\end{aligned}
\tag{A43}
$$
,

doi:10.6342/NTU202502508

$$
\begin{aligned}
C_{ij3} = {} & (15a^3MN)^{-1}\lambda^6(30a^3b^3J_{ij}^{(3)}(r_0)\lambda^{-2}N\{2a\lambda[15a \\
& +(2a^3-3ab^2+b^3)\lambda^2]\cosh[\lambda(a-r_0)] \\
& +[-30a+2(-7a^3+3ab^2+b^3)\lambda^2]\sinh[\lambda(a-r_0)]-30a\lambda r_0 \\
& +(a-b)^2(a+2b)\lambda^3r_0\}+60b^3J_{ij}^{(0)}(r_0)\lambda^{-4}Nr_0\{6ab^3\lambda^3+a^3(a-b)^2(a+2b)\lambda^5 \\
& -\sinh[\lambda(a-r_0)][-45a+3\lambda^2(-7a^3+3ab^2+b^3+15a^2r_0-5ar_0^2) \\
& +\lambda^4r_0(6a^4-9a^2b^2-7a^3r_0+b^3r_0+3ab^2(b+r_0))] \\
& -\lambda\cosh[\lambda(a-r_0)][45a(a-r_0)+a(2a^3-3ab^2+b^3)\lambda^4r_0^2 \\
& +3\lambda^2(2a^4-7a^3r_0+b^3r_0+ab^2(b+3r_0)+a^2(-3b^2+5r_0^2))]\} \\
& -a^5J_{ij}^{(5)}(b)\lambda^{-2}N(6a\lambda[180b+(-40a^3+54a^2b-5b^3)\lambda^2]r_0 \\
& -3\sinh[\lambda(a-r_0)]\{180a(-b+r_0) \\
& +\lambda^4[2a^3(8a^3-15a^2b+5b^38a^3-15a^2b+5b^3) \\
& +a(-4a^3+9a^2b-5b^3)r_0^2+(8a^3-15a^2b+5b^3)r_0^3] \\
& +\lambda^2[40a^4+15b^3r_0+24a^3(-6b+r_0)-45a^2r_0(b+4r_0) \\
& +20a(b^3+9br_0^2+3r_0^3)]\} \\
& +\lambda\cosh[\lambda(a-r_0)]\{a(4a^3-9a^2b+5b^3)\lambda^4(2a^3+r_0^3) \\
& -540a[a(b-r_0)+r_0(b+r_0)]+3\lambda^2[40a^5-15b^3r_0^2 \\
& +4a^4(-21b+r_0)-3a^3r_0(3b+8r_0)+5abr_0(b^2-12r_0^2)+5a^2(4b^3+9br_0^2+12r_0^3)]\}) \\
& +10a^2b^3J_{ij}^{(2)}(b)\lambda^{-2}N(6a(-10a^3+b^3)\lambda^3r_0 \\
& -3\sinh[\lambda(a-r_0)]\{45ar_0+\lambda^2(10a^4-4ab^3+6a^3r_0-3b^3r_0-45a^2r_0^2+15ar_0^3) \\
& +\lambda^4[4a^6-a^4r_0^2+ab^3r_0^2-b^3r_0^3+2a^3(-b^3+r_0^3)]\} \\
& +\lambda\cosh[\lambda(a-r_0)]\{135a(a-r_0)r_0+a(a^3-b^3)\lambda^4(2a^3+r_0^3) \\
& +3\lambda^2[10a^5+a^4r_0-ab^3r_0-6a^3r_0^2+3b^3r_0^2+a^2(-4b^3+15r_0^3)]\}) \\
& +15a^3b^3J_{ij}^{(3)}(b)\lambda^{-2}N(6a\lambda[20+(6a^2-b^2)\lambda^2]r_0 \\
& +\sinh[\lambda(a-r_0)]\{60a+\lambda^4[10a^5+3ab^2r_0^2+5a^2r_0^3-3b^2r_0^3-3a^3(2b^2+r_0^2)] \\
& +3\lambda^2[16a^3+5a^2r_0-3b^2r_0-4a(b^2+5r_0^2)]\} \\
& -\lambda\cosh[\lambda(a-r_0)]\{60a(a+r_0)+a(a^2-b^2)\lambda^4(2a^3+r_0^3) \\
& +\lambda^2[28a^4+3a^3r_0+9b^2r_0^2-3a^2(4b^2+5r_0^2)+a(-3b^2r_0+20r_0^3)]\}) \\
& +ab^5J_{ij}^{(0)}(b)\lambda^2(a^2\lambda^{-2}M\{2a(-3a+b)\lambda\cosh[\lambda(a-r_0)]+2(3a+b)\sinh[\lambda(a-r_0)] \\
& +(-3a+2b)\lambda r_0\}-5b\{-2a\lambda[15a+(2a^3-3ab^2+b^3)\lambda^2]\cosh[\lambda(a-r_0)] \\
& +2[15a+(7a^3-3ab^2-b^3)\lambda^2]\sinh[\lambda(a-r_0)]+30a\lambda r_0 \\
& -(a-b)^2(a+2b)\lambda^3r_0\}\{6\lambda[24b^3+a^2(a^3-12ab^2+8b^3)\lambda^2]r_0 \\
& +3\sinh[\lambda(a-r_0)][6b^2(4b-9r_0)+a(a-b)^2(a+2b)\lambda^4(2a^3-ar_0^2+r_0^3) \\
& +\lambda^2\{4a^2(a^3-3ab^2+5b^3)+3a(a-b)^2(a+2b)r_0+6(9a-4b)b^2r_0^2-18b^2r_0^3\}] \\
& -\lambda\cosh[\lambda(a-r_0)][18b^2(4ab-9ar_0+4br_0+9r_0^2)
\end{aligned}
$$

doi:10.6342/NTU202502508

$$+a^2(a-b)^2(a+2b)\lambda^4(2a^3+r_0^3)+3\lambda^2\{4a^3(a^3-3ab^2+3b^3)$$
$$+a^2(a-b)^2(a+2b)r_0-3a(a-b)^2(a+2b)r_0^2+2b^2(-9a+4b)r_0^3\}]\})$$
$$+30b^3J_{ij}^{(\alpha)}(r_0)[\lambda\sinh(\lambda a)r_0\{3a\lambda[1800a^2b^3-60a^2(a^5-4a^2b^3+3b^5)\lambda^2$$
$$+(a-b)^4(12a^5+33a^4b+36a^3b^2+28a^2b^3+4ab^4-8b^5)\lambda^4]r_0$$
$$+3\lambda\cosh[\lambda(a-r_0)][-900a^2b^3(a^2+r_0^2)$$
$$+(a-b)^3\lambda^4\{2a^2(2a^2+2ab-b^2)(4a^4+5a^3b+6a^2b^2+2ab^3-2b^4)$$
$$+(a-b)^2(a+b)(a+2b)(2a^2+ab+2b^2)r_0^2\}$$
$$+30a\lambda^2\{a^2(4a^6-3a^5b-9a^3b^3+12ab^5-4b^6)$$
$$+(-2a^6+3a^5b+a^3b^3-6ab^5+4b^6)r_0^2\}]$$
$$+\sinh[\lambda(a-r_0)][2700a^2b^3(a-r_0)$$
$$+(a-b)^5(a+b)(a+2b)(2a^2+ab+2b^2)\lambda^6(2a^3+r_0^3)$$
$$-90a\lambda^2\{a(4a^6-3a^5b-19a^3b^3+12ab^5-4b^6)$$
$$+(a-b)^2(2a^4+a^3b-2ab^3-4b^4)r_0+10ab^3r_0^3\}$$
$$-3(a-b)^2\lambda^4\{2a[28a^7+35a^6b+30a^5b^2$$
$$-19a^4b^3-59a^3b^4-12a^2b^5+6ab^6+6b^7]$$
$$-(a-b)^3(a+b)(a+2b)(2a^2+ab+2b^2)r_0$$
$$+10a(2a^4+a^3b-2ab^3-4b^4)r_0^3\}]\}$$
$$+\cosh(\lambda r_0)(-6a^4\lambda^3[20a^6\lambda^2-27a^5b\lambda^2+2b^6\lambda^2$$
$$+5a^3b(-18+b^2\lambda^2)]r_0+\sinh[\lambda(a-r_0)]\{2700a^2b^3r_0$$
$$+(a-b)^4(a+2b)\lambda^6[2a^3(4a^4+11a^3b+18a^2b^2+10ab^3+2b^4)$$
$$-3a(4a^4+5a^3b+6a^2b^2+2ab^3-2b^4)r_0^2$$
$$+(4a^4+11a^3b+18a^2b^2+10ab^3+2b^4)r_0^3]$$
$$+3(a-b)^2\lambda^4[4ab^3(-a^4+a^3b+18a^2b^2+10ab^3+2b^4)$$
$$+(a-b)^2(a+2b)(4a^4+11a^3b+18a^2b^2+10ab^3+2b^4)r_0$$
$$+30a^3(4a^3+5a^2b+6ab^2+3b^3)r_0^2$$
$$-10a(4a^4+11a^3b+18a^2b^2+11ab^3+4b^4)r_0^3]$$
$$-90a\lambda^2[4a^6r_0+3a^5br_0-14a^3b^3r_0+4b^6r_0$$
$$+30a^2b^3r_0^2+a(4b^6+3b^5r_0-10b^3r_0^3)]\}$$
$$+\lambda\cosh[\lambda(a-r_0)]\{-2700a^2b^3(a-r_0)r_0$$
$$-a(a-b)^4(a+2b)(4a^4+5a^3b+6a^2b^2+2ab^3-2b^4)\lambda^6(2a^3+r_0^3)$$
$$-3(a-b)^2\lambda^4[-4a^2(a-b)b^3(a^3+6a^2b-2b^3)$$
$$+a(a-b)^2(a+2b)(4a^4+5a^3b+6a^2b^2+2ab^3-2b^4)r_0$$

doi:10.6342/NTU202502508

$$-(a-b)^2(a+2b)(4a^4+11a^3b+18a^2b^2+10ab^3+2b^4)r_0^2$$
$$-10a^3(4a^3+5a^2b+6ab^2+3b^3)r_0^3]$$
$$+90a\lambda^2[4a^7r_0-4a^4b^3r_0-3a^5br_0^2+14a^3b^3r_0^2-3ab^5r_0^2$$
$$-4b^6r_0^2-a^6r_0(3b+4r_0)+a^2(4b^6+3b^5r_0-10b^3r_0^3)]\})$$
$$-\cosh(\lambda a)r_0(3\lambda[1800a^2b^3-60a(a^6+3a^5b-14a^3b^3+3ab^5+4b^6)\lambda^2$$
$$+(a-b)^3(32a^6+57a^5b+51a^4b^2+12a^3b^3-48a^2b^4-36ab^5-8b^6)\lambda^4]r_0$$
$$+3\sinh[\lambda(a-r_0)][900a^2b^3+(a-b)^5(a+b)(a+2b)(2a^2+ab+2b^2)\lambda^6r_0^2$$
$$-30a\lambda^2(4a^6+3a^5b-29a^3b^3+12ab^5+4b^6+30ab^3r_0^2)$$
$$-2(a-b)^2\lambda^4\{28a^7+77a^6b+114a^5b^2+33a^4b^3-51a^3b^4$$
$$-48a^2b^5-16ab^6-2b^7+15a(2a^4+a^3b-2ab^3-4b^4)r_0^2\}]$$
$$+\lambda\cosh[\lambda(a-r_0)][-2700a^2b^3(a+r_0)$$
$$+(a-b)^5(a+b)(a+2b)(2a^2+ab+2b^2)\lambda^6(2a^3+r_0^3)$$
$$+3(a-b)^2\lambda^4\{2a(8a^7+22a^6b+24a^5b^2+5a^4b^3-17a^3b^4-12a^2b^5+2ab^6-2b^7)$$
$$+(a-b)^3(a+b)(a+2b)(2a^2+ab+2b^2)r_0$$
$$-10a(2a^4+a^3b-2ab^3-4b^4)r_0^3\}$$
$$+90a\lambda^2\{4a^7-19a^4b^3+12a^2b^5+a^6(3b-2r_0)$$
$$+3a^5br_0+a^3b^3r_0+4b^6r_0+2a(2b^6-3b^5r_0-5b^3r_0^3)\}])]$$
$$-30b^3J_{ij}^{(\beta)}(r_0)(\lambda\cosh(\lambda a)r_0\{3a\lambda[1800a^2b^3$$
$$-60a^2(a^5-4a^2b^3+3b^5)\lambda^2$$
$$+(a-b)^4(12a^5+33a^4b+36a^3b^2+28a^2b^3+4ab^4-8b^5)\lambda^4]r_0$$
$$+3\lambda\cosh[\lambda(a-r_0)][-900a^2b^3(a^2+r_0^2)$$
$$+(a-b)^3\lambda^4\{2a^2(2a^2+2ab-b^2)(4a^4+5a^3b+6a^2b^2+2ab^3-2b^4)$$
$$+(a-b)^2(a+b)(a+2b)(2a^2+ab+2b^2)r_0^2\}$$
$$+30a\lambda^2\{a^2(4a^6-3a^5b-9a^3b^3+12ab^5-4b^6)$$
$$+(-2a^6+3a^5b+a^3b^3-6ab^5+4b^6)r_0^2\}]$$
$$+\sinh[\lambda(a-r_0)][2700a^2b^3(a-r_0)$$
$$+(a-b)^5(a+b)(a+2b)(2a^2+ab+2b^2)\lambda^6(2a^3+r_0^3)$$
$$-90a\lambda^2\{a(4a^6-3a^5b-19a^3b^3+12ab^5-4b^6)$$
$$+(a-b)^2(2a^4+a^3b-2ab^3-4b^4)r_0+10ab^3r_0^3\}$$
$$-3(a-b)^2\lambda^4\{2a(28a^7+35a^6b+30a^5b^2-19a^4b^3$$
$$-59a^3b^4-12a^2b^5+6ab^6+6b^7)$$
$$-(a-b)^3(a+b)(a+2b)(2a^2+ab+2b^2)r_0$$
$$+10a(2a^4+a^3b-2ab^3-4b^4)r_0^3\}]\}$$
$$+\sinh(\lambda r_0)(-6a^4\lambda^3[20a^6\lambda^2-27a^5b\lambda^2+2b^6\lambda^2$$
$$+5a^3b(-18+b^2\lambda^2)]r_0+\sinh[\lambda(a-r_0)][2700a^2b^3r_0$$
$$+(a-b)^4(a+2b)\lambda^6\{2a^3(4a^4+11a^3b+18a^2b^2+10ab^3+2b^4)$$

doi:10.6342/NTU202502508

$$
\begin{aligned}
&-3a(4a^4+5a^3b+6a^2b^2+2ab^3-2b^4)r_0^2\\
&+(4a^4+11a^3b+18a^2b^2+10ab^3+2b^4)r_0^3\}\\
&3(a-b)^2\lambda^4\{4ab^3(-a^4+a^3b+18a^2b^2+10ab^3+2b^4)\\
&+(a-b)^2(a+2b)(4a^4+11a^3b+18a^2b^2+10ab^3+2b^4)r_0\\
&+30a^3(4a^3+5a^2b+6ab^2+3b^3)r_0^2\\
&-10a(4a^4+11a^3b+18a^2b^2+11ab^3+4b^4)r_0^3\}\\
&-90a\lambda^2\{4a^6r_0+3a^5br_0-14a^3b^3r_0+4b^6r_0+30a^2b^3r_0^2\\
&+a(4b^6+3b^5r_0-10b^3r_0^3)\}]\\
&+\lambda\cosh[\lambda(a-r_0)][-2700a^2b^3(a-r_0)r_0\\
&-a(a-b)^4(a+2b)(4a^4+5a^3b+6a^2b^2+2ab^3-2b^4)\lambda^6(2a^3+r_0^3)\\
&-3(a-b)^2\lambda^4\{-4a^2(a-b)b^3(a^3+6a^2b-2b^3)\\
&+a(a-b)^2(a+2b)(4a^4+5a^3b+6a^2b^2+2ab^3-2b^4)r_0\\
&-(a-b)^2(a+2b)(4a^4+11a^3b+18a^2b^2+10ab^3+2b^4)r_0^2\\
&-10a^3(4a^3+5a^2b+6ab^2+3b^3)r_0^3\}\\
&+90a\lambda^2\{4a^7r_0-4a^4b^3r_0-3a^5br_0^2+14a^3b^3r_0^2-3ab^5r_0^2\\
&-4b^6r_0^2-a^6r_0(3b+4r_0)+a^2(4b^6+3b^5r_0-10b^3r_0^3)\}])\\
&-\sinh(\lambda a)r_0(3\lambda\{1800a^2b^3-60a(a^6+3a^5b-14a^3b^3+3ab^5+4b^6)\lambda^2\\
&+(a-b)^3(32a^6+57a^5b+51a^4b^2+12a^3b^3-48a^2b^4-36ab^5-8b^6)\lambda^4\}r_0\\
&+3\sinh[\lambda(a-r_0)][900a^2b^3+(a-b)^5(a+b)(a+2b)(2a^2+ab+2b^2)\lambda^6r_0^2\\
&-30a\lambda^2(4a^6+3a^5b-29a^3b^3+12ab^5+4b^6+30ab^3r_0^2)\\
&-2(a-b)^2\lambda^4\{28a^7+77a^6b+114a^5b^2+33a^4b^3\\
&-51a^3b^4-48a^2b^5-16ab^6-2b^7+15a(2a^4+a^3b-2ab^3-4b^4)r_0^2\}]\\
&+\lambda\cosh[\lambda(a-r_0)][-2700a^2b^3(a+r_0)\\
&+(a-b)^5(a+b)(a+2b)(2a^2+ab+2b^2)\lambda^6(2a^3+r_0^3)\\
&+3(a-b)^2\lambda^4\{2a(8a^7+22a^6b+24a^5b^2+5a^4b^3\\
&-17a^3b^4-12a^2b^5+2ab^6-2b^7)\\
&+(a-b)^3(a+b)(a+2b)(2a^2+ab+2b^2)r_0\\
&-10a(2a^4+a^3b-2ab^3-4b^4)r_0^3\}\\
&+90a\lambda^2\{4a^7-19a^4b^3+12a^2b^5+a^6(3b-2r_0)\\
&+3a^5br_0+a^3b^3r_0+4b^6r_0+2a(2b^6-3b^5r_0-5b^3r_0^3)\}])]) \qquad ,
\end{aligned}
\tag{A44}
$$

doi:10.6342/NTU202502508

$$
\begin{aligned}
C_{ij4} = {} & (15O)^{-1}\lambda^4\{2\mathrm{e}^{(a+r_0)\lambda}(90r_0[(4a^3+3a^2b-b^3)J_{ij}^{(\alpha)}(r_0) \\
& +a(a-b)(4a^2+ab+b^2)J_{ij}^{(\beta)}(r_0)\lambda]\cosh(\lambda a) \\
& +\lambda(-90J_{ij}^{(0)}(r_0)r_0[-4a^4+ab^3+3a^2br_0-b^3r_0+a^3(3b+4r_0)] \\
& +3[4ab^6J_{ij}^{(0)}(b)+40a^7(J_{ij}^{(3)}(b)-J_{ij}^{(3)}(r_0)) \\
& +10a^4b^3(2J_{ij}^{(0)}(b)-J_{ij}^{(3)}(b)+J_{ij}^{(3)}(r_0)) \\
& +6a^6b(-10J_{ij}^{(2)}(b)+J_{ij}^{(5)}(b)+5J_{ij}^{(3)}(r_0)) \\
& +\{-9ab^5J_{ij}^{(0)}(b)+4b^6J_{ij}^{(0)}(b)+5a^3b^3(J_{ij}^{(0)}(b)+3J_{ij}^{(2)}(b)-2J_{ij}^{(3)}(b)) \\
& +2a^6(5J_{ij}^{(3)}(b)-3J_{ij}^{(5)}(b))+3a^5b(-5J_{ij}^{(2)}(b)+2J_{ij}^{(5)}(b))\}r_0 \\
& +3\{3b^5J_{ij}^{(0)}(b)+15a^4bJ_{ij}^{(2)}(b) \\
& -5a^2b^3(J_{ij}^{(0)}(b)+J_{ij}^{(2)}(b))+2a^5(-5J_{ij}^{(3)}(b)+J_{ij}^{(5)}(b))\}r_0^{\,2} \\
& +10a(a-b)(4a^2+ab+b^2)J_{ij}^{(0)}(r_0)r_0^{\,3}]\lambda^2 \\
& +(a-b)[5a^2b^3J_{ij}^{(0)}(b)+5ab^4J_{ij}^{(0)}(b)-4b^5J_{ij}^{(0)}(b) \\
& +5a^4b(-3J_{ij}^{(2)}(b)+2J_{ij}^{(3)}(b))+5a^3b^2(-3J_{ij}^{(2)}(b)+2J_{ij}^{(3)}(b)) \\
& +2a^5(5J_{ij}^{(3)}(b)-3J_{ij}^{(5)}(b))](2a^3+r_0^{\,3})\lambda^4)\cosh[(a-r_0)\lambda] \\
& +30[3J_{ij}^{(\alpha)}(r_0)\{-6a^3b+(a-b)^2(2a+b)r_0\} \\
& +3(a-b)^2(2a+b)J_{ij}^{(\beta)}(r_0)r_0^{\,2}\lambda \\
& +(a-b)^2(2a+b)J_{ij}^{(\alpha)}(r_0)(2a^3+r_0^{\,3})\lambda^2]\cosh(\lambda r_0) \\
& +6r_0[90a^3bJ_{ij}^{(0)}(r_0)\lambda-\{4b^6J_{ij}^{(0)}(b) \\
& +5a^3b^3(J_{ij}^{(0)}(b)+2J_{ij}^{(0)}(r_0)-2J_{ij}^{(3)}(b)+J_{ij}^{(3)}(r_0)) \\
& +10a^6(2J_{ij}^{(0)}(r_0)+J_{ij}^{(3)}(b)+J_{ij}^{(3)}(r_0)) \\
& -3a^5b(10J_{ij}^{(0)}(r_0)+5J_{ij}^{(2)}(b)-2J_{ij}^{(5)}(b)+5J_{ij}^{(3)}(r_0))\}\lambda^3 \\
& -15\{(4a^3+3a^2b-b^3)J_{ij}^{(\beta)}(r_0) \\
& +a(a-b)(4a^2+ab+b^2)J_{ij}^{(\alpha)}(r_0)\lambda\}\sinh\{\lambda a\}] \\
& -3[30(4a^3+3a^2b-b^3)J_{ij}^{(0)}(r_0)r_0 \\
& +\{4b^6J_{ij}^{(0)}(b)+40a^6(J_{ij}^{(3)}(b)-J_{ij}^{(3)}(r_0))-9b^5J_{ij}^{(0)}(b)r_0 \\
& +30ab^3J_{ij}^{(0)}(r_0)r_0^{\,2}-10b^3J_{ij}^{(0)}(r_0)r_0^{\,3} \\
& -15a^4r_0(3bJ_{ij}^{(2)}(b)+8J_{ij}^{(0)}(r_0)r_0) \\
& -6a^5(10bJ_{ij}^{(2)}(b)-bJ_{ij}^{(5)}(b)+5bJ_{ij}^{(3)}(r_0)-5J_{ij}^{(3)}(b)r_0+J_{ij}^{(5)}(b)r_0) \\
& +15a^2br_0[b^2(J_{ij}^{(0)}(b)+J_{ij}^{(2)}(b))+2J_{ij}^{(0)}(r_0)r_0^{\,2}] \\
& +10a^3[b^3(2J_{ij}^{(0)}(b)-J_{ij}^{(3)}(b)+J_{ij}^{(3)}(r_0))+9bJ_{ij}^{(0)}(r_0)r_0^{\,2}+4J_{ij}^{(0)}(r_0)r_0^{\,3}]\}\lambda^2 \\
& +\{-6a^3b^5J_{ij}^{(0)}(b)-30a^7bJ_{ij}^{(2)}(b)+10a^5b^3(J_{ij}^{(0)}(b)+J_{ij}^{(2)}(b)) \\
& +4a^8(5J_{ij}^{(3)}(b)-J_{ij}^{(5)}(b))+[9ab^5J_{ij}^{(0)}(b)-4b^6J_{ij}^{(0)}(b)
\end{aligned}
$$

doi:10.6342/NTU202502508

$$
\begin{aligned}
&-5a^3b^3(J_{ij}^{(0)}(b)+3J_{ij}^{(2)}(b)-2J_{ij}^{(3)}(b))+3a^5b(5J_{ij}^{(2)}(b)-2J_{ij}^{(5)}(b))\\
&+a^6(-10J_{ij}^{(3)}(b)+6J_{ij}^{(5)}(b))]r_0{}^2+[-3b^5J_{ij}^{(0)}(b)-15a^4bJ_{ij}^{(2)}(b)\\
&+5a^2b^3(J_{ij}^{(0)}(b)+J_{ij}^{(2)}(b))+2a^5(5J_{ij}^{(3)}(b)-J_{ij}^{(5)}(b))]r_0{}^3\}\lambda^4]\sinh[(a-r_0)\lambda]\\
&-30\{3J_{ij}^{(\beta)}(r_0)[-6a^3b+(a-b)^2(2a+b)r_0]\\
&+3(a-b)^2(2a+b)J_{ij}^{(\alpha)}(r_0)r_0{}^2\lambda\\
&+(a-b)^2(2a+b)J_{ij}^{(\beta)}(r_0)(2a^3+r_0{}^3)\lambda^2\}\sinh(\lambda r_0))]\},
\end{aligned}
\tag{A45}
$$

doi:10.6342/NTU202502508

$$
\begin{aligned}
C_{ij5} = {} & (3a^2M)^{-1}\lambda^2\{-6[180a^3J_{ij}^{(\alpha)}(r_0)+180a^3(a-b)J_{ij}^{(\beta)}(r_0)\lambda \\
& +3(a-b)^3(8a^2+9ab+3b^2)J_{ij}^{(\alpha)}(r_0)\lambda^2 \\
& +(a-b)^4(4a^2+7ab+4b^2)J_{ij}^{(\beta)}(r_0)\lambda^3]\cosh(a\lambda)r_0 \\
& -2\lambda\cosh[\lambda(a-r_0)][540a^3J_{ij}^{(0)}(r_0)(a-b-r_0)r_0 \\
& +\lambda^4\{a^3[a^3b^3\{3(4J_{ij}^{(0)}(b)+10J_{ij}^{(2)}(b)-5J_{ij}^{(3)}(b)+J_{ij}^{(5)}(b))-10J_{ij}^{(3)}(r_0)\} \\
& +2b^6\{3(J_{ij}^{(0)}(b)+J_{ij}^{(2)}(b))-2J_{ij}^{(3)}(r_0)\}-9ab^5(2J_{ij}^{(0)}(b)+J_{ij}^{(3)}(b)-J_{ij}^{(3)}(r_0)) \\
& +4a^6(6J_{ij}^{(3)}(b)-3J_{ij}^{(5)}(b)-J_{ij}^{(3)}(r_0))+9a^5b(-4J_{ij}^{(2)}(b)+J_{ij}^{(5)}(b)+J_{ij}^{(3)}(r_0))] \\
& +(a-b)^4(4a^2+7ab+4b^2)J_{ij}^{(0)}(r_0)r_0^3\}+3\lambda^2\{30[a^4b^3J_{ij}^{(0)}(b) \\
& +2a^7(J_{ij}^{(3)}(b)-J_{ij}^{(3)}(r_0))+a^6b(-3J_{ij}^{(2)}(b)+2J_{ij}^{(3)}(r_0))] \\
& +(a-b)J_{ij}^{(0)}(r_0)r_0[(a-b)^3(4a^2+7ab+4b^2)-3(a-b)^2(8a^2+9ab+3b^2)r_0 \\
& +60a^3r_0^2]\}]+6(-2J_{ij}^{(\alpha)}(r_0)\{20a^6\lambda^2-27a^5b\lambda^2+2b^6\lambda^2 \\
& +5a^3b(-18+b^2\lambda^2)\}\cosh(\lambda r_0)+2J_{ij}^{(\beta)}(r_0)\{20a^6\lambda^2-27a^5b\lambda^2 \\
& +2b^6\lambda^2+5a^3b(-18+b^2\lambda^2)\}\sinh(\lambda r_0) \\
& +\lambda\{-180a^3bJ_{ij}^{(0)}(r_0)+2[2b^6J_{ij}^{(0)}(r_0)+5a^3b^3(3J_{ij}^{(0)}(b)+J_{ij}^{(0)}(r_0)) \\
& -9a^5b(3J_{ij}^{(0)}(r_0)+5J_{ij}^{(2)}(b))+10a^6(2J_{ij}^{(0)}(r_0)+3J_{ij}^{(3)}(b))]\lambda^2 \\
& +a^2[2b^6(-J_{ij}^{(0)}(b)+J_{ij}^{(2)}(b))+3ab^5(J_{ij}^{(0)}(b)-J_{ij}^{(3)}(b)) \\
& +3a^5b(J_{ij}^{(2)}(b)-J_{ij}^{(5)}(b))+2a^6(-J_{ij}^{(3)}(b)+J_{ij}^{(5)}(b)) \\
& +a^3b^3(-J_{ij}^{(0)}(b)-5J_{ij}^{(2)}(b)+5J_{ij}^{(3)}(b)+J_{ij}^{(5)}(b))]\lambda^4\}r_0 \\
& +\{180a^3J_{ij}^{(\beta)}(r_0)+180a^3(a-b)J_{ij}^{(\alpha)}(r_0)\lambda \\
& +3(a-b)^3(8a^2+9ab+3b^2)J_{ij}^{(\beta)}(r_0)\lambda^2 \\
& +(a-b)^4(4a^2+7ab+4b^2)J_{ij}^{(\alpha)}(r_0)\lambda^3\}\sinh(a\lambda)r_0 \\
& +\sinh[\lambda(a-r_0)][180a^3J_{ij}^{(0)}(r_0)r_0+\lambda^4\{a^2[2b^6(-J_{ij}^{(0)}(b)+J_{ij}^{(2)}(b)) \\
& +a^3b^3(14J_{ij}^{(0)}(b)+10J_{ij}^{(2)}(b)+5J_{ij}^{(3)}(b)+J_{ij}^{(5)}(b)-10J_{ij}^{(3)}(r_0)) \\
& -3a^5b(14J_{ij}^{(2)}(b)+J_{ij}^{(5)}(b)-5J_{ij}^{(3)}(r_0)) \\
& +4a^6(7J_{ij}^{(3)}(b)-J_{ij}^{(5)}(b)-2J_{ij}^{(3)}(r_0))-3ab^5(2J_{ij}^{(0)}(b)+J_{ij}^{(3)}(b)-J_{ij}^{(3)}(r_0))] \\
& +(a-b)^3J_{ij}^{(0)}(r_0)r_0^2[-(a-b)(4a^2+7ab+4b^2)+(8a^2+9ab+3b^2)r_0]\} \\
& +3\lambda^2\{10[a^3b^3J_{ij}^{(0)}(b)-3a^5bJ_{ij}^{(2)}(b)+2a^6(J_{ij}^{(3)}(b)-J_{ij}^{(3)}(r_0))] \\
& +J_{ij}^{(0)}(r_0)r_0[(a-b)^3(8a^2+9ab+3b^2)+20a^3r_0(-3a+3b+r_0)]\}])\},
\end{aligned}
\tag{A46}
$$

doi:10.6342/NTU202502508

$$
\begin{aligned}
C_{ij6} = {} & (3a^5 M)^{-1}\{2[6a^3 r_0 \lambda^3\{90a^3 b J_{ij}^{(3)}(r_0) \\
& -[9a^5 b(J_{ij}^{(5)}(b) - 3J_{ij}^{(3)}(r_0)) + 20a^6 J_{ij}^{(3)}(r_0) \\
& +2b^6(3J_{ij}^{(0)}(b) + J_{ij}^{(3)}(r_0)) + 5a^3 b^3(-3J_{ij}^{(3)}(b) + J_{ij}^{(3)}(r_0))]\lambda^2 \\
& +a^2[2b^6(-J_{ij}^{(0)}(b) + J_{ij}^{(2)}(b)) + 3ab^5(J_{ij}^{(0)}(b) - J_{ij}^{(3)}(b)) \\
& +3a^5 b(J_{ij}^{(2)}(b) - J_{ij}^{(5)}(b)) + 2a^6(-J_{ij}^{(3)}(b) + J_{ij}^{(5)}(b)) \\
& +a^3 b^3(-J_{ij}^{(0)}(b) - 5J_{ij}^{(2)}(b) + 5J_{ij}^{(3)}(b) + J_{ij}^{(5)}(b))]\lambda^4\} \\
& -6r_0\{-270a^3 b J_{ij}^{(\alpha)}(r_0) - 270a^4 b J_{ij}^{(\beta)}(r_0)\lambda \\
& +6(10a^6 - 36a^5 b + 10a^3 b^3 + b^6)J_{ij}^{(\alpha)}(r_0)\lambda^2 \\
& +6a(10a^6 - 21a^5 b + 10a^3 b^3 + b^6)J_{ij}^{(\beta)}(r_0)\lambda^3 \\
& +3a^3(a-b)^3(8a^2 + 9ab + 3b^2)J_{ij}^{(\alpha)}(r_0)\lambda^4 \\
& +a^3(a-b)^4(4a^2 + 7ab + 4b^2)J_{ij}^{(\beta)}(r_0)\lambda^5\}\cosh(\lambda a) \\
& +\lambda\{1620a^3 b J_{ij}^{(0)}(r_0)(a - r_0)r_0 - 18[2ab^6 J_{ij}^{(0)}(r_0)r_0 \\
& +5a^3 b^3(3J_{ij}^{(0)}(b) - 4J_{ij}^{(0)}(r_0))r_0^2 - 2b^6 J_{ij}^{(0)}(r_0)r_0^2 + 9a^5 b(8J_{ij}^{(0)}(r_0) - 5J_{ij}^{(2)}(b))r_0^2 \\
& +10a^7(3bJ_{ij}^{(3)}(r_0) + 2J_{ij}^{(0)}(r_0)r_0 - 3J_{ij}^{(3)}(b)r_0) \\
& +a^6 r_0(-42bJ_{ij}^{(0)}(r_0) + 45bJ_{ij}^{(2)}(b) - 20J_{ij}^{(0)}(r_0)r_0 + 30J_{ij}^{(3)}(b)r_0) \\
& -5a^4 b r_0\{b^2(3J_{ij}^{(0)}(b) - 4J_{ij}^{(0)}(r_0)) + 6J_{ij}^{(0)}(r_0)r_0^2\}]\lambda^2 \\
& +3a[4a^3(10a^6 - 21a^5 b + 10a^3 b^3 + b^6)J_{ij}^{(3)}(r_0) \\
& +a^2\{2b^6(3J_{ij}^{(0)}(b) - 4J_{ij}^{(0)}(r_0) + 3J_{ij}^{(2)}(b)) - 9ab^5(2J_{ij}^{(0)}(b) - 2J_{ij}^{(0)}(r_0) + J_{ij}^{(3)}(b)) \\
& +9a^5 b(2J_{ij}^{(0)}(r_0) - 4J_{ij}^{(2)}(b) + J_{ij}^{(5)}(b)) \\
& +a^3 b^3(12J_{ij}^{(0)}(b) - 20J_{ij}^{(0)}(r_0) + 30J_{ij}^{(2)}(b) - 15J_{ij}^{(3)}(b) + 3J_{ij}^{(5)}(b)) \\
& -4a^6(2J_{ij}^{(0)}(r_0) - 6J_{ij}^{(3)}(b) + 3J_{ij}^{(5)}(b))\}r_0 \\
& +3a\{2b^6(J_{ij}^{(0)}(b) - J_{ij}^{(2)}(b)) + 3ab^5(2J_{ij}^{(0)}(b) - 2J_{ij}^{(0)}(r_0) + J_{ij}^{(3)}(b)) \\
& +3a^5 b(-10J_{ij}^{(0)}(r_0) + 14J_{ij}^{(2)}(b) + J_{ij}^{(5)}(b)) + 4a^6(4J_{ij}^{(0)}(r_0) - 7J_{ij}^{(3)}(b) + J_{ij}^{(5)}(b)) \\
& -a^3 b^3(14J_{ij}^{(0)}(b) - 20J_{ij}^{(0)}(r_0) + 10J_{ij}^{(2)}(b) + 5J_{ij}^{(3)}(b) + J_{ij}^{(5)}(b))\}r_0^2 \\
& -2\{2b^6 J_{ij}^{(0)}(r_0) + 5a^3 b^3(-3J_{ij}^{(0)}(b) + 4J_{ij}^{(0)}(r_0)) + a^5 b(-42J_{ij}^{(0)}(r_0) + 45J_{ij}^{(2)}(b)) \\
& +10a^6(2J_{ij}^{(0)}(r_0) - 3J_{ij}^{(3)}(b))\}r_0^3]\lambda^4 \\
& +a^3[2a^3(a-b)^4(4a^2 + 7ab + 4b^2)J_{ij}^{(3)}(r_0) \\
& +\{2b^6(3J_{ij}^{(0)}(b) - 4J_{ij}^{(0)}(r_0) + 3J_{ij}^{(2)}(b)) \\
& -9ab^5(2J_{ij}^{(0)}(b) - 2J_{ij}^{(0)}(r_0) + J_{ij}^{(3)}(b)) + 9a^5 b(2J_{ij}^{(0)}(r_0) - 4J_{ij}^{(2)}(b) + J_{ij}^{(5)}(b))
\end{aligned}
$$

doi:10.6342/NTU202502508

$$
\begin{aligned}
&+a^3b^3(12J_{ij}^{(0)}(b)-20J_{ij}^{(0)}(r_0)+30J_{ij}^{(2)}(b)-15J_{ij}^{(3)}(b)+3J_{ij}^{(5)}(b))\\
&-4a^6(2J_{ij}^{(0)}(r_0)-6J_{ij}^{(3)}(b)+3J_{ij}^{(5)}(b))\}r_0{}^3]\lambda^6\}\cosh[(a-r_0)\lambda]\\
&-3\{12ab^6J_{ij}^{(0)}(r_0)r_0{}^2\lambda^4+16a^{11}J_{ij}^{(3)}(r_0)\lambda^6-30a^{10}bJ_{ij}^{(3)}(r_0)\lambda^6\\
&-4b^6J_{ij}^{(0)}(r_0)r_0\lambda^2(3+r_0{}^2\lambda^2)-2a^2b^6(J_{ij}^{(0)}(b)-J_{ij}^{(2)}(b))r_0\lambda^4(3+r_0{}^2\lambda^2)\\
&-a^5br_0\lambda^2[-144J_{ij}^{(0)}(r_0)+90J_{ij}^{(2)}(b)\\
&-b^2(14J_{ij}^{(0)}(b)-20J_{ij}^{(0)}(r_0)+10J_{ij}^{(2)}(b)+5J_{ij}^{(3)}(b)+J_{ij}^{(5)}(b))\lambda^2](3+r_0{}^2\lambda^2)\\
&+4a^9\lambda^4[10J_{ij}^{(3)}(r_0)+(2J_{ij}^{(0)}(r_0)-6J_{ij}^{(3)}(b)+3J_{ij}^{(5)}(b))r_0{}^2\lambda^2]\\
&+3a^4br_0{}^2\lambda^2[-180J_{ij}^{(0)}(r_0)+10b^2(-3J_{ij}^{(0)}(b)+4J_{ij}^{(0)}(r_0))\lambda^2\\
&+3b^4(2J_{ij}^{(0)}(b)-2J_{ij}^{(0)}(r_0)+J_{ij}^{(3)}(b))\lambda^4]+a^3b[540J_{ij}^{(0)}(r_0)r_0\\
&+30r_0\{b^2(3J_{ij}^{(0)}(b)-4J_{ij}^{(0)}(r_0))+6J_{ij}^{(0)}(r_0)r_0{}^2\}\lambda^2\\
&+b^2\{4b^3J_{ij}^{(3)}(r_0)-9b^2(2J_{ij}^{(0)}(b)-2J_{ij}^{(0)}(r_0)+J_{ij}^{(3)}(b))r_0\\
&+10(3J_{ij}^{(0)}(b)-4J_{ij}^{(0)}(r_0))r_0{}^3\}\lambda^4\\
&-b^4r_0{}^2\{b(6J_{ij}^{(0)}(b)-8J_{ij}^{(0)}(r_0)+6J_{ij}^{(2)}(b))\\
&+3(2J_{ij}^{(0)}(b)-2J_{ij}^{(0)}(r_0)+J_{ij}^{(3)}(b))r_0\}\lambda^6]\\
&+3a^7r_0\lambda^4[20(2J_{ij}^{(0)}(r_0)-3J_{ij}^{(3)}(b))r_0\\
&+b(10J_{ij}^{(0)}(r_0)-14J_{ij}^{(2)}(b)-J_{ij}^{(5)}(b))(3+r_0{}^2\lambda^2)] \qquad \text{(A47)}\\
&+a^8\lambda^4[-144bJ_{ij}^{(3)}(r_0)+20b^3J_{ij}^{(3)}(r_0)\lambda^2\\
&-9b(2J_{ij}^{(0)}(r_0)-4J_{ij}^{(2)}(b)+J_{ij}^{(5)}(b))r_0{}^2\lambda^2\\
&-4(4J_{ij}^{(0)}(r_0)-7J_{ij}^{(3)}(b)+J_{ij}^{(5)}(b))r_0(3+r_0{}^2\lambda^2)]\\
&+a^6\lambda^2[-6b^5J_{ij}^{(3)}(r_0)\lambda^4-20(2J_{ij}^{(0)}(r_0)-3J_{ij}^{(3)}(b))r_0(3+r_0{}^2\lambda^2)\\
&+18b\{-10J_{ij}^{(3)}(r_0)+(-14J_{ij}^{(0)}(r_0)+15J_{ij}^{(2)}(b))r_0{}^2\lambda^2\}\\
&+b^3\lambda^2\{40J_{ij}^{(3)}(r_0)+(-12J_{ij}^{(0)}(b)+20J_{ij}^{(0)}(r_0)-30J_{ij}^{(2)}(b)\\
&+15J_{ij}^{(3)}(b)-3J_{ij}^{(5)}(b))r_0{}^2\lambda^2\}]\}\sinh[(a-r_0)\lambda]\\
&+6r_0\{[-270a^3bJ_{ij}^{(\beta)}(r_0)-270a^4bJ_{ij}^{(\alpha)}(r_0)\lambda\\
&+6(10a^6-36a^5b+10a^3b^3+b^6)J_{ij}^{(\beta)}(r_0)\lambda^2\\
&+6a(10a^6-21a^5b+10a^3b^3+b^6)J_{ij}^{(\alpha)}(r_0)\lambda^3\\
&+3a^3(a-b)^3(8a^2+9ab+3b^2)J_{ij}^{(\beta)}(r_0)\lambda^4\\
&+a^3(a-b)^4(4a^2+7ab+4b^2)J_{ij}^{(\alpha)}(r_0)\lambda^5]\sinh(\lambda a) \qquad ,\\
&+[20a^6\lambda^2-27a^5b\lambda^2+2b^6\lambda^2\\
&+5a^3b(-18+b^2\lambda^2)][\{3J_{ij}^{(\beta)}(r_0)r_0\lambda+J_{ij}^{(\alpha)}(r_0)(3+r_0{}^2\lambda^2)\}\cosh(\lambda r_0)\\
&-\{3J_{ij}^{(\alpha)}(r_0)r_0\lambda+J_{ij}^{(\beta)}(r_0)(3+r_0{}^2\lambda^2)\}\sinh(\lambda r_0)]\}]\}
\end{aligned}
$$

doi:10.6342/NTU202502508

$$
\begin{aligned}
C_{ij7} = {}& (a^5 \lambda M)^{-1} \{6\cosh(\lambda a)[r_0 \lambda\{180 a^3 b J_{ij}^{(0)}(r_0) \\
& -2[2b^6 J_{ij}^{(0)}(r_0) + 5a^3 b^3(-3J_{ij}^{(0)}(b) + 4J_{ij}^{(0)}(r_0)) \\
& +9a^5 b(-8J_{ij}^{(0)}(r_0) + 5J_{ij}^{(2)}(b)) \\
& +10a^6(2J_{ij}^{(0)}(r_0) - 3J_{ij}^{(3)}(b) + 3J_{ij}^{(3)}(r_0))]\lambda^2 \\
& +a^2[2b^6(-J_{ij}^{(0)}(b) + J_{ij}^{(2)}(b)) + a^3 b^3(14J_{ij}^{(0)}(b) - 20J_{ij}^{(0)}(r_0) \\
& +10J_{ij}^{(2)}(b) + 5J_{ij}^{(3)}(b) + J_{ij}^{(5)}(b) - 10J_{ij}^{(3)}(r_0)) \\
& +3ab^5(-2J_{ij}^{(0)}(b) + 2J_{ij}^{(0)}(r_0) - J_{ij}^{(3)}(b) + J_{ij}^{(3)}(r_0)) \\
& -4a^6(4J_{ij}^{(0)}(r_0) - 7J_{ij}^{(3)}(b) + J_{ij}^{(5)}(b) + 2J_{ij}^{(3)}(r_0)) \\
& +3a^5 b(10J_{ij}^{(0)}(r_0) - 14J_{ij}^{(2)}(b) - J_{ij}^{(5)}(b) + 5J_{ij}^{(3)}(r_0))]\lambda^4\} \\
& +\{180a^3 J_{ij}^{(\alpha)}(r_0)(-b + r_0) + 180a^3 J_{ij}^{(\beta)}(r_0) r_0^{\,2} \lambda \\
& +J_{ij}^{(\alpha)}(r_0)[4(10a^6 - 36a^5 b + 10a^3 b^3 + b^6) \\
& +3(a-b)^3(8a^2 + 9ab + 3b^2) r_0 + 60a^3 r_0^{\,3}]\lambda^2 \\
& +3(a-b)^3(8a^2 + 9ab + 3b^2) J_{ij}^{(\beta)}(r_0) r_0^{\,2} \lambda^3 \\
& +(a-b)^3(8a^2 + 9ab + 3b^2) J_{ij}^{(\alpha)}(r_0)(2a^3 + r_0^{\,3})\lambda^4\}\cosh(\lambda r_0) \\
& -\{180a^3 J_{ij}^{(\beta)}(r_0)(-b + r_0) + 180a^3 J_{ij}^{(\alpha)}(r_0) r_0^{\,2} \lambda \\
& +J_{ij}^{(\beta)}(r_0)[4(10a^6 - 36a^5 b + 10a^3 b^3 + b^6) \\
& +3(a-b)^3(8a^2 + 9ab + 3b^2) r_0 + 60a^3 r_0^{\,3}]\lambda^2 \\
& +3(a-b)^3(8a^2 + 9ab + 3b^2) J_{ij}^{(\alpha)}(r_0) r_0^{\,2} \lambda^3 \\
& +(a-b)^3(8a^2 + 9ab + 3b^2)(2a^3 + r_0^{\,3}) J_{ij}^{(\beta)}(r_0)\lambda^4\}\sinh(\lambda r_0)] \\
& +2\lambda[6J_{ij}^{(\beta)}(r_0) r_0\{20a^6\lambda^2 - 27a^5 b\lambda^2 + 2b^6\lambda^2 + 5a^3 b(-18 + b^2\lambda^2)\} \\
& +ar_0\lambda\{-540a^3 b J_{ij}^{(0)}(r_0) + 6[2b^6 J_{ij}^{(0)}(r_0) \\
& +5a^3 b^3(-3J_{ij}^{(0)}(b) + 4J_{ij}^{(0)}(r_0)) \\
& +10a^6(2J_{ij}^{(0)}(r_0) - 3J_{ij}^{(3)}(b) + 3J_{ij}^{(3)}(r_0)) \\
& -3a^5 b(14J_{ij}^{(0)}(r_0) - 15J_{ij}^{(2)}(b) + 10J_{ij}^{(3)}(r_0))]\lambda^2 \\
& +a^2[9ab^5(2J_{ij}^{(0)}(b) - 2J_{ij}^{(0)}(r_0) + J_{ij}^{(3)}(b) \\
& -J_{ij}^{(3)}(r_0)) - 9a^5 b(2J_{ij}^{(0)}(r_0) - 4J_{ij}^{(2)}(b) + J_{ij}^{(5)}(b) + J_{ij}^{(3)}(r_0)) \\
& +4a^6(2J_{ij}^{(0)}(r_0) - 6J_{ij}^{(3)}(b) + 3J_{ij}^{(5)}(b) + J_{ij}^{(3)}(r_0)) \\
& +2b^6(-3J_{ij}^{(0)}(b) + 4J_{ij}^{(0)}(r_0) - 3J_{ij}^{(2)}(b) + 2J_{ij}^{(3)}(r_0)) \\
& +a^3 b^3(-12J_{ij}^{(0)}(b) + 20J_{ij}^{(0)}(r_0) - 30J_{ij}^{(2)}(b) \\
& +15J_{ij}^{(3)}(b) - 3J_{ij}^{(5)}(b) + 10J_{ij}^{(3)}(r_0))]\lambda^4\}\sinh(\lambda a)
\end{aligned}
$$

doi:10.6342/NTU202502508

$$
\begin{aligned}
&+\cosh(\lambda r_0)\{-540a^3bJ_{ij}^{(0)}(r_0)r_0+6[2b^6J_{ij}^{(0)}(r_0)r_0\\
&+9a^5b(-3J_{ij}^{(0)}(r_0)+5J_{ij}^{(2)}(b))r_0\\
&+10a^6(3bJ_{ij}^{(3)}(r_0)+2J_{ij}^{(0)}(r_0)r_0-3J_{ij}^{(3)}(b)r_0)\\
&+5a^3br_0(b^2(-3J_{ij}^{(0)}(b)+J_{ij}^{(0)}(r_0))-6J_{ij}^{(0)}(r_0){r_0}^2)]\lambda^2\\
&+[-2a^3\{20a^6J_{ij}^{(3)}(r_0)+2b^6(-3J_{ij}^{(0)}(b)+J_{ij}^{(3)}(r_0))\\
&+5a^3b^3(3J_{ij}^{(3)}(b)+J_{ij}^{(3)}(r_0))-9a^5b(J_{ij}^{(5)}(b)+3J_{ij}^{(3)}(r_0))\}\\
&+3a^2\{2b^6(J_{ij}^{(0)}(b)-J_{ij}^{(2)}(b))+3ab^5(-J_{ij}^{(0)}(b)+J_{ij}^{(3)}(b))\\
&+a^3b^3(J_{ij}^{(0)}(b)+5J_{ij}^{(2)}(b)-5J_{ij}^{(3)}(b)-J_{ij}^{(5)}(b))\\
&+2a^6(J_{ij}^{(3)}(b)-J_{ij}^{(5)}(b))+3a^5b(-J_{ij}^{(2)}(b)+J_{ij}^{(5)}(b))\}r_0\\
&+2\{2b^6J_{ij}^{(0)}(r_0)+5a^3b^3(-3J_{ij}^{(0)}(b)+J_{ij}^{(0)}(r_0))\\
&+9a^5b(-3J_{ij}^{(0)}(r_0)+5J_{ij}^{(2)}(b))\\
&+10a^6(2J_{ij}^{(0)}(r_0)-3J_{ij}^{(3)}(b))\}{r_0}^3]\lambda^4\\
&+a^2(a-b)^2\{2b^4(J_{ij}^{(0)}(b)-J_{ij}^{(2)}(b))\\
&+6a^2b^2(-J_{ij}^{(2)}(b)+J_{ij}^{(3)}(b))\\
&+ab^3(J_{ij}^{(0)}(b)-4J_{ij}^{(2)}(b)+3J_{ij}^{(3)}(b))+2a^4(J_{ij}^{(3)}(b)-J_{ij}^{(5)}(b))\\
&-a^3b(3J_{ij}^{(2)}(b)-4J_{ij}^{(3)}(b)+J_{ij}^{(5)}(b))\}(2a^3+{r_0}^3)\lambda^6\\
&-\{-540a^3J_{ij}^{(\alpha)}(r_0)[a(b-r_0)+br_0]+540a^3(a-b)J_{ij}^{(\beta)}(r_0){r_0}^2\lambda\\
&+3J_{ij}^{(\alpha)}(r_0)[4a(10a^6-21a^5b+10a^3b^3+b^6)\\
&+(a-b)^4(4a^2+7ab+4b^2)r_0\\
&+60a^3(a-b){r_0}^3]\lambda^2+3(a-b)^4(4a^2+7ab+4b^2)J_{ij}^{(\beta)}(r_0){r_0}^2\lambda^3\\
&+(a-b)^4(4a^2+7ab+4b^2)J_{ij}^{(\alpha)}(r_0)(2a^3+{r_0}^3)\lambda^4\}\sinh(\lambda a)\}\\
&+\{3{r_0}^2\lambda[180a^3bJ_{ij}^{(0)}(r_0)-2\{2b^6J_{ij}^{(0)}(r_0)+5a^3b^3(-3J_{ij}^{(0)}(b)+J_{ij}^{(0)}(r_0))\\
&+9a^5b(-3J_{ij}^{(0)}(r_0)+5J_{ij}^{(2)}(b))+10a^6(2J_{ij}^{(0)}(r_0)-3J_{ij}^{(3)}(b))\}\lambda^2\\
&+a^2\{2b^6(-J_{ij}^{(0)}(b)+J_{ij}^{(2)}(b))+3ab^5(J_{ij}^{(0)}(b)-J_{ij}^{(3)}(b))+3a^5b(J_{ij}^{(2)}(b)-J_{ij}^{(5)}(b))\\
&+2a^6(-J_{ij}^{(3)}(b)+J_{ij}^{(5)}(b))+a^3b^3(-J_{ij}^{(0)}(b)-5J_{ij}^{(2)}(b)+5J_{ij}^{(3)}(b)+J_{ij}^{(5)}(b))\}\lambda^4]\\
&+[-540a^3J_{ij}^{(\beta)}(r_0)\{a(b-r_0)+br_0\}+540a^3(a-b)J_{ij}^{(\alpha)}(r_0){r_0}^2\lambda\\
&+3J_{ij}^{(\beta)}(r_0)\{4a(10a^6-21a^5b+10a^3b^3+b^6)\\
&+(a-b)^4(4a^2+7ab+4b^2)r_0+60a^3(a-b){r_0}^3\}\lambda^2\\
&+3(a-b)^4(4a^2+7ab+4b^2)J_{ij}^{(\alpha)}(r_0){r_0}^2\lambda^3\\
&+(a-b)^4(4a^2+7ab+4b^2)J_{ij}^{(\beta)}(r_0)(2a^3+{r_0}^3)\lambda^4]\sinh(\lambda a)\}\sinh(\lambda r_0)]\}
\end{aligned}
\quad , \tag{A48}
$$

doi:10.6342/NTU202502508

$$C_{ij8}=(a^5\lambda M)^{-1}\{2r_0\lambda[-6J_{ij}^{(\alpha)}(r_0)\{20a^6\lambda^2-27a^5b\lambda^2$$

$$+2b^6\lambda^2+5a^3b(-18+b^2\lambda^2)\}+\{540a^4bJ_{ij}^{(0)}(r_0)\lambda$$

$$-6a[2b^6J_{ij}^{(0)}(r_0)+5a^3b^3(-3J_{ij}^{(0)}(b)+4J_{ij}^{(0)}(r_0))$$

$$+10a^6(2J_{ij}^{(0)}(r_0)-3J_{ij}^{(3)}(b)+3J_{ij}^{(3)}(r_0))$$

$$-3a^5b(14J_{ij}^{(0)}(r_0)-15J_{ij}^{(2)}(b)+10J_{ij}^{(3)}(r_0))]\lambda^3$$

$$+a^3[a^3b^3(12J_{ij}^{(0)}(b)-20J_{ij}^{(0)}(r_0)+30J_{ij}^{(2)}(b)$$

$$-15J_{ij}^{(3)}(b)+3J_{ij}^{(5)}(b)-10J_{ij}^{(3)}(r_0))+2b^6(3J_{ij}^{(0)}(b)$$

$$-4J_{ij}^{(0)}(r_0)+3J_{ij}^{(2)}(b)-2J_{ij}^{(3)}(r_0))+9ab^5(-2J_{ij}^{(0)}(b)$$

$$+2J_{ij}^{(0)}(r_0)-J_{ij}^{(3)}(b)+J_{ij}^{(3)}(r_0))+9a^5b(2J_{ij}^{(0)}(r_0)-4J_{ij}^{(2)}(b)$$

$$+J_{ij}^{(5)}(b)+J_{ij}^{(3)}(r_0))-4a^6(2J_{ij}^{(0)}(r_0)-6J_{ij}^{(3)}(b)+3J_{ij}^{(5)}(b)$$

$$+J_{ij}^{(3)}(r_0))]\lambda^5\}\cosh(\lambda a)+3\{-180a^3bJ_{ij}^{(0)}(r_0)$$

$$+2[2b^6J_{ij}^{(0)}(r_0)+5a^3b^3(-3J_{ij}^{(0)}(b)+4J_{ij}^{(0)}(r_0))$$

$$+9a^5b(-8J_{ij}^{(0)}(r_0)+5J_{ij}^{(2)}(b))$$

$$+10a^6(2J_{ij}^{(0)}(r_0)-3J_{ij}^{(3)}(b)+3J_{ij}^{(3)}(r_0))]\lambda^2$$

$$+a^2[2b^6(J_{ij}^{(0)}(b)-J_{ij}^{(2)}(b))-a^3b^3(14J_{ij}^{(0)}(b)$$

$$-20J_{ij}^{(0)}(r_0)+10J_{ij}^{(2)}(b)+5J_{ij}^{(3)}(b)+J_{ij}^{(5)}(b)-10J_{ij}^{(3)}(r_0))$$

$$+3a^5b(-10J_{ij}^{(0)}(r_0)+14J_{ij}^{(2)}(b)+J_{ij}^{(5)}(b)-5J_{ij}^{(3)}(r_0))$$

$$+3ab^5(2J_{ij}^{(0)}(b)-2J_{ij}^{(0)}(r_0)+J_{ij}^{(3)}(b)-J_{ij}^{(3)}(r_0))$$

$$+4a^6(4J_{ij}^{(0)}(r_0)-7J_{ij}^{(3)}(b)+J_{ij}^{(5)}(b)+2J_{ij}^{(3)}(r_0))]\lambda^4\}\sinh(\lambda a)]$$

$$+2\cosh(\lambda r_0)[3{r_0}^2\lambda^2\{-180a^3bJ_{ij}^{(0)}(r_0)$$

$$+2[2b^6J_{ij}^{(0)}(r_0)+5a^3b^3(-3J_{ij}^{(0)}(b)+J_{ij}^{(0)}(r_0))$$

$$+9a^5b(-3J_{ij}^{(0)}(r_0)+5J_{ij}^{(2)}(b))+10a^6(2J_{ij}^{(0)}(r_0)-3J_{ij}^{(3)}(b))]\lambda^2$$

$$+a^2[2b^6(J_{ij}^{(0)}(b)-J_{ij}^{(2)}(b))+3ab^5(-J_{ij}^{(0)}(b)+J_{ij}^{(3)}(b))$$

$$+a^3b^3(J_{ij}^{(0)}(b)+5J_{ij}^{(2)}(b)-5J_{ij}^{(3)}(b)-J_{ij}^{(5)}(b))$$

$$+2a^6(J_{ij}^{(3)}(b)-J_{ij}^{(5)}(b))+3a^5b(-J_{ij}^{(2)}(b)+J_{ij}^{(5)}(b))]\lambda^4\}$$

$$+\lambda\{-540a^3J_{ij}^{(\alpha)}(r_0)[a(b-r_0)+br_0]+540a^3\left(a-b\right)J_{ij}^{(\beta)}(r_0){r_0}^2\lambda$$

$$+3J_{ij}^{(\alpha)}(r_0)[4a(10a^6-21a^5b+10a^3b^3+b^6)$$

$$+(a-b)^4(4a^2+7ab+4b^2)r_0+60a^3(a-b){r_0}^3]\lambda^2$$

$$+3(a-b)^4(4a^2+7ab+4b^2)J_{ij}^{(\beta)}(r_0){r_0}^2\lambda^3$$

$$+(a-b)^4(4a^2+7ab+4b^2)J_{ij}^{(\alpha)}(r_0)(2a^3+{r_0}^3)\lambda^4\}\cosh(\lambda a)$$

$$-3\{180a^3J_{ij}^{(\alpha)}(r_0)(-b+r_0)+180a^3J_{ij}^{(\beta)}(r_0){r_0}^2\lambda$$

doi:10.6342/NTU202502508

$$
\begin{aligned}
&+J_{ij}^{(\alpha)}(r_0)[4(10a^6-36a^5b+10a^3b^3+b^6)\\
&+3(a-b)^3(8a^2+9ab+3b^2)r_0+60a^3{r_0}^3]\lambda^2\\
&+3(a-b)^3(8a^2+9ab+3b^2)J_{ij}^{(\beta)}(r_0){r_0}^2\lambda^3\\
&+(a-b)^3(8a^2+9ab+3b^2)J_{ij}^{(\alpha)}(r_0)(2a^3+{r_0}^3)\lambda^4\}\sinh(\lambda a)]\\
&-2[-540a^3bJ_{ij}^{(0)}(r_0)r_0\lambda+6\{2b^6J_{ij}^{(0)}(r_0)r_0\\
&+9a^5b(-3J_{ij}^{(0)}(r_0)+5J_{ij}^{(2)}(b))r_0+10a^6(3bJ_{ij}^{(3)}(r_0)\\
&+2J_{ij}^{(0)}(r_0)r_0-3J_{ij}^{(3)}(b)r_0)\\
&+5a^3br_0[b^2(-3J_{ij}^{(0)}(b)+J_{ij}^{(0)}(r_0))-6J_{ij}^{(0)}(r_0){r_0}^2]\}\lambda^3\\
&+\{-2a^3[20a^6J_{ij}^{(3)}(r_0)+2b^6(-3J_{ij}^{(0)}(b)+J_{ij}^{(3)}(r_0))\\
&+5a^3b^3(3J_{ij}^{(3)}(b)+J_{ij}^{(3)}(r_0))-9a^5b(J_{ij}^{(5)}(b)+3J_{ij}^{(3)}(r_0))]\\
&+3a^2[2b^6(J_{ij}^{(0)}(b)-J_{ij}^{(2)}(b))+3ab^5(-J_{ij}^{(0)}(b)+J_{ij}^{(3)}(b))\\
&+a^3b^3(J_{ij}^{(0)}(b)+5J_{ij}^{(2)}(b)-5J_{ij}^{(3)}(b)-J_{ij}^{(5)}(b))\\
&+2a^6(J_{ij}^{(3)}(b)-J_{ij}^{(5)}(b))+3a^5b(-J_{ij}^{(2)}(b)+J_{ij}^{(5)}(b))]r_0\\
&+2[2b^6J_{ij}^{(0)}(r_0)+5a^3b^3(-3J_{ij}^{(0)}(b)+J_{ij}^{(0)}(r_0))\\
&+9a^5b(-3J_{ij}^{(0)}(r_0)+5J_{ij}^{(2)}(b))\\
&+10a^6(2J_{ij}^{(0)}(r_0)-3J_{ij}^{(3)}(b))]{r_0}^3\}\lambda^5\\
&+a^2(a-b)^2[2b^4(J_{ij}^{(0)}(b)-J_{ij}^{(2)}(b))\\
&+6a^2b^2(-J_{ij}^{(2)}(b)+J_{ij}^{(3)}(b))\\
&+ab^3(J_{ij}^{(0)}(b)-4J_{ij}^{(2)}(b)+3J_{ij}^{(3)}(b))\\
&+2a^4(J_{ij}^{(3)}(b)-J_{ij}^{(5)}(b))\\
&-a^3b(3J_{ij}^{(2)}(b)-4J_{ij}^{(3)}(b)+J_{ij}^{(5)}(b))](2a^3+{r_0}^3)\lambda^7\\
&+\lambda\{-540a^3J_{ij}^{(\beta)}(r_0)[a(b-r_0)+br_0]\\
&+540a^3(a-b)J_{ij}^{(\alpha)}(r_0){r_0}^2\lambda\\
&+3J_{ij}^{(\beta)}(r_0)[4a(10a^6-21a^5b+10a^3b^3+b^6)\\
&+(a-b)^4(4a^2+7ab+4b^2)r_0\\
&+60a^3(a-b){r_0}^3]\lambda^2+3(a-b)^4(4a^2+7ab+4b^2)J_{ij}^{(\alpha)}(r_0){r_0}^2\lambda^3\\
&+(a-b)^4(4a^2+7ab+4b^2)J_{ij}^{(\beta)}(r_0)(2a^3+{r_0}^3)\lambda^4\}\cosh(\lambda a)\\
&-3\{180a^3J_{ij}^{(\beta)}(r_0)(-b+r_0)+180a^3J_{ij}^{(\alpha)}(r_0){r_0}^2\lambda\\
&+J_{ij}^{(\beta)}(r_0)[4(10a^6-36a^5b+10a^3b^3+b^6)\\
&+3(a-b)^3(8a^2+9ab+3b^2)r_0+60a^3{r_0}^3]\lambda^2\\
&+3(a-b)^3(8a^2+9ab+3b^2)J_{ij}^{(\alpha)}(r_0){r_0}^2\lambda^3\\
&+(a-b)^3(8a^2+9ab+3b^2)J_{ij}^{(\beta)}(r_0)(2a^3+{r_0}^3)\lambda^4\}\sinh(\lambda a)]\sinh(r_0\lambda)\}
\end{aligned}
\quad , \qquad (A49)
$$

doi:10.6342/NTU202502508

where $(i,j)=(0,1)$, $(1,0)$, $(0,2)$, $(1,1)$, and $(2,0)$,

$$\begin{aligned}
M =& -12\lambda^5[20a^6\lambda^2-27a^5b\lambda^2+2b^6\lambda^2+5a^3b(-18+b^2\lambda^2)]r_0 \\
&+\lambda^5\cosh[\lambda(a-r_0)]\{(a-b)^4(4a^2+7ab+4b^2)\lambda^4(2a^3+r_0^3) \\
&+3\lambda^2[40a^7-84a^6b+40a^4b^3+4ab^6+(a-b)^4(4a^2+7ab+4b^2)r_0 \\
&-3(a-b)^3(8a^2+9ab+3b^2)r_0^2+60a^3(a-b)r_0^3]-540a^3[ab+r_0(-a+b+r_0)]\}, \\
&-3\lambda^4\sinh[\lambda(a-r_0)]\{180a^3(-b+r_0)+(a-b)^3\lambda^4[2a^3(8a^2+9ab+3b^2) \\
&-(a-b)(4a^2+7ab+4b^2)r_0^2+(8a^2+9ab+3b^2)r_0^3] \\
&+\lambda^2[4(10a^6-36a^5b+10a^3b^3+b^6)+3r_0((a-b)^3(8a^2+9ab+3b^2) \\
&+20a^3r_0(-3a+3b+r_0))]\}
\end{aligned} \tag{A50}$$

$$\begin{aligned}
N =& \lambda^4\{30ab^3r_0\lambda+(a-b)^3(a+b)(2a^2+ab+2b^2)r_0\lambda^3 \\
&+\lambda a[-30ab^3+(4a^6-3a^5b-5a^3b^3+6ab^5-2b^6)\lambda^2]\cosh[(a-r_0)\lambda], \\
&-[-30ab^3+(4a^6+3a^5b-15a^3b^3+6ab^5+2b^6)\lambda^2]\sinh[(a-r_0)\lambda]\}
\end{aligned} \tag{A51}$$

$$\begin{aligned}
O =& 2e^{\lambda(a+r_0)}\lambda^4\{2a\lambda[-270a^3b+6(10a^6-21a^5b+10a^3b^3+b^6)\lambda^2 \\
&+a^2(a-b)^4(4a^2+7ab+4b^2)\lambda^4]\cosh[\lambda(a-r_0)] \\
&-6[-90a^3b+2(10a^6-36a^5b+10a^3b^3+b^6)\lambda^2 \\
&+a^3(a-b)^3(8a^2+9ab+3b^2)\lambda^4]\sinh[\lambda(a-r_0)] \\
&+r_0[-12\lambda\{20a^6\lambda^2-27a^5b\lambda^2+2b^6\lambda^2+5a^3b(-18+b^2\lambda^2)\} \\
&+\lambda\cosh[\lambda(a-r_0)]\{540a^3(a-b)+3(a-b)^4(4a^2+7ab+4b^2)\lambda^2, \\
&-9[60a^3+(a-b)^3(8a^2+9ab+3b^2)\lambda^2]r_0 \\
&+\lambda^2[180a^3(a-b)+(a-b)^4(4a^2+7ab+4b^2)\lambda^2]r_0^2\} \\
&+3\sinh[\lambda(a-r_0)]\{-180a^3-3(a-b)^3(8a^2+9ab+3b^2)\lambda^2 \\
&+\lambda^2r_0[180a^3(a-b)+(a-b)^4(4a^2+7ab+4b^2)\lambda^2 \\
&+\{-60a^3-(a-b)^3(8a^2+9ab+3b^2)\lambda^2\}r_0]\}]\}
\end{aligned} \tag{A52}$$

doi:10.6342/NTU202502508

Appendix B
Basic Governing Equations in Chapter 2 and Section 3.1

Starting with the steady state mass transport differential equation in the absence of chemical reaction, the conservation of ionic species is governed by

$$\nabla \cdot \mathbf{J}_{\pm} = 0, \tag{B1}$$

where, for dilute electrolyte solution, the ionic fluxes follow the Nernst-Plank equation with a convection term,

$$\mathbf{J}_{\pm} = n_{\pm}\mathbf{u} - D_{\pm}(\nabla n_{\pm} \pm \frac{Zen_{\pm}}{kT}\nabla\psi). \tag{B2}$$

Since the electrochemical potential is defined as $\mu_{\pm} = \mu_{\pm}^{0} + kT\ln n_{\pm} \pm Ze\psi$, its gradient is accordingly given by

$$\nabla\mu_{\pm} = kT\frac{\nabla n_{\pm}}{n_{\pm}} \pm Ze\nabla\psi. \tag{B3}$$

Substitute Equations (B2) and (B3) into Equation (B1), the ionic continuity equation is

$$\nabla \cdot [n_{\pm}\mathbf{u} - n_{\pm}\frac{D_{\pm}}{kT}\nabla\mu_{\pm}] = 0. \tag{B4}$$

Combining Equations (B4), (1) and (7), we can obtain Equation (4).

The Poisson equation for a symmetric electrolyte solution modified to account for the fixed charge density in the porous layer can be expressed as

doi:10.6342/NTU202502508

$$\nabla^2\psi = -\frac{1}{\varepsilon}[Ze(n_+ - n_-) + h(r)Q]. \tag{B5}$$

At equilibrium, ionic concentrations obey the Boltzmann distribution

$$n_\pm^{(\mathrm{eq})} = n_0^\infty \exp[\mp \frac{Ze\psi^{(\mathrm{eq})}}{kT}]. \tag{B6}$$

Substitute Equations (1), (3) and (B6) into Equation (B5), we can obtain the governing equation for the perturbed electrical potential shown in Equation (6), and the governing equation for the equilibrium electrical potential is given by

$$\nabla^2\psi^{(\mathrm{eq})} = -\frac{Zen_0^\infty}{\varepsilon}\left[\exp\left(-\frac{Ze\psi^{(\mathrm{eq})}}{kT}\right) - \exp\left(\frac{Ze\psi^{(\mathrm{eq})}}{kT}\right)\right]. \tag{B7}$$

Solving Equation (B7) with appropriate boundary conditions yields the equilibrium electrical potential profile provided in Equations (13)-(17) [38].

For quasi-steady low Reynolds number flow, the Stokes-Brinkman equation modified to incorporate electrostatic effect takes the form

$$\eta\nabla^2\mathbf{u} - \eta\lambda^2 h(r)\mathbf{u} = \nabla p + Ze(n_+ - n_-)\nabla\psi. \tag{B8}$$

Within the porous layer, where $h(r) = 1$, Equation (B8) becomes the modified Brinkman equation; outside the porous layer, where $h(r) = 0$, Equation (B8) reduces to the Stokes equation modified with electrostatic effect. With the substitution of Equations (1)-(3) into Equation (B8), we obtain Equations (5).

doi:10.6342/NTU202502508